Journal of Immunology Research

Advances in Immunology of Neglected Tropical Diseases: New Control Tools and Prospects for Disease Elimination

Lead Guest Editor: Barbara C. Figueiredo
Guest Editors: Carina S. Pinheiro, Fabio V. Marinho, and Nestor A. Guerrero

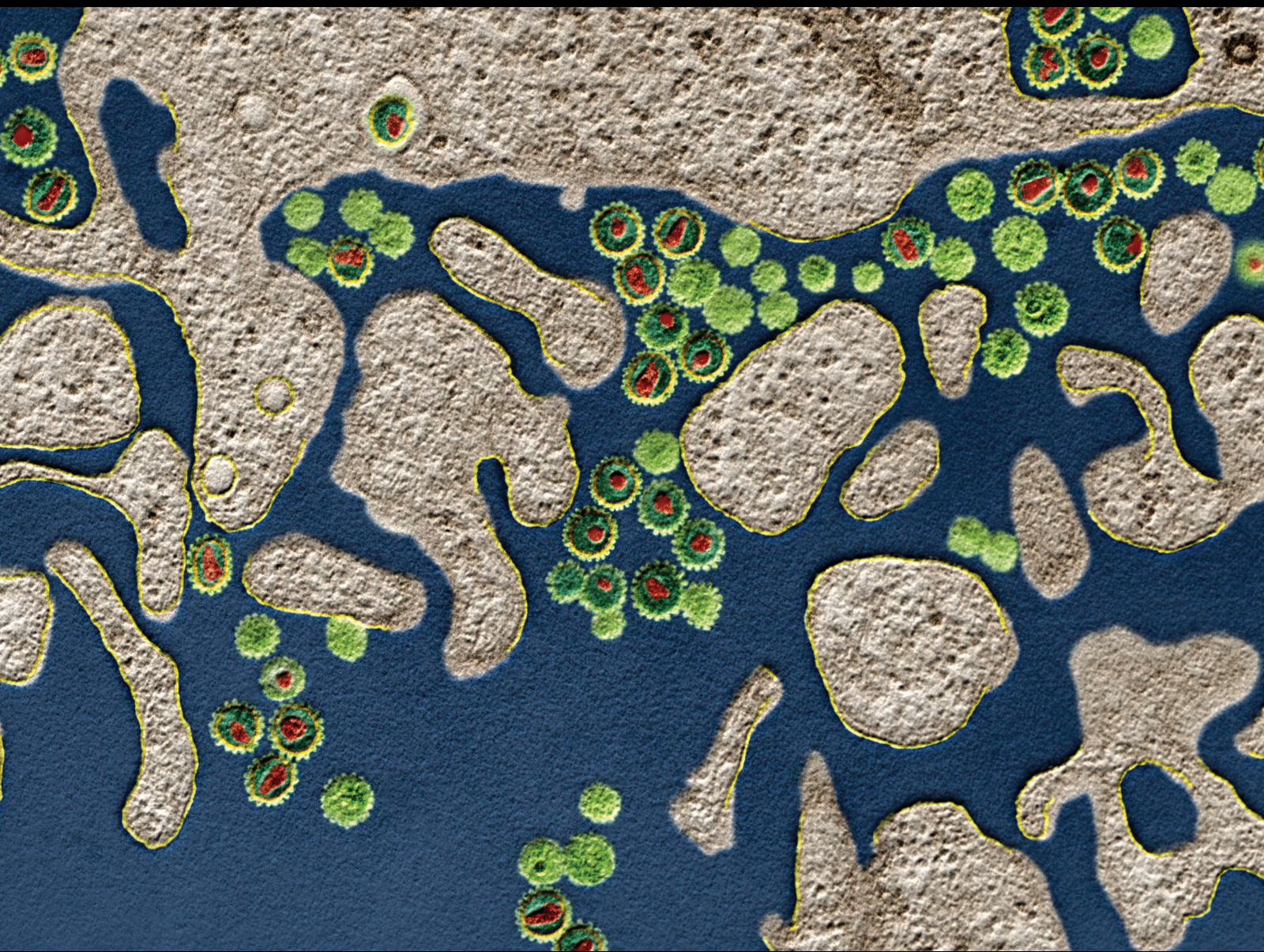

Advances in Immunology of Neglected Tropical Diseases: New Control Tools and Prospects for Disease Elimination

Journal of Immunology Research

Advances in Immunology of Neglected Tropical Diseases: New Control Tools and Prospects for Disease Elimination

Lead Guest Editor: Barbara C. Figueiredo
Guest Editors: Carina S. Pinheiro, Fabio V. Marinho, and Nestor A. Guerrero

Contents

Hindawi
Journal of Immunology Research
Volume 2020, Article ID 9361518, 2 pages
https://doi.org/10.1155/2020/9361518

Editorial

Advances in Immunology of Neglected Tropical Diseases: New Control Tools and Prospects for Disease Elimination

Barbara Castro-Pimentel Figueiredo,[1] **Carina Silva Pinheiro**,[2] **Fabio Vitarelli Marinho**,[3] **and Nestor Adrian Guerrero**[4]

[1]*Departamento de Bioquimica e Biofisica, Universidade Federal da Bahia, Salvador, BA, Brazil*
[2]*Departamento de Biointeracao, Universidade Federal da Bahia, Salvador, BA, Brazil*
[3]*Departamento de Bioquimica e Imunologia, Universidade Federal de Minas Gerais, Belo Horizonte, MG, Brazil*
[4]*Centro de Biologia Molecular Severo Ochoa, Universidad Autonoma de Madrid, Madrid, Spain*

Correspondence should be addressed to Barbara Castro-Pimentel Figueiredo; barbaracpf@ufba.br

Received 3 March 2020; Accepted 3 March 2020; Published 16 March 2020

Neglected tropical diseases (NTD) comprise a group of infectious viral, bacterial, and parasitic diseases with high endemicity in tropical and subtropical regions, disproportionately affecting the developing countries [1]. The WHO currently classifies 20 diseases and conditions as NTDs. The great diversity of parasites comprising NTDs hinders the development of strategies of management and the treatment of these diseases. Besides that, another barrier to overcome is the poverty and the lack of health care, sanitation, and clean water in endemic countries [2]. Due to inefficient diagnosis and also inadequate access to drugs, most of NTD infections are left untreated, which has catastrophic consequences, triggering high rates of disease spread, disability, and even death [3, 4]. It is estimated that more than one billion people worldwide are affected by NTD in 149 undeveloped countries [1]. The research on this field is also challenged by the socioeconomic, cultural, demographic, and political factors, which compromises the interest of many scientists worldwide. Although they are few compared to other fields in health science, NTD researchers have made a lot of advances in disease comprehension and novel tools for prophylaxis, diagnosis, and treatment, including vector control, vaccines, diagnostic tests, and new drugs. Without these new tools, NTD control and elimination will not happen [5, 6].

The control and elimination of NTD involve both the comprehension of immune mechanisms during parasite establishment in the host and the development of better tools to improve detection and minimize transmission. Research in this field is critical to comprehend each organism that causes these diseases and to develop new treatment for them. The immune response to NTD agents was previously investigated over the last decades. The new discoveries in this field enabled NTD researchers to better understand parasite evasion, modulation of host immune responses, and the immunopathology of infections. In this special issue, we present two manuscripts providing new insights on these topics. Quental and colleagues evaluate puerperal colostrum, discover that maternal Zika infection increases colostrum viscosity, and also modify cytokine concentrations. The altered levels of cytokines are possibly what changes colostrum viscosity, which represents a possible mechanism of adaptation of breastfeeding against Zika virus. In another original research, Duan and colleagues find that CCAAT/enhancer-binding homologous protein (CHOP), a transcriptional regulator induced by endoplasmic reticulum stress, plays a critical role in liver pathology associated with *S. japonicum* infection. Their results suggest that this protein promotes the progression of liver fibrosis, through alternative activation of macrophages. Immunological research is also important in the development of clinical tools available to address such diseases: vaccines, diagnostics, and drugs. In this issue, Bernardes and colleagues intend to investigate an antigen of *S. mansoni*

as a target for vaccine development. This manuscript relates a complete analysis concerning humoral and cellular responses investigation and also the worm burden after vaccination and infection in murine model. Regarding the diagnostic based on immunological tools, Takeuchi and colleagues measure serum total and specific anti-*Ascaris* IgE to evaluate wheezing in children. They cluster these kids and investigate the relationship between wheezing and *Ascaris* infection. When it comes to leishmaniasis, Aleka and colleagues monitored visceral leishmaniasis treatment efficacy by measuring the production of cytokines before, during, and at the end of treatment. Their work presents a unique cohort study using a novel methodology to discriminate active from cured leishmaniasis patients.

In summary, this current special issue publishes five original research articles on recent findings about NTD immunology. The few number of papers published in this special edition reflects the major difficulties among NTD research and also the limited interest of the scientific community to this topic. Although the content of this special issue only covers a few topics, it reports the newest discoveries on the field and provides new data that enhance the knowledge in the field and stimulate researchers to keep investigating the NTD in the future. These diseases take many lives yearly and challenge many researches around the world, so the works published here enhance the understanding of NTDs and help experts in this inspiring field.

Conflicts of Interest

The authors declare they have no conflict of interest.

Barbara Castro-Pimentel Figueiredo
Carina Silva Pinheiro
Fabio Vitarelli Marinho
Nestor Adrian Guerrero

References

[1] World Health Organization, "Neglected tropical diseases," 2020, January 2020, https://www.who.int/neglected_diseases/diseases/en/.

[2] P. J. Hotez, S. Aksoy, P. J. Brindley, and S. Kamhawi, "World neglected tropical diseases day," *PLoS Neglected Tropical Diseases*, vol. 14, no. 1, article e0007999, 2020.

[3] D. H. Molyneux, L. Savioli, and D. Engels, "Neglected tropical diseases: progress towards addressing the chronic pandemic," *The Lancet*, vol. 389, no. 10066, pp. 312–325, 2017.

[4] N. I. Nii-Trebi, "Emerging and neglected infectious diseases: insights, advances, and challenges," *BioMed Research International*, vol. 2017, Article ID 5245021, 15 pages, 2017.

[5] P. J. Hotez, B. Pecoul, S. Rijal et al., "Eliminating the neglected tropical diseases: translational science and new technologies," *PLoS Neglected Tropical Diseases*, vol. 10, no. 3, article e0003895, 2016.

[6] G. Ortu and O. Williams, "Neglected tropical diseases: exploring long term practical approaches to achieve sustainable disease elimination and beyond," *Infectious Diseases of Poverty*, vol. 6, no. 1, article 147, 2017.

Hindawi
Journal of Immunology Research
Volume 2020, Article ID 8385672, 12 pages
https://doi.org/10.1155/2020/8385672

Research Article

Whole Blood Stimulation Assay as a Treatment Outcome Monitoring Tool for VL Patients in Ethiopia: A Pilot Evaluation

Yetemwork Aleka,[1] Ana Victoria Ibarra-Meneses,[2] Meseret Workineh,[1] Fitsumbrhan Tajebe,[1] Amare Kiflie,[1] Mekibib Kassa Tessema,[3] Roma Melkamu,[3] Azeb Tadesse,[3] Javier Moreno,[2] Johan van Griensven,[4] Eugenia Carrillo,[2] and Wim Adriaensen[4]

[1]*Department of Immunology and Molecular Biology, University of Gondar, Gondar, Ethiopia*
[2]*WHO Collaborating Centre for Leishmaniasis, National Centre for Microbiology, Instituto de Salud Carlos III, Majadahonda, Madrid, Spain*
[3]*Leishmaniasis Research and Treatment Centre, University of Gondar, Gondar, Ethiopia*
[4]*Unit of Neglected Tropical Diseases, Department of Clinical Sciences, Institute of Tropical Medicine, Antwerp, Belgium*

Correspondence should be addressed to Eugenia Carrillo; ecarrillo@isciii.es

Yetemwork Aleka and Ana Victoria Ibarra-Meneses contributed equally to this work.

Received 9 September 2019; Accepted 4 December 2019; Published 23 January 2020

Guest Editor: Nestor A. Guerrero

Visceral leishmaniasis (VL) is a lethal disease if left untreated. Current treatments produce variable rates of treatment failure and toxicity without sterile cure, rendering treatment efficacy monitoring essential. To avoid repeated invasive tissue aspirates as well as empirical treatment, there is a need for new tools that allow a less-invasive and early assessment of treatment efficacy in the field. Cross-sectional studies have suggested levels of cytokines/chemokines after whole blood stimulation as good markers of cure, but longitudinal studies are lacking. In this study, we followed 13 active VL cases in an endemic area in Ethiopia by measuring the production of IFN-γ, TNF-α, IP-10, IL-2, IL-10, MCP-1, and MIG before, during, and at the end of treatment. After 24 hours of stimulation of whole blood with soluble *Leishmania* antigen, we observed an early, robust, and incremental increase of IFN-γ, TNF-α, and IP-10 levels in all patients during treatment. Moreover, based on the IFN-γ levels that showed an average 13-fold increase from the time of diagnosis until the end of treatment, we could almost perfectly discriminate active from cured status. Similar concentrations and patterns were found in stimulation assays with the two main *Leishmania* species. The levels of IFN-γ, IP-10, or TNF-α also seemed to be inversely associated with the parasite load at baseline. Despite a 1/10 drop in concentrations, similar patterns were observed in IFN-γ and IP-10 levels when dried plasma spots were stored at 4°C for an average of 225 days. All the above evidence suggests a detectable restoration of cell-mediated immunity in VL and its association with parasite clearance. With a potential application in rural settings by means of dried plasma spots, we recommend to further explore the early diagnostic value of such assays for treatment efficacy monitoring in large cohort studies including treatment failure cases.

1. Introduction

Visceral leishmaniasis (VL) is a neglected vector-borne protozoan disease, prevalent in the tropics, subtropics, and Mediterranean basin. It is responsible for an estimated 50,000-90,000 annual cases globally and lethal if left untreated [1, 2]. Over 90% of the cases are concentrated in Bangladesh, India, Brazil, Sudan, South Sudan, and Ethiopia [2]. It is characterized by persistent low-grade fever, weight loss, anemia, pancytopenia, hepatosplenomegaly, edema, muscle wasting, diarrhea, and hypergammaglobulinemia. Through time, it may cause bleeding due

to thrombocytopenia which may progress to sepsis and severe cachexia [3, 4]. The limited range of drugs currently used for treatment includes pentavalent antimonials, pentamidine, amphotericin B deoxycholate and its lipid formulations, miltefosine, and paromomycin. However, they all produce considerable but variable rates of treatment failure (10-59%) and sterile cure is almost never achieved [5–10]. Due to the latter, the World Health Organization (WHO) defines "true cure" as a patient with no relapse episode in 3-6 months after treatment stop. In addition, the treatments are lengthy, have a high toxicity with regular side effects, and are often expensive [11]. Taken together, the need to monitor drug efficacy is paramount.

Considering the lack of comparable alternatives, WHO recommends a splenic, bone marrow or lymph node aspirate as a test for diagnosis but also as a test of cure [12]. Nevertheless, patients are often discharged purely following improvement of clinical signs in more rural settings, due to the need of an experienced health worker to perform the procedure or bleeding risk. To avoid repeated invasive tissue aspirates as well as empirical treatment, there is a need for quick, easy-to-use, and sensitive tools that allow a less-invasive assessment of treatment efficacy. Such tools could aid clinicians in making decisions about the continuation or change of treatment regimens. Moreover, markers able to identify the initiation of a successful treatment might help to shorten the treatment duration.

Serological techniques cannot be used for this purpose as antibodies remain high for several years. Molecular techniques seem promising, but could be less suitable as the parasitic load mostly decreases steeply after two days of treatment and gives no information on the host's immunological recovery [13–15]. Following the latter, one of the key immunological characteristics of active disease is a profound immunosuppression and impaired production of interferon-γ (IFN-γ) and associated cytokines. Activation of infected macrophages by IFN-γ triggers the production of nitric *oxide synthases*/reactive oxygen species (NOS/ROS) that facilitates parasite killing, indicating the importance of cellular sources of IFN-γ [16, 17]. The host's *Leishmania*-specific cell-mediated immunity is thus a key determinant in resistance and clearance of a *Leishmania* infection and could serve as a proxy measurement of the host's capacity to maintain future recrudescence or to resist reinfections of *Leishmania* as it is known to last for several years [18]. Therefore, techniques such as the whole blood stimulation assay (WBA) which measures the *in vitro* cell-mediated immune response after stimulation with soluble *Leishmania* antigens have been proposed to monitor disease recovery [19, 20]. Recent findings in cross-sectional studies of Ethiopia, Spain, and Bangladesh further enforced the idea that gradual increases in IFN-γ or in IFN-γ-induced protein 10 (IP-10 or CXCL10), monokine induced by IFN-γ (MIG or CXCL9), tumor necrosis factor-alpha (TNF-α), and monocyte chemoattractant protein 1 (MCP-1 or CCL2) levels in soluble *Leishmania* antigen- (SLA-) stimulated whole blood could indicate that treatment has been successful and could be targeted as biomarkers of clinical cure in VL [20–23]. The search for a robust marker is still ongoing, as different cytokines and chemokines have been proposed, but vary by geographical area, *Leishmania* strain, and outcome identification (asymptomatic, active, cured). To date, this assay has never been evaluated longitudinally to monitor individual *L. donovani*-infected patients during the course of treatment. And only one cross-sectional study reported on its value in the East African *L. donovani* setting, which was restricted to the IFN-γ and interleukin- (IL-) 10 analytes. In remote regions, a simpler storage and transportation method would be highly needed. Protein Saver 903 cards have shown potential as an alternative method for transporting SLA-stimulated plasma samples, even at ambient temperature, for the later analysis of IL-2, IFN-γ, IP-10, MIG, and MCP-1 concentrations [24].

The main aim of this pilot study was to further validate the usefulness of this assay as a treatment efficacy monitoring tool in Ethiopian VL patients by means of a first-in-its-kind longitudinal evaluation of individual patients during the course of treatment. To further fine-tune the development and implementation of a WBA in research and clinical activities among VL patients in East Africa, we also assessed strain specificity, a more field-adapted method, and demonstrated the value of seven previously proposed cytokine/chemokine markers.

2. Materials and Methods

2.1. Study Design. An institutional-based cohort study was conducted from March to September 2018 in which a total of 21 VL patients were recruited at time of diagnosis (referred to as day zero (D0)). A 2 ml venous blood sample was collected in a lithium-heparin tube at D0, after the first week of the treatment (W1), and at end of treatment (EOT). Sociodemographic data was collected by questionnaire and clinical data was collected from the patient's medical record by using a case report format. One patient died during treatment because he suffered from acute kidney injury and anemia. In addition, three were lost to follow-up during treatment and four had a missing time point. Therefore, a total of 13 VL patients with complete follow-up during treatment was included in the main analyses. A total of 19 VL patients were used for baseline analyses.

The study protocol was reviewed and approved by the research ethics committee of the School of Biomedical and Laboratory Sciences, College of Medicine and Health Sciences, University of Gondar, and the Institutional Review Board of the Institute of Tropical Medicine. All study participants provided informed consent.

2.2. Study Population. Patients were recruited and followed at the Leishmaniasis Research and Treatment Centre (LRTC) at the University of Gondar, Ethiopia. The center is located in the northwestern part of Ethiopia close to the high VL-endemic areas along the border with Sudan. Only microscopically confirmed VL cases (by the spleen or bone marrow aspiration) were included in the study. Patients with a concurrent medical emergency (unconscious and severely ill individuals), documented coinfection (tuberculosis (TB), human immunodeficiency virus (HIV), and helminthic

infection), records of any immune suppressive drugs, or who were younger than 18 or older than 65 years were considered noneligible.

2.3. Operational Definitions. Body mass index (BMI) was defined as the weight in kilograms divided by the square of the height in meters (kg/m^2), and the following criteria were used: underweight (BMI < 18.5 kg/m^2) and normal or healthy weight (BMI within the range of 18.5-25 kg/m^2) [25]. Fever was considered if the body temperature was above 37°C.

Cure from leishmaniasis was defined at clinical discharge based on the absence of clinical signs or if a repeated splenic or bone marrow aspirate was taken, negative microscopy at end of treatment [26]. Following WHO guidelines, seven of the 13 VL patients (54%) confirmed "true cure" status at six months after therapy and six patients were lost to follow-up.

After splenic/bone marrow aspiration, parasites were detected with standard Giemsa staining. The parasite density score was determined using a logarithmic scale ranging from 0 (no parasites per 1000 oil immersion fields), 1+ (1–10 parasites per 1000 fields), 2+ (1–10 parasites per 100 fields), 3+ (1–10 parasites per 10 fields), 4+ (1–10 parasites per field), 5+ (10–100 parasites per field) to +6 (>100 parasites per field) [27].

2.4. Preparation of Soluble Leishmania Antigen (SLA). *L. donovani* and *L. infantum* antigens were prepared from promastigote cultures in the stationary phase (S-698 strain MHOM/ET/67/HU3 and JPC strain MCAN/ES/98/LLM-722, respectively) as previously described [28, 29]. The parasites were first washed with 1X phosphate-buffered saline (PBS) and centrifuged at 1000 g for 20 min at 4°C. The supernatant was discarded, and the pellet resuspended in lysis buffer (50 mM Tris/5 mM EDTA/HCl, pH 7). These samples were subjected to three cycles of freezing/thawing and then sonicated three times (40 W for 20 s) before being centrifuged again at 27,000 g for 20 min at 4°C. The supernatants were collected and centrifuged at 100,000 g for 4 hours at 4°C, to remove the membrane antigens. Finally, the supernatants were divided into aliquots and stored at -80°C until use. The protein content was quantified following the bicinchoninic acid method (BCA), using the Pierce BCA Protein Assay Kit (Bio-Rad, USA).

2.5. Whole Blood Stimulation Assay (WBA). Whole blood samples were stimulated as previously described [20]. Briefly, for each sample, an aliquot of 500 μl blood was transferred in a control tube (unstimulated), two tubes containing 10 μg/ml SLA from *L. donovani* and 10 μg/ml SLA from *L. infantum*, and a positive control tube with phytohemagglutinin (PHA). The latter and SLA of both species were lyophilized for utility and preservation in the field. Next, all of tubes were incubated at 37°C for 24 h. After incubation time, the supernatants were collected and stored at -80°C until cytokine/-chemokine determination.

2.6. Storage of Stimulated Plasma Samples in Filter Paper. In parallel with freezing down stimulated plasma, 40 μl was dropped onto two premarked 1.2 cm diameter circles on separate Protein Saver 903 cards (Whatman, Maidstone, UK) and dried for 3–4 h at ambient temperature (AT) in a horizontal position on the bench to produce dried plasma spots (DPS). The cards were then placed in zip-lock plastic bags (Whatman, Maidstone, UK) containing a desiccant and maintained at 4°C up to 8 months.

After this period, a biopsy punch (Integra Miltex, NY, USA) was used to cut out two discs from the cards of each patient. The discs were placed in the 96-well plate and 70 μl of the elution buffer (2% BSA, 0.1% Tween-20 in PBS 1X) was added. The plate was incubated at ambient temperature for 1 hour in a shaker to elute all cytokines and chemokines of plasma deposited on filter paper.

2.7. Cytometric Bead Array (CBA) Assay. Levels of IFN-γ, TNF-α, IP-10, IL-2, IL-10, MIG, and MCP-1 were quantified in frozen plasma and DPS-elucidated sample from control and SLA-stimulated and PHA-stimulated whole blood using the BD Cytometric Bead Array Human Flex Set (Becton Dickinson Biosciences, USA) following the manufacturer's instructions. Briefly, 50 μl of the plasma of each patient was incubated for 1 h at ambient temperature with 50 μl of capture beads. After incubation, 50 μl of the detection antibody was added and the mixture was placed 2 hours at ambient temperature. Data were acquired using a FACSCalibur flow cytometer and analysed using the Flow Cytometric Analysis Program Array (BD Biosciences, USA) by manual clustering. Cytokines and chemokine concentrations (expressed in pg/ml) produced in response to SLA or PHA stimulation were determined by subtracting background levels measured in the negative control samples (nonstimulated tube).

2.8. Data Analysis. Data analysis was performed with GraphPad Prism v6.0 software (GraphPad Software, USA). Continuous data was presented as the median with interquartile ranges (IQR) and the normality of data was checked by the Shapiro-Wilk test. The concentrations of analytes before and after treatment were compared using the nonparametric Wilcoxon signed-rank test. The cut-off values for each cytokine and chemokine shown in Figures 1 and 2 were determined by calculating the optimal point in the receiver operating characteristic (ROC) curves for discriminating active disease from cured status. Spearman correlation coefficients were calculated between baseline parasite load and cytokine/chemokine concentrations or *L. infantum*- and *L. donovani*-stimulated cytokine levels. A p value $\leq$ 0.05 was considered as statistically significant.

3. Results

3.1. Sociodemographic and Clinical Characteristics of VL Patients. A total of 13 confirmed primary VL cases were included. All the patients were male with a median age of 22 years and only five (38.4%) were literate. Almost all (92.31%) were migrant workers, functioning as farmers or daily labourers (see Table 1). Related to their clinical condition, the median body mass index (BMI) was 16.4 kg/m^2, classifying 12 (92.3%) patients as being underweight. Other pathologies were diagnosed in three (23.1%) patients, such as pneumonia ($n = 1$), malaria ($n = 1$), and giardia ($n = 1$).

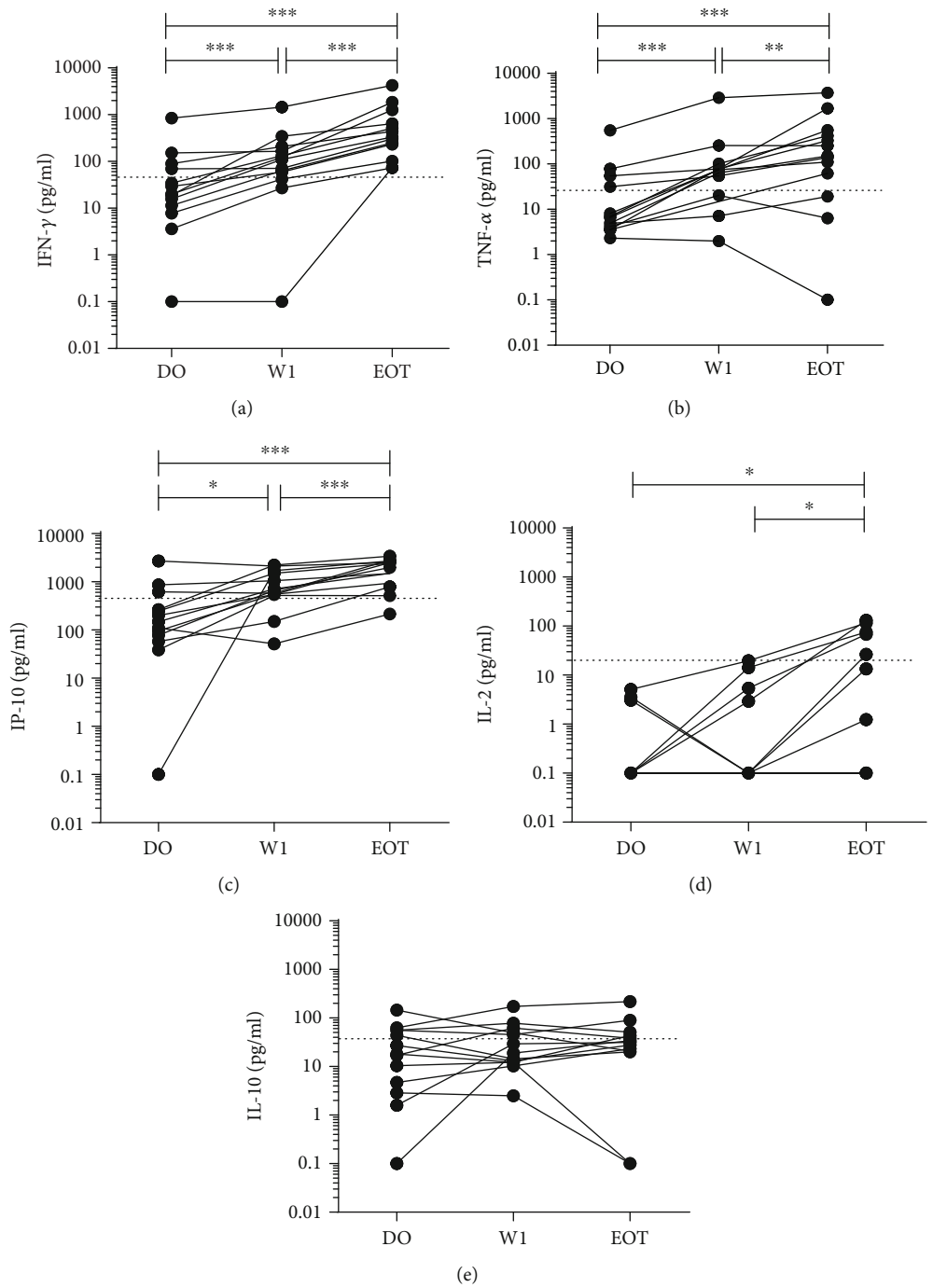

Figure 1: IFN-γ (a), TNF-α (b), IP-10 (c), IL-2 (d), and IL-10 (e) levels in soluble *L. donovani* antigen-stimulated plasma of 13 VL patients at active disease (D0), after one week of treatment (W1), and at the end of treatment (EOT). Each line curve represents an individual during follow-up. Comparison of medians was made using the Wilcoxon paired *t*-test. $^{*}p < 0.05$; $^{**}p < 0.01$; $^{***}p < 0.001$. Dotted line represents the best cut-off for each cytokine/chemokine based on ROC analyses to discriminate active from cured status.

Regarding the treatment of leishmaniasis, 10 (76.9%) of them were treated with a combination treatment of paromomycin (PM) and sodium stibogluconate (SSG) while three patients (38.5%) were treated with AmBisome monotherapy. All patients were successfully treated and discharged.

3.2. IFN-γ, TNF-α, and IP-10 in SLA-Stimulated Plasma as Potential Biomarkers for Treatment Efficacy Monitoring in VL Patients. The cytokine/chemokine concentrations were measured in the soluble *L. donovani* antigen-stimulated plasma of VL patients at time of diagnosis (D0), during treatment (W1), and at the end of treatment (EOT) (Figure 1). The levels of IFN-γ, TNF-α, and IP-10 increased significantly after one week of treatment (median (IQR ; p value) = 110.70 pg/ml (50.81-187.30; <0.01); 74.63 pg/ml (28.72-

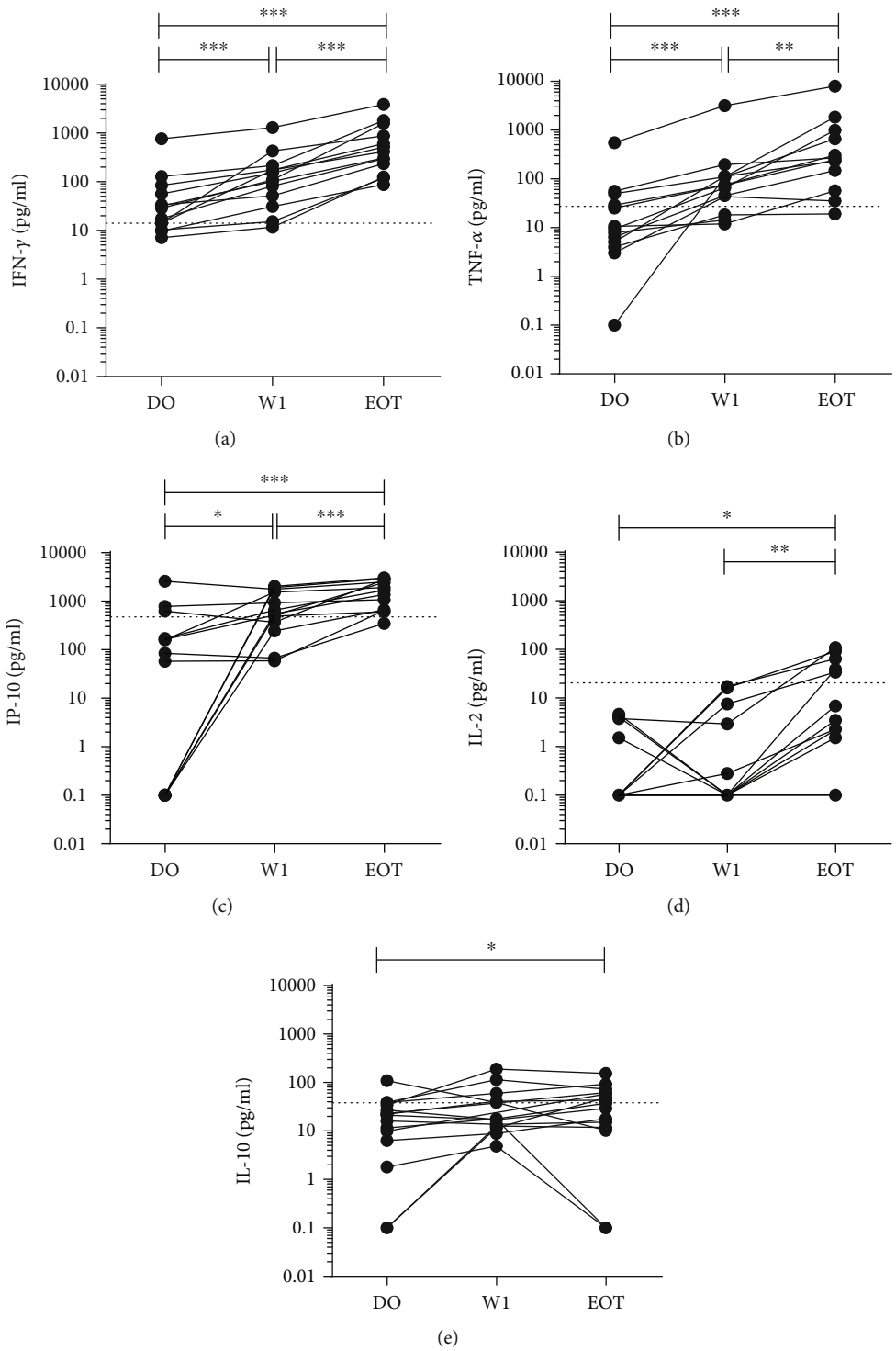

Figure 2: IFN-γ (a), TNF-α (b), IP-10 (c), IL-2 (d), and IL-10 (e) levels in soluble *L. infantum* antigen-stimulated plasma of 13 VL patients at the active moment (D0), during one week of treatment (W1), and the end of treatment (EOT). Each line curve represents an individual during follow-up. Comparison of medians was made using the Wilcoxon paired *t*-test. $^{*}p < 0.05$; $^{**}p < 0.01$; $^{***}p < 0.001$. Dotted lines represent the best cut-off for each cytokine/chemokine based on ROC analyses to discriminate the active from cured status.

95.61; <0.01); and 667.90 pg/ml (533.80-1601; 0.01), respectively) compared to a baseline levels (D0) (median (IQR) = 19.96 pg/ml (9.62–79.85); 6.56 pg/ml (3.86–43.25); and 149.40 pg/ml (68.01-440.90), respectively). The levels of these cytokines/chemokines also presented a significant increase at the end of treatment with a dose-response like relationship (median (IQR; p value) = IFN-γ: 331.7 pg/ml (167.80-950.80; <0.01); TNF-α: 150.60 pg/ml (40.68-489.30; <0.01); and IP-10: 1979 pg/ml (863.30-2603; <0.01)) (Figures 1(a)–1(c)). The concentration of IL-2 was not significantly

Table 1: Sociodemographic and clinical characteristics of study participants in Gondar, Ethiopia.

Variables		VL patients ($n = 13$)
Demographic characteristics		
Male gender, *n* (%)		13 (100)
Age (years), median (min–max)		22 (17-27)
Occupation, *n* (%)		
Farmer		6 (46.1)
Daily labourer		7 (53.9)
Literacy, *n* (%)		5 (38.4)
Marital status, *n* (%)		
Single		12 (92.3)
Married		1 (7.7)
Migrant worker, *n* (%)		12 (92.3)
Clinical characteristics		
BMI, median (kg/m^2) (min–max)		16.4 (13.6-18.4)
Fever, *n* (%)		9 (69.2)
Conjunctival pallor, *n* (%)		12 (92.3)
Edema, *n* (%)		6 (46.2)
Other pathology, *n* (%)		3 (23.1)
Palpable spleen size (cm), mean ± SD		9.1 ± 4.8
Parasite load (parasites/field), median (min–max)		3 (1-6)
Type of treatment, *n* (%)	PM+SSG	10 (76.9)
	AmBisome	3 (38.5)
Treatment duration (days), median (min–max)	PM+SSG	17 (15-20)
	AmBisome	19 (14-22)

min: minimum; max: maximum; *n*: total number; SD: standard deviation; PM: paromomycin; SSG: sodium stibogluconate.

increased at W1 (median (IQR ; p value) = 0.1 pg/ml (0.10-4.16; <0.5)), but significantly increased at EOT (median (IQR; p value) = 1.24 pg/ml (0.10-71.57; <0.05)), compared to D0 (0.1 pg/ml) (Figure 1(d)). IL-10 did not show significant differences between the different time points (Figure 1(e)). MCP-1 and MIG concentrations were lacking a defined pattern across the different time points of the study (data not shown).

To assess the specificity against the *L. donovani* strain used in the assay, we performed a simultaneous stimulation with the soluble *L. infantum* antigen. We found that the stimulation with SLA from *L. infantum* showed the same pattern of cytokine and chemokine production than stimulation with SLA from *L. donovani* (Figure 2). The results show a significant increase in IFN-γ, TNF-α, and IP-10 after one week of treatment (W1, median (IQR ; p value) = 108.9 pg/ml (41.34-194.50; <0.001); 74.38 pg/ml (30.81-111.70; <0.001); and 552.10 pg/ml (306.00-1659; <0.05)) compared to baseline levels (D0) of IFN-γ, TNF-α, and IP-10 (median (IQR) = 28.64 pg/ml (12.15-70.48); 9.38 pg/ml (4.54-39.40); and 84.81 pg/ml (0.10-399.50), respectively). The levels of these cytokines/chemokines also presented a significant increase at the end of treatment compared to D0 (EOT, median (IQR ; p value) = IFN $-\gamma$: 361.20 pg/ml (108.20-1221; <0.001); TNF-α: 247.50 pg/ml (80.12-908.60; <0.001); and IP-10: 1284 pg/ml (651.00-2646; <0.001)) (Figures 2(a)–2(c)). IL-2, IL-10, MIG, and MCP-1 also showed very similar patterns as previously described using the *L. donovani* antigen (Figures 2(d)–2(e)). Moreover, excellent correlation scores were observed for IFN-γ ($r = 0.97$; $p < 0.001$), TNF-α ($r = 0.95$; $p < 0.001$), and IP-10 ($r = 0.97$; $p < 0.001$) levels with *L. infantum* and *L. donovani* antigen stimulation. We also observed good correlations for IL-2 ($r = 0.78$; $p < 0.001$), IL-10 ($r = 0.84$; $p < 0.001$), MIG ($r = 0.86$; $p < 0.001$), and MCP-1 ($r = 0.74$; $p < 0.001$) levels with *L. infantum* and *L. donovani* antigen stimulation.

Comparative results were also obtained in response to the general T cell mitogen PHA, which showed a low production of cytokines and chemokines before treatment that increased during treatment (see in Table S1 in Supplementary Material). This indicated a good cell viability and immunocompetence after cell activation for all samples, but also confirmed the overall hyporesponsiveness observed during active VL disease and its restoration upon successful treatment.

3.3. IFN-γ Showed the Highest Fold Increase after SLA Stimulation Plasma at the End of Treatment. The fold change in each cytokine/chemokine concentration after one week of treatment (W1) and at the end of the treatment (EOT), in relation to their concentration at the time of active disease (D0), is shown in Figure 3. The concentration of IFN-γ ($p < 0.001$) in the SLA-stimulated plasma increased 3.8 times after one week of treatment, while TNF-α ($p = 0.001$) and IP-10 ($p = 0.013$) increased around fivefold (Figure 3). At the end of the treatment, the concentrations of IFN-γ ($p < 0.001$), TNF-α ($p < 0.001$), and IP-10 ($p < 0.001$) increased significantly by 13.1, 10.8, and 9.9 times, respectively. IL-2 levels were also increased 1.3 times from D0 to EOT in a statistically significant manner ($p = 0.023$). In addition, we found very similar fold changes using the soluble *L. infantum* antigen as specific stimulation (see Figure S1 in Supplementary Material).

Without exception, all 13 patients experienced a steep and incremental increase during treatment in IFN-γ and TNF-α levels towards successful disease recovery, arguing to investigate its prognostic value in larger cohorts including treatment failures as a potential pretest-posttest.

3.4. IFN-γ Levels Showed Highest Discriminatory Power to Determine a Cured Status in VL Patients at End of Treatment. To investigate the possibility of a general, single-time point-based test instead of a pre-post treatment evaluation, we calculated the optimal cut-off values to determine a cured (EOT) status by means of ROC analyses. For IFN-γ, TNF-α, IP-10, IL-2, and IL-10 with *L. donovani* stimulation, the optimal cut-off values were 48.13 pg/ml, 25.35 pg/ml, 452.90 pg/ml, 20.02 pg/ml, and 37.29 pg/ml, respectively (depicted as dotted lines in Figures 1 and 2). Table 2 shows the proportion of patients that produced levels above the respective cut-off values after SLA stimulation. Results showed that active VL patients recovered their ability to mount a specific cellular immune response against

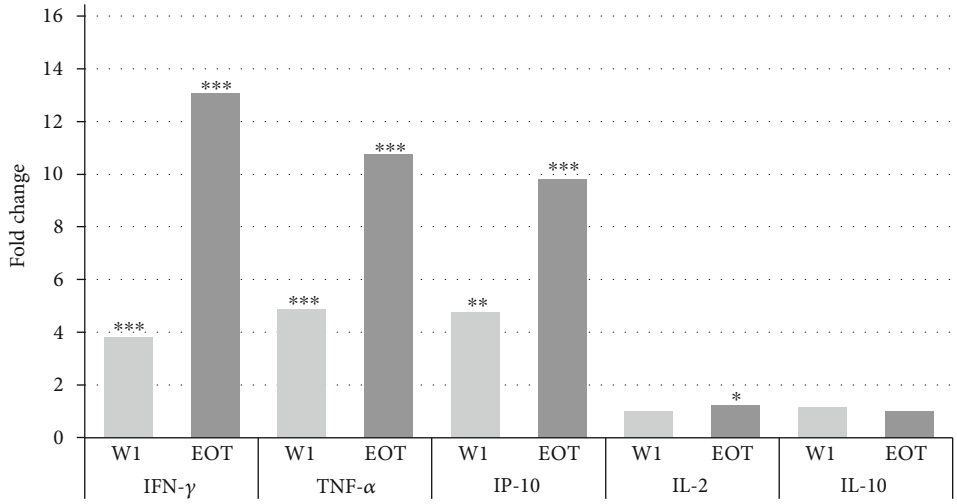

Figure 3: Fold changes in cytokine/chemokine concentrations during treatment of 13 VL patients, measured in soluble *L. donovani* antigen-stimulated plasma. Fold increase during W1 and EOT compared to D0 was calculated by dividing the value of (W1, EOT) by D0 values. p values are represented for comparison with baseline concentration at the time of diagnosis (D0). $^{*}p < 0.05$; $^{**}p < 0.01$; $^{***}p < 0.001$.

Table 2: Proportion of patients that produced levels above the calculated optimal cut-off values after SLA stimulation of a whole blood sample.

Analytes (cut-off value)	*L. donovani*			*L. infantum*		
	D0	W1	EOT	D0	W1	EOT
	N (%)	*N* (%)	*N* (%)	*N* (%)	*N* (%)	*N* (%)
IFN-γ (48.1 pg/ml)	4/13 (31)	10/13 (77)	13/13 (100)	4/13 (31)	10/13 (77)	13/13 (100)
TNF-α (25.4 pg/ml)	4/13 (31)	9/13 (69)	10/13 (77)	4/13 (31)	10/13 (77)	11/13 (85)
IP-10 (452.9 pg/ml)	3/13 (23)	11/13 (85)	12/13 (92)	3/13 (23)	9/13 (69)	12/13 (92)
IL-2 (20.0 pg/ml)	0/13 (0)	0/13 (0)	5/13 (38)	0/13 (0)	0/13 (0)	5/13 (38)
IL-10 (37.3 pg/ml)	5/13 (38)	5/13 (38)	4/13 (31)	3/13 (23)	5/13 (38)	5/13 (38)

D0: active moment, day zero; W1: first week of the treatment; EOT: end of treatment; *N*: number of patients; %: percentage of positives patients that produce cytokines/chemokines.

Leishmania during the treatment period, producing IFN-γ, TNF-α, IP-10, and IL-2 (with the exception of IL-10). IFN-γ, TNF-α, and IP-10 seemed to be the most promising biomarkers after one week of treatment. At end of treatment, a production of IFN-γ and IP-10 above the cut-off was able to identify 100% and 92% of the cured patients, arguing for further research towards a universal cut-off value to define cure. Yet, 3-4 VL patients did produce cytokine levels above the cut-off value at D0 (see Table 2), arguing for further optimization towards a universal cut-off value to define cure. These 4 patients all showed a median increase of 5.0, 1.7, and 7.6 times at EOT for IFN-γ, TNF-α, and IP-10, respectively.

3.5. IFN-γ and IP-10 Are Stable Markers in Filter Paper. After elution of the SLA-stimulated plasma (*L. donovani* or *L. infantum* antigen) from the filter paper (DPS) that was stored at 4 °C for a median of 225 (IQR: 106-266) days and shipped at ambient temperature, we found that IFN-γ and IP-10 were the most stable analytes (Figure 4). It is important to highlight that the levels of TNF-α, IL-2, and IL-10 after elution of filter paper were below the detection limit of the technique, and that MIG and MCP-1 values after elution of the filter paper were also on the low side and, in comparison with frozen plasma, lacking a defined pattern across the different time points of the study. Compared to the frozen plasma method, concentrations were around 1/10 lower, indicating a significant loss of material due to the nature of the preservation method, as previously described [24]. Nevertheless, we could still observe similar patterns and IFN-γ and IP-10 levels significantly increased after one week of treatment with soluble *L. donovani* stimulation (median (IQR ; p value) = 11.22 pg/ml (5.10-20.68; 0.0327) and 57.23 pg/ml (34.47-144.50; 0.1909), respectively) compared to baseline levels (D0). The levels of these cytokines/chemokines also presented a statistically significant increase at the end of treatment compared to D0 (median (IRQ ; p value) = 58.37 pg/ml (42.7-141.9; 0.0002) and 501.4 pg/ml (156.50-855; 0.0002), respectively) (Figure 4(a)).

With *L. infantum* stimulation, we observed similar differences (Figure 4(b)). These findings indicate the stability of the patterns of the IFN-γ and IP-10 in a more field-adapted preservation method and robustness of the findings.

3.6. IP-10, TNF-α, and IFN-γ Concentrations Showed Significant Correlation with the Parasite Load at Baseline. To assess whether produced cytokine/chemokine levels in

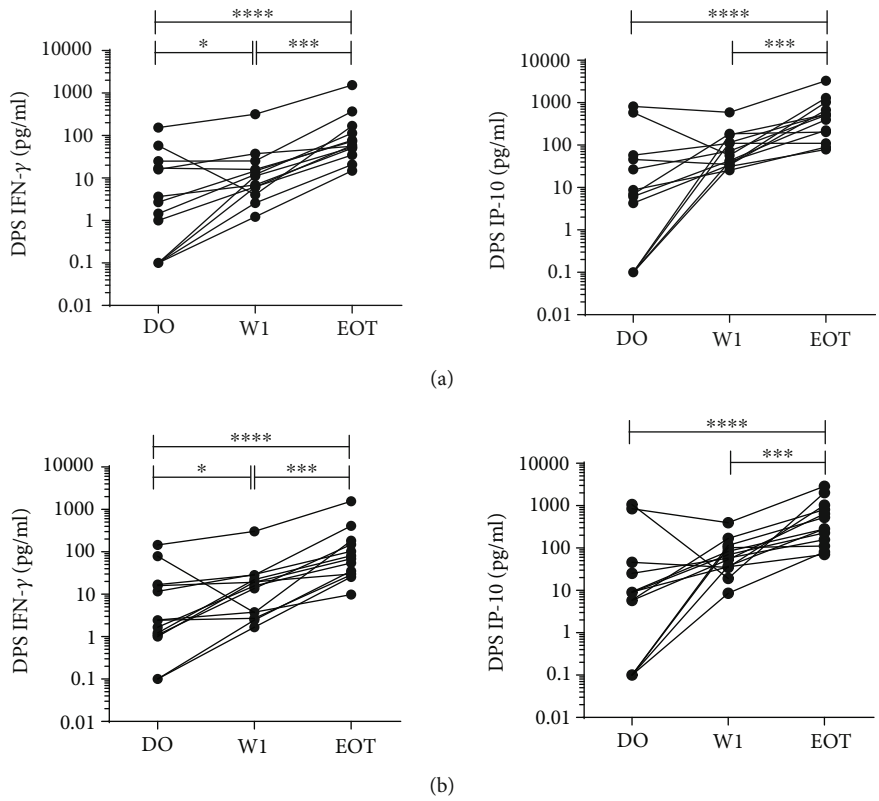

Figure 4: Levels of IFN-γ and IP-10 eluted from dried plasma spots (DPS) stored at 4°C for a median of 255 days in VL patients at D0, W1, and EOT. Blood was stimulated with lyophilized (a) *L. donovani* antigen or (b) *L. infantum* antigen. Each line curve represents one individual. The Wilcoxon test was used to compare paired samples. $^{*}p < 0.05$; $^{***}p < 0.001$; $^{****}p < 0.0001$.

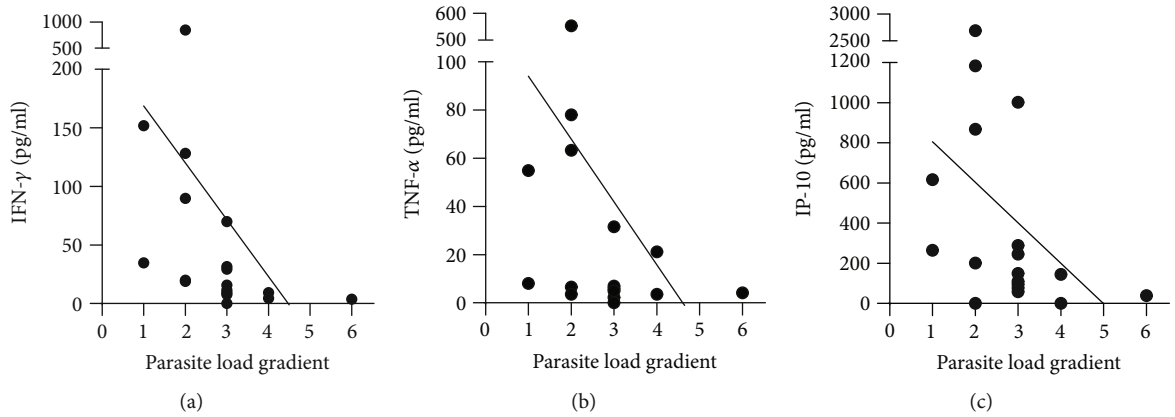

Figure 5: Correlation of baseline parasite load with IFN-γ (a), TNF-α (b), and IP-10 (c) levels after SLA *L. donovani* stimulation at D0. Correlation between analyte concentrations with parasitic load was based on all active VL cases of which baseline data was available ($n = 19$), by means of the nonparametric Spearman test.

stimulated blood are reflecting parasite reduction in the spleen, we studied the correlation between spleen baseline parasite load and SLA-stimulated responses in whole blood.

Of all cytokines tested, an inverse correlation between the baseline concentration of IFN-γ ($r = -0.74$, $p < 0.001$), TNF-α ($r = -0.52$, $p = 0.022$), or IP-10 ($r = -0.56$, $p = 0.012$) and the baseline parasite load could be observed (Figure 5). This inverse relationship suggests that a recovery in cytokine/-chemokine production after SLA stimulation could be used as a proxy for parasite reduction at end of treatment.

4. Discussion

In this small but unique cohort study of primary VL cases, 13 Ethiopian patients with successful treatment all showed a steep and incremental restoration of cellular IFN-γ

production upon *in vitro* stimulation with soluble *Leishmania* antigens during treatment. This reflected a detectable restoration of the profound immunosuppression previously reported in active VL patients [30]. Despite being in contrast with a previous cross-sectional study in India where no statistically significant differences were found after quantification of IFN-γ levels between active and cured VL patients [31], our results consolidated the findings of the sole East African report. The latter reported on an incremental increase in IFN-γ levels in cured individuals living in Northwest Ethiopia as compared to active patients but could not detect differences in IL-10 levels. Similar findings were reported in Turkish, Indian, Iranian, Spanish, and Bangladeshi VL patients [20, 21, 23, 32, 33], indicating a typical cellular hyporesponsiveness during active disease that restores after successful therapy, as was also reported in studies using peripheral blood mononuclear cell (PBMC). This was also reflected in the gradual increase in nonspecific PHA stimulation which suggests a broad mechanism of immunosuppression that merits further investigation. Studies in Spain and Ethiopia demonstrated that a long-lasting memory response remains in cured patients and increased levels of IFN-γ and IFN-γ-inducible protein 10 (IP-10) could be detected in almost all patients at 6 and 12 months after treatment [21, 23]. This is, however, the first time that a longitudinal study in diseased individuals was performed with an early measurement at one week of treatment. It showed an early almost dose-response-like rate of recovery with 9 to 13-fold increases in IFN-γ, IP-10, or TNF-α levels after therapy (EOT).

Due to the sharp 13-fold increase in IFN-γ levels during treatment, it was almost possible to perfectly discriminate between diseased (D0) and cured (EOT) status. Although we did not have splenic parasite counts at end of treatment, the levels of IFN-γ, IP-10, or TNF-α seemed to be inversely associated with the parasite load at baseline and therefore could reflect parasite clearance. This further argues for the development and validation of this assay as an alternative test of cure in larger cohort studies including treatment failure cases to establish its prognostic and diagnostic value in early to late stages of the treatment.

Because IFN-γ is produced in rather low quantities, other IFN-γ-associated cytokines and chemokines have been proposed to show better performance. The production of IP-10 has a role in the host response to VL by initiation of early immune responses and further increasing the production of IFN-γ, which indirectly promotes killing of the intracellular parasite [34]. In our study, plasma concentrations of IP-10 after SLA stimulation were also significantly increased during successful treatment, but not as robustly in all individual patients as IFN-γ or TNF-α. A previous study also showed IP-10 as an accurate global marker of infection and cure [21]. We found similar results for TNF-α levels during treatment. TNF-α has an indirect role for parasite clearance by stimulating the production of IFN-γ. Previously, a significantly elevated production of TNF-α was also observed in VL-cured solid organ transplant subjects and VL-cured individuals from Spain after 6 months of treatment [20, 35].

Even though Th1 cell-mediated immunity for parasite control is associated with production of IL-2 by activated T cells [16], it was produced at much lower concentration and there was no significant production of IL-2 during treatment but only at the end of treatment. In previous studies, its concentration was also below detection limit during active infection while cured individuals were able to produce a significant concentration of this cytokine [20, 21]. This suggests that production of IL-2 is rather a late signature of cure.

High levels of the anti-inflammatory cytokine IL-10 have been associated with the depressed cell-mediated immunity (CMI) during active VL, and PBMC-based assays have showed elevated production of this cytokine during active infections that decreased over time [20, 36]. Nevertheless, we observed no changes in IL-10 levels during treatment which was also reported by Adem et al. in a very similar patient population [23]. These challenge the common dogma in PBMC assays or point towards other sources of IL-10. In a similar manner, our findings showed no specific pattern for MIG levels during treatment with SLA or PHA stimulation, although a previous study in Spain reported MIG to be a good biomarker of cure in *L. infantum*-infected individuals [21].

A similar whole blood interferon-γ release assay is being used in tuberculosis patients to identify specific immunity during latent infection (commercialized as QuantiFERON®) [37]. The *Leishmania*-specific whole blood stimulation assay has also been evaluated in different endemic areas of *Leishmania* spp. for the detection of subjects with asymptomatic infection [36, 38, 39]. However, specificity problems of the soluble *Leishmania* antigens used, in particular cross-reactivity with similar pathogens like *Trypanosoma cruzi* and *Toxoplasma gondii*, could be problematic when targeting a diagnostic or predictive tool in coendemic countries, which may be of lesser concern for its development as a test-of-cure. Field applicability is also important when testing for asymptomatic infection in the rural settings of endemic areas. We found comparable patterns in cytokine/chemokine expressions of frozen plasma and dried plasma spots that were stored at 4°C for up to 8 months and shipped at ambient temperature. Similar results were also obtained on negative control subjects and asymptomatic individuals from Spain and Bangladesh, where the samples stored for 10 days at ambient temperature or -20°C [24]. This indicates that an adapted version of the WBA with dry stimulated plasma spots instead of frozen supernatants could be developed for the rural less-equipped health centers, thereby avoiding a cold-chain transport and decreasing the cost of transport to reference centers. Despite a loss in quantity, the ratio between D0 and EOT remained identical by which a pretest-posttest would be advised. In addition, no significant differences in cytokine/chemokine expressions between SLA from *L. infantum* and SLA from *L. donovani* stimulation were observed. Similar results were reported in studies determining the CMI at endemic areas for *L. infantum* and *L. donovani* [21]. This suggests that many immunodominant antigens are shared across the species and a global assay could be developed [40].

Despite a number of inherent and important limitations such as the lack of treatment failure cases, low number of

individuals, and lack of long-term follow-up after treatment stop, we believe these findings can spur and steer larger cohort studies to evaluate its diagnostic and prognostic value as a treatment monitoring tool.

5. Conclusion

This pilot study indicated a detectable restoration of cell-mediated immunity against VL that could be used to follow up treatment efficacy and enable better patient management. This longitudinal pilot study showed that IFN-γ had a steady and on average 13-fold increase from time of diagnosis until end of treatment in successfully treated VL patients and would be the recommended analyte out of a panel of 7 previously proposed markers to be prioritized. We hope the recommendations in this work on the use of WBA in combination with filter paper will facilitate treatment monitoring studies of more VL patients in the search for an alternative less-invasive test-of-cure. In particular, an early marker of treatment efficacy would be highly warranted to limit the duration or steer the chemotherapeutic choice of treatment.

Data Availability

The data used to support the findings of this study are restricted by the research ethics committee of the School of Biomedical and Laboratory Sciences, College of Medicine and Health Sciences, University of Gondar, and the Institutional Review Board of the Institute of Tropical Medicine in order to protect patient privacy. Data are available from Wim Adriaensen for researchers who meet the criteria for access to confidential data.

Conflicts of Interest

The authors declare that there is no conflict of interest regarding the publication of this paper.

Authors' Contributions

Yetemwork Aleka and Ana Victoria Ibarra-Meneses contributed equally to this work. WA and EC equally contributed in the project design, coordination, administration, and funding acquisition. MW, AK, and FT supervised the sample processing and day-to-day work. MK, RM, and AT recruited the patients and collected the samples. YA and AVIM equally contributed in the data curation and formal analyses of the data. YA, AVIM, EC, and WA interpreted the data. YA, AVIM, EC, and WA drafted and edited the manuscript. JM, JG, MW, AK, and FT reviewed and edited the manuscript. YA, AVIM, MW, FT, MK, RM, AT, JM, JG, EC, and WA approved the final version of the manuscript.

Acknowledgments

We would like to say our words of gratitude to study participants, for their willingness to be a part of this study. We also want to acknowledge the University of Gondar, Department of Immunology and Molecular Biology, for allowing and supporting us to conduct this study. In particular, we would like to thank the Belgian Directorate-General for Development Cooperation (DGDC) for the financial support and the involved staff at the Institute of Tropical Medicine (ITM) and the Leishmaniasis Research and Treatment Center and the National Center for Microbiology (CNM-ISCIII) for their scientific support. Funding was provided by the Belgian Directorate-General for Development Cooperation under the ITM-DGDC framework agreement FA-IIII. WA is personally supported by a Research Foundation Flanders postdoctoral fellowship. In addition, this work was funded by the Instituto de Salud Carlos III via the project PI18CIII/00029 and via the Red de Enfermedades Tropicales, Subprograma RETICS del Plan Estatal de I+D+I 2013-2016, which is cofunded by FEDER "Una manera de hacer Europa" funds, via projects RD16/0027/0017 and RD16CIII/0003/0002.

Supplementary Materials

Supplementary Table 1 showed the levels of cytokines and chemokines produced after PHA stimulation whole blood from VL patients in the active moment, during the treatment and the end of treatment. In the Supplementary Figure 1, we showed the fold change in each cytokine/chemokine concentration after one week of treatment (W1) and at the end of the treatment (EOT), in relation to their concentration at the time of active disease (D0) after SLA stimulation from *L. infantum*. *(Supplementary Materials)*

References

[1] WHO, "Leishmaniasis in high-burden countries: an epidemiological update based on data reported in 2014," *Weekly Epidemiological Record*, vol. 91, no. 22, pp. 287–296, 2016.

[2] J. Alvar, I. D. Velez, C. Bern et al., "Leishmaniasis worldwide and global estimates of its incidence," *PLoS One*, vol. 7, no. 5, article e35671, 2012.

[3] H. W. Murray, "Treatment of visceral leishmaniasis (kala-azar): a decade of progress and future approaches," *International Journal of Infectious Diseases*, vol. 4, no. 3, pp. 158–177, 2000.

[4] D. Sacks and S. Kamhawi, "Molecular aspects of parasite-vector and vector-host interactions in leishmaniasis," *Annual Review of Microbiology*, vol. 55, pp. 453–483, 2001.

[5] A. K. Haldar, P. Sen, and S. Roy, "Use of antimony in the treatment of leishmaniasis: current status and future directions," *Molecular Biology International*, vol. 2011, Article ID 571242, 23 pages, 2011.

[6] T. A. Patel and D. N. Lockwood, "Pentamidine as secondary prophylaxis for visceral leishmaniasis in the immunocompromised host: report of four cases," *Tropical Medicine & International Health*, vol. 14, no. 9, pp. 1064–1070, 2009.

[7] S. Sundar and J. Chakravarty, "Liposomal amphotericin B and leishmaniasis: dose and response," *Journal of Global Infectious Diseases*, vol. 2, no. 2, pp. 159–166, 2010.

[8] S. Sundar and P. L. Olliaro, "Miltefosine in the treatment of leishmaniasis: clinical evidence for informed clinical risk management," *Therapeutics and Clinical Risk Management*, vol. 3, no. 5, pp. 733–740, 2007.

[9] A. M. Musa, B. Younis, A. Fadlalla et al., "Paromomycin for the treatment of visceral leishmaniasis in Sudan: a randomized, open-label, dose-finding study," *PLoS Neglected Tropical Diseases*, vol. 4, no. 10, article e855, 2010.

[10] A. Ponte-Sucre, F. Gamarro, J. C. Dujardin et al., "Drug resistance and treatment failure in leishmaniasis: a 21st century challenge," *PLoS Neglected Tropical Diseases*, vol. 11, no. 12, article e0006052, 2017.

[11] E. M. Moore and D. N. Lockwood, "Treatment of visceral leishmaniasis," *Journal of Global Infectious Diseases*, vol. 2, no. 2, pp. 151–158, 2010.

[12] L. Gradoni, R. López-Vélez, and M. Mokni, *Manual on case management and surveillance of the leishmaniases in the WHO European Region*, World Health Organization Regional Office for Europe, Copenhagen, 2017, http://www.euro.who.int/en/publications/abstracts/manual-on-case-management-and-surveillance-of-the-leishmaniases-in-the-who-european-region-2017.

[13] B. Pourabbas, A. Ghadimi Moghadam, G. Pouladfar, Z. Rezaee, and A. Alborzi, "Quantification of *Leishmania infantum* kinetoplast DNA for monitoring the response to meglumine antimoniate therapy in visceral leishmaniasis," *The American Journal of Tropical Medicine and Hygiene*, vol. 88, no. 5, pp. 868–871, 2013.

[14] C. Mary, F. Faraut, L. Lascombe, and H. Dumon, "Quantification of *Leishmania infantum* DNA by a real-time PCR assay with high sensitivity," *Journal of Clinical Microbiology*, vol. 42, no. 11, pp. 5249–5255, 2004.

[15] C. Mary, F. Faraut, M. P. Drogoul et al., "Reference values for *Leishmania infantum* parasitemia in different clinical presentations: quantitative polymerase chain reaction for therapeutic monitoring and patient follow-up," *The American Journal of Tropical Medicine and Hygiene*, vol. 75, no. 5, pp. 858–863, 2006.

[16] P. M. Kaye and T. Aebischer, "Visceral leishmaniasis: immunology and prospects for a vaccine," *Clinical Microbiology and Infection*, vol. 17, no. 10, pp. 1462–1470, 2011.

[17] V. Rodrigues, A. Cordeiro-da-Silva, M. Laforge, R. Silvestre, and J. Estaquier, "Regulation of immunity during visceral *Leishmania* infection," *Parasites & Vectors*, vol. 9, no. 1, p. 118, 2016.

[18] K. Gidwani, A. Picado, B. Ostyn et al., "Persistence of *Leishmania donovani* antibodies in past visceral leishmaniasis cases in India," *Clinical and Vaccine Immunology*, vol. 18, no. 2, pp. 346–348, 2011.

[19] O. P. Singh, K. Gidwani, R. Kumar et al., "Reassessment of immune correlates in human visceral leishmaniasis as defined by cytokine release in whole blood," *Clinical and Vaccine Immunology*, vol. 19, no. 6, pp. 961–966, 2012.

[20] A. V. Ibarra-Meneses, E. Carrillo, C. Sanchez et al., "Interleukin-2 as a marker for detecting asymptomatic individuals in areas where *Leishmania infantum* is endemic," *Clinical Microbiology and Infection*, vol. 22, no. 8, pp. 739.e1–739.e4, 2016.

[21] A. V. Ibarra-Meneses, P. Ghosh, F. Hossain et al., "IFN-γ, IL-2, IP-10, and MIG as biomarkers of exposure to *Leishmania* spp., and of cure in human visceral leishmaniasis," *Frontiers in Cellular and Infection Microbiology*, vol. 7, 200 pages, 2017.

[22] A. V. Ibarra-Meneses, C. Sanchez, J. Alvar, J. Moreno, and E. Carrillo, "Monocyte chemotactic protein 1 in plasma from soluble *Leishmania* antigen-stimulated whole blood as a potential biomarker of the cellular immune response to *Leishmania infantum*," *Frontiers in Immunology*, vol. 8, p. 1208, 2017.

[23] E. Adem, F. Tajebe, M. Getahun et al., "Successful treatment of human visceral leishmaniasis restores antigen-specific IFN-γ, but not IL-10 production," *PLoS Neglected Tropical Diseases*, vol. 10, no. 3, article e0004468, 2016.

[24] A. V. Ibarra-Meneses, D. Mondal, J. Alvar, J. Moreno, and E. Carrillo, "Cytokines and chemokines measured in dried SLA-stimulated whole blood spots for asymptomatic *Leishmania infantum* and *Leishmania donovani* infection," *Scientific Reports*, vol. 7, no. 1, p. 17266, 2017.

[25] D. R. Wagner and V. H. Heyward, "Measures of body composition in blacks and whites: a comparative review," *The American Journal of Clinical Nutrition*, vol. 71, no. 6, pp. 1392–1402, 2000.

[26] WHO, "Control of the leishmaniases," *World Health Organization technical report series*, vol. 949, pp. xii–xiii, 2010, 1-186, back cover.

[27] J. D. Chulay and A. D. Bryceson, "Quantitation of amastigotes of *Leishmania donovani* in smears of splenic aspirates from patients with visceral leishmaniasis," *The American Journal of Tropical Medicine and Hygiene*, vol. 32, no. 3, pp. 475–479, 1983.

[28] A. Sassi, B. Largueche-Darwaz, A. Collette et al., "Mechanisms of the natural reactivity of lymphocytes from noninfected individuals to Membrane-Associated *Leishmania infantum* Antigens," *The Journal of Immunology*, vol. 174, no. 6, pp. 3598–3607, 2005.

[29] L. Botana, A. V. Ibarra-Meneses, C. Sanchez et al., "Asymptomatic immune responders to *Leishmania* among HIV positive patients," *PLoS Neglected Tropical Diseases*, vol. 13, no. 6, article e0007461, 2019.

[30] H. Akuffo, C. Costa, J. van Griensven, S. Burza, J. Moreno, and M. Herrero, "New insights into leishmaniasis in the immunosuppressed," *PLoS Neglected Tropical Diseases*, vol. 12, no. 5, article e0006375, 2018.

[31] K. Gidwani, S. Jones, R. Kumar, M. Boelaert, and S. Sundar, "Interferon-gamma release assay (modified QuantiFERON) as a potential marker of infection for *Leishmania donovani*, a proof of concept study," *PLoS Neglected Tropical Diseases*, vol. 5, no. 4, article e1042, 2011.

[32] N. Turgay, I. C. Balcioglu, S. O. Toz, Y. Ozbel, and S. L. Jones, "Quantiferon-*Leishmania* as an epidemiological tool for evaluating the exposure to *Leishmania* infection," *The American Journal of Tropical Medicine and Hygiene*, vol. 83, no. 4, pp. 822–824, 2010.

[33] M. H. Alimohammadian, S. L. Jones, H. Darabi et al., "Assessment of interferon-γ levels and leishmanin skin test results in persons recovered for leishmaniasis," *The American Journal of Tropical Medicine and Hygiene*, vol. 87, no. 1, pp. 70–75, 2012.

[34] S. Gasperini, M. Marchi, F. Calzetti et al., "Gene expression and production of the monokine induced by IFN-gamma (MIG), IFN-inducible T cell alpha chemoattractant (I-TAC), and IFN-gamma-inducible protein-10 (IP-10) chemokines by human neutrophils," *Journal of Immunology*, vol. 162, no. 8, pp. 4928–4937, 1999.

[35] E. Carrillo, N. Carrasco-Anton, F. Lopez-Medrano et al., "Cytokine release assays as tests for exposure to *Leishmania*, and for confirming cure from leishmaniasis, in solid organ transplant recipients," *PLoS Neglected Tropical Diseases*, vol. 9, no. 10, article e0004179, 2015.

[36] O. P. Singh, C. B. Stober, A. K. Singh, J. M. Blackwell, and S. Sundar, "Cytokine responses to novel antigens in an Indian population living in an area endemic for visceral

leishmaniasis," *PLoS Neglected Tropical Diseases*, vol. 6, no. 10, article e1874, 2012.

[37] G. H. Mazurek, J. Jereb, A. Vernon, K. G. Castro, S. Goldberg, and P. LoBue, "Updated guidelines for using interferon gamma release assays to detect *Mycobacterium tuberculosis* infection - United States, 2010," *Morbidity and mortality weekly report. Recommendations and reports*, vol. 59, no. RR-5, pp. 1–25, 2010.

[38] A. V. Ibarra-Meneses, E. Carrillo, J. Nieto et al., "Prevalence of asymptomatic *Leishmania* infection and associated risk factors, after an outbreak in the south-western Madrid region, Spain, 2015," *Euro surveillance: bulletin Européen sur les maladies transmissibles = European communicable disease bulletin*, vol. 24, no. 22, 2019.

[39] G. N. Porcino, K. S. S. Carvalho, D. C. Braz, V. Costa Silva, C. H. N. Costa, and I. K. F. de Miranda Santos, "Evaluation of methods for detection of asymptomatic individuals infected with *Leishmania infantum* in the state of Piauí, Brazil," *PLOS Neglected Tropical Diseases*, vol. 13, no. 7, article e0007493, 2019.

[40] D. R. Abanades, L. V. Arruda, E. S. Arruda et al., "Immunodominant antigens of *Leishmania chagasi* associated with protection against human visceral leishmaniasis," *PLoS Neglected Tropical Diseases*, vol. 6, no. 6, article e1687, 2012.

Hindawi
Journal of Immunology Research
Volume 2019, Article ID 4236825, 8 pages
https://doi.org/10.1155/2019/4236825

Research Article

Classification of Wheezing Children in Rural Bangladesh by Intensity of *Ascaris* Infection, Total and Specific IgE Levels, History of Pneumonia, and Other Risk Factors

Haruko Takeuchi,[1] **Md Alfazal Khan**,[2] **Khalequz Zaman**,[3] **Sayaka Takanashi**,[4] **S. M. Tafsir Hasan**,[2] **Mohammad Yunus**,[5] **and Tsutomu Iwata**[6]

[1]*Department of Community and Global Health, Graduate School of Medicine, The University of Tokyo, 7-3-1 Hongo, Bunkyo-ku, Tokyo 113-0033, Japan*
[2]*Nutrition and Clinical Services Division, International Centre for Diarrhoeal Disease Research, Bangladesh (icddr,b), 68 Shaheed Tajuddin Ahmed Sarani, Mohakhali, Dhaka 1212, Bangladesh*
[3]*Maternal and Child Health Division, icddr,b, 68 Shaheed Tajuddin Ahmed Sarani, Mohakhali, Dhaka 1212, Bangladesh*
[4]*Department of Developmental Medical Sciences, Graduate School of Medicine, The University of Tokyo, 7-3-1 Hongo, Bunkyo-ku, Tokyo 113-0033, Japan*
[5]*Emeritus Scientist, Maternal and Child Health Division, International Centre for Diarrhoeal Disease Research, Bangladesh (icddr,b), 68 Shaheed Tajuddin Ahmed Sarani, Mohakhali, Dhaka 1212, Bangladesh*
[6]*The Graduate School of Humanities and Life Sciences, Tokyo Kasei University, Tokyo, Japan*

Correspondence should be addressed to Haruko Takeuchi; htakeuchi-tky@umin.net

Received 5 August 2019; Accepted 16 November 2019; Published 5 December 2019

Guest Editor: Barbara C. Figueiredo

Ascaris lumbricoides is the most common soil-transmitted helminth and infects 447 million people in impoverished areas worldwide. It causes serious morbidity including wheezing and influences various aspects of human immunity, such as type 2 innate lymphoid cells, regulatory T cell function, and acquired immunity. Thus, it is crucial to elucidate its influence on human immunity. We aimed to classify wheezing children based on their *Ascaris* infection intensity and other risk factors using hierarchical cluster analysis to determine the mechanisms of and the degree to which *Ascaris* contributes to childhood wheezing in rural Bangladesh. We analyzed relevant data collected in 2001. The participants included 219 5-year-old wheezing children who were randomly selected from 1705 children living in the Matlab Health and Demographic Surveillance area of the International Centre for Diarrhoeal Disease Research, Bangladesh. Hierarchical cluster analysis was conducted using variables of history of pneumonia, total and specific immunoglobulin E levels, *Ascaris* infection intensity, and parental asthma. Three distinct wheezing groups were identified. Children in Cluster 1 ($n = 50$) had the highest titers of the total, anti-*Ascaris*, anti-*Dermatophagoides pteronyssinus*, and anticockroach IgEs and experienced the fewest episodes of pneumonia. Cluster 2 ($n = 114$), the largest group, experienced few episodes of pneumonia and had the lowest titers of the total, anti-*Ascaris*, anti-Dp, and anticockroach IgEs. Cluster 3 ($n = 32$) consisted of participants with the most episodes of pneumonia and lower titers of the total and specific IgEs. The extremely high prevalence of *Ascaris* infection found in Clusters 1-3 was 78%, 77%, and 72%, respectively. Childhood wheezing in rural Bangladesh could be divided into three groups, with 26% of wheezing attributable to anti-*Ascaris* IgE and 16% to history of pneumonia during early childhood, and 58% might have been due to *Ascaris* infection without elevated anti-*Ascaris* IgE.

1. Introduction

Ascaris lumbricoides is the most common soil-transmitted helminth (STH), and *Ascaris* infection is one of 13 neglected tropical diseases of great concern. The STH affects approximately 1.5 billion people worldwide, and *Ascaris* infects 447 million people in impoverished areas of Africa, Asia, and Central and South America [1, 2]. The people at risk are preschool children and school-age children [1]. The WHO has implemented a program since 2001 for people at risk in endemic areas in order to eliminate STH infections to reduce intensity of infection and to protect infected individuals from morbidity related to the worms harbored [1]. Although the eradication program of helminthic infections has been on the way, an unacceptably large number of individuals continue to suffer from them despite the program [2]. The morbidity related to the worms harbored includes abdominal pain, general malaise and weakness, intestinal obstruction, and impaired cognitive and physical development. In addition to these symptoms, *Ascaris* causes wheezing; it migrates through the lungs during maturation, where it induces the type 2 inflammatory response, called Löffler's syndrome [3].

A potential explanation for the role of *Ascaris* infection in wheezing might be pulmonary inflammation of type 2 immunity induced by type 2 innate lymphoid cells (ILC2s). Animal worms, such as *Nippostrongylus*, known as the rat hookworm, which have a larval stage in the lungs, have been linked to lung damage, type 2 immune responses, and long-term changes in lung function and structure in nonhuman hosts, which are consistent with allergic airway disease [4]. Migration of *Nippostrongylus* larvae through the lungs causes damage to the epithelium, promoting the release of damage-associated molecular patterns from epithelial cells in the airway [4–6]. The release of interleukin-33 (IL-33) and IL-25 promotes the activation of ILC2s, leading to an increase in the release of the type 2 cytokines, IL-4, IL-5, and IL-13 [4, 6], which have been found to be part of a pathway in both the innate and adaptive responses to lung larval migration in mice [5, 6]. Furthermore, *Ascaris* larval migration causes significant pulmonary damage, including bronchial hyperreactivity (BHR) and type 2 inflammatory lung pathology resembling an extreme form of allergic airway disease in mice [7].

On the other hand, the sharp rise in the worldwide prevalence of bronchial asthma since the 1970s, with children living in industrial and urban areas experiencing higher asthma rates than those in rural area [8–12], has led to the hypothesis that helminthic infections might provide protection against asthma by suppressing the host's immune response. Helminthic infections activate regulatory T cells and induce the production of IL-10, thereby playing a protective role against asthma and allergies. Studies have shown that IL-10 induced in chronic schistosomiasis suppresses atopy in African children [13], and infection with *Schistosoma mansoni* has been associated with a reduced course of asthma [14]. However, we found concurrent decreases in the prevalence of *Ascaris* infection and wheezing from no less than 72% in 2001, to 18% in 2016, and from 16% to 9%, respectively, after implementation of a national deworming program, indicating that the decrease in the prevalence of *Ascaris* infection did not increase wheezing [15].

It appears likely that *Ascaris* infections are associated with increased wheezing. A systematic review and meta-analysis of 22 studies found an association between *Ascaris* infection and wheezing [16]. Another systematic review conducted in Latin America reported an association of a higher risk of asthma or wheezing with an *Ascaris* infestation [17]. However, this relationship remains controversial because the results of multiple epidemiological studies both support and refute the protective effects of helminths on asthma and allergies [13–18].

In 2001, we also reported that anti-*Ascaris* IgE was an increasing risk factor for childhood wheezing in rural areas of Bangladesh [19], and in 2005, we found that anti-*Ascaris* IgE was an increasing risk factor for childhood BHR in the same rural areas [20]. In these studies, *Ascaris* infection itself was not a risk factor for wheezing. The antiparasite role of IgE antibody against helminths is thought to be a normal component of the protective response of the host during infection, and they are not usually associated with allergic symptoms. However, allergic manifestations have been described in some helminth infections such as *Ascariasis* and *Anisakiasis* [21].

Ascaris influences on various aspects of human immunity, such as type 2 innate lymphoid cells (ILC2s), Treg function, and acquired immunity; hence, childhood wheezing in rural Bangladesh might be attributable to *Ascaris* infection through a complex interplay between innate, regulatory, and acquired immunity. The mechanism by which *Ascaris* is involved in the development of wheezing and asthma symptoms has caught attention given the serious morbidity caused by this helminth. Therefore, the study's purpose was to classify wheezing children, who participated in the 2001 study, based on the intensity of their *Ascaris* infection, total and specific IgEs including anti-*Ascaris* IgE, parental asthma, and other risk factors to determine the mechanism by which *Ascaris* causes childhood wheezing in this rural area of Bangladesh and the degree to which it contributes to the development of wheezing.

2. Methods

The present study reanalyzed the data collected in 2001. The procedures used for the data collection used are described elsewhere [19]. In short, the study population consisted of 1705 5-year-old children randomly selected from Matlab, a riverine rural area located 55 km southeast of Dhaka, the capital of Bangladesh. Children ($n = 256$) who had experienced wheezing during the previous 12 months were identified using a questionnaire adapted from the standardized questionnaire of the International Study of Asthma and Allergies in Childhood (ISAAC) [22]. We retrieved information about the children's history of pneumonia from the routine data-collection system of the International Centre for Diarrhoeal Disease Research, Bangladesh (icddr,b) in the Matlab Health and Demographic Surveillance System (HDSS) area [23]. We also collected blood and stool samples to measure serum total

and specific IgEs and to detect helminth infections among the 219 wheezing children whose guardians gave us written informed consent. At that time, the risk factors that were assessed for childhood wheezing included family history of allergies, serum total and anti-*Ascaris* IgE levels, and frequency of pneumonia episodes at 0 years, 1 year, and 2 years of age.

The dataset of the 2001 study included information about wheezing, family history of allergies, socioeconomic status, environmental factors, helminth infections, serum total and antigen-specific IgE levels, and the frequency of pneumonia episodes during the earliest years of childhood. We included the following variables in the present analysis: frequency of pneumonia episodes when the children were 0, 1, and 2 years of age; total, anti-*Ascaris*, anti-*Dermatophagoides pteronyssinus* (Dp), and anticockroach IgE levels; history of parental asthma; and helminth infections.

SPSS 22 (IBM Japan, Tokyo, Japan) was used to perform the cluster analysis with Ward's minimum-variance hierarchical clustering method. The variables were standardized to equalize the standard deviation of the scales. To compare differences among the clusters, analysis of variance (ANOVA) was used for parametric tests of the continuous variables and the Chi-square test was used to analyze the categorical variables. The significance level for all statistical analyses was set at $P < 0.05$.

The Ethics Committee of Tokyo Kasei University approved the study's protocol (Sayama H27-09), and the Ethics Committee of The University of Tokyo approved the protocol (11956). The dataset of the study conducted in 2001 was used in the current study, and the protocol (2000-038) was approved by the Ethical Review Committee of the icddr,b. The 2001 study involved human participants; therefore, it followed the ethical principles of the Declaration of Helsinki. Written informed consent was obtained from the legal guardians of all the participants.

3. Results

3.1. Characteristics of the Participants. The initial study's dataset contained 1705 children who were selected using random-cluster sampling and 1580 of them agreed to participate in the first questionnaire survey. Two hundred fifty-six (16.2%) children were found to have wheezing during the previous 12 months (current wheezing), and 219 participated in the subsequent nested case-control study and submitted blood and stool samples. The information collected from these 219 current wheezing children was used for the cluster analysis. Two hundred fifty-six of the 1324 children with no current wheezing had been randomly selected as the control group and 183 of them agreed to participate in the nested case-control study. The children without current wheezing were divided into two groups. One of the groups consisted of 122 children who had never experienced wheezing (never wheezing) and the other group included 61 children who had experienced wheezing (ever wheezing), but not within the previous 12 months. Data from the 122 children who had never experienced wheezing were used as the comparison group (Figure 1). Tables 1 and 2 show the characteristics of the current- and never-wheezing participants and the three clusters.

3.2. Cluster Analysis. We identified three clusters through the analysis (Figure 2). Table 1 shows the physical status, family history, and sociodemographic characteristics of the three groups. Table 2 shows the total and specific IgE levels, prevalence and intensity of *Ascaris* infection, and pneumonia history. The first group consisted of 50 (26%) children who had the highest titers of the total, anti-*Ascaris* IgEs, anti-Dp, and anticockroach IgEs and the lowest frequency of pneumonia episodes. The second group consisted of 114 (58%) children who had a moderate level of pneumonia history and the lowest titers of the total and anti-*Ascaris* IgEs. The third group consisted of 32 (16%) children who had the highest frequency of pneumonia episodes and low IgEs.

3.2.1. Cluster 1. Twenty-six percent of the participants ($n = 50$) were grouped into Cluster 1. This cluster was characterized by significantly high serum levels of the total and anti-*Ascaris* IgE levels, and high anti-Dp and anticockroach IgE levels, and a significantly lower number of children with a history of pneumonia when they were 0, 1, and 2 years of age. A significantly lower number of the mothers in Cluster 1 were educated at the primary level, and their household income (monthly) was lower than that of the households in the other groups, although the difference was not significant. We found no significant differences from other groups, with respect to sex, physical measurements, parental history of asthma, or type of cooking fuel. Cluster 1 had the highest prevalence and intensity of *Ascaris* infection (78%) although the differences between the three groups were not significant.

3.2.2. Cluster 2. Cluster 2 was the largest group ($n = 114$; 58%) of participants. It consisted of children with a moderate frequency of pneumonia episodes and the lowest serum levels of the total, anti-*Ascaris*, anti-Dp, and anticockroach IgE, which were comparable to the levels of the never-wheezing children. Their mothers had significantly more education, a relatively high household income (monthly), and a higher prevalence of asthma than the mothers did in Cluster 3, although the differences were not significant. The prevalence (77%) and intensity (37.7%) of *Ascaris* infection were as high as Cluster 1.

3.2.3. Cluster 3. Cluster 3, which was the smallest cluster ($n = 32$; 16%), was characterized by their frequency of pneumonia episodes when they were 0, 1, and 2 years old. They experienced a significantly higher frequency of pneumonia episodes than the children in the other groups did. They had more *Trichuris* infections, and their mothers had a lower rate of asthma than the mothers did in the other two groups, although the differences were not significant. The prevalence (71.9%) and intensity (21.9%) of *Ascaris* infection were lower in Cluster 3 than in the other two groups and were almost comparable to the never-wheezing group (71.6% and 29.4%, respectively).

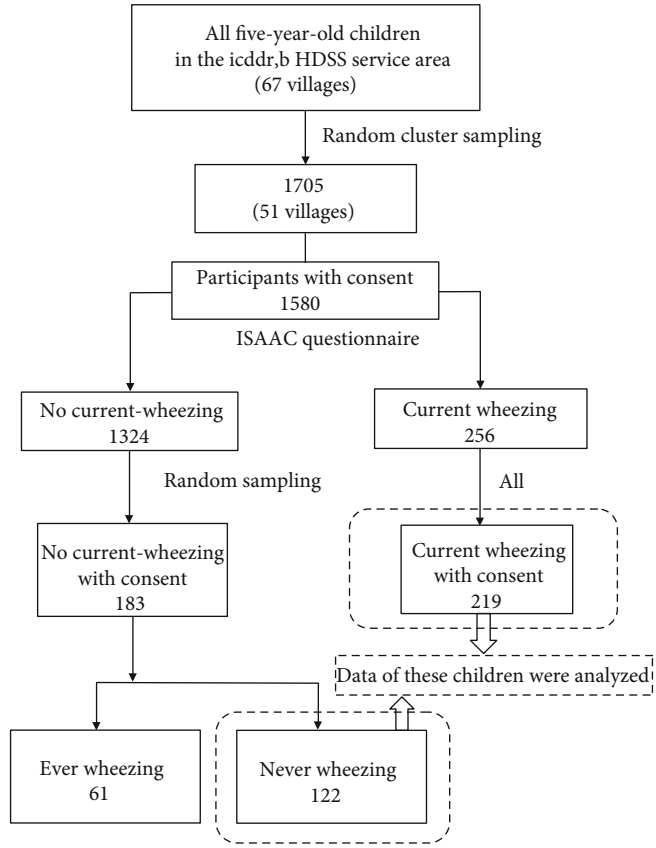

Figure 1: Flowchart of the sampling procedure for the dataset.

Table 1: Comparisons of physical status, family history, and sociodemographic characteristics of the three groups.

	Total	Cluster 1	Cluster 2	Cluster 3		Never-wheezing
n	219	50	114	32	*P*=	122
Sex, female (%)	108 (49)	22 (44)	63 (55)	12 (38)	0.138	66 (49)
Physical measurements (*n*)	194	49	113	32		122
Height (cm)	103.0	102.4	103.6	102.3	0.213	103.7
Weight (kg)	14.7	14.5	14.8	14.5	0.492	14.8
DPT3 vaccine coverage (%)	185 (94.4)	45 (90.0)	108 (94.7)	32 (100)	0.154	
Measles vaccine coverage (%)	188 (95.9)	47 (94.0)	109 (95.6)	32 (100)	0.395	
Family history						
Mother's asthma (%)	42 (19)	11 (22.0)	26 (22.8)	2 (6.3)	0.106	12 (9.8)
Father's asthma (%)	25 (12)	4 (8.2)	16 (14.0)	4 (12.5)	0.578	2 (1.7)
Dry leaves as fuel	183 (86)	42 (89)	93 (83)	28 (88)	0.548	91 (75)
Mother's education (none) (%)	93 (43)	29 (58)	41 (36)	17 (53)	0.018	48 (39)
Monthly income (BTk)	3943	2896	4164	3712	0.054	4755

DPT3: diphtheria, pertussis, tetanus vaccine; BTk: Bangladesh Taka.

4. Discussion

The major finding of this analysis was that three distinct clusters of wheezing children in rural Bangladesh were identified, with children having a high titer of anti-*Ascaris* IgE comprising Cluster 1. Participants in this group ($n = 50$) had higher titers of the total IgE, anti-*Ascaris* IgE, anti-Dp IgE, and anticockroach IgE levels and experienced fewer episodes of pneumonia. Children in Cluster 2 ($n = 114$) had a low frequency of pneumonia episodes and lower titers of the total, anti-*Ascaris*, anti-Dp, and anticockroach IgE. Cluster 3 ($n = 32$) consisted of children with a higher frequency of pneumonia episodes and lower titers of the total and specific IgEs. The prevalence of *Ascaris* infection was high in all

Table 2: Comparisons of serum IgE levels, helminth infections, and pneumonia history among the three groups.

	Total	Cluster 1	Cluster 2	Cluster 3		Never-wheezing
n (%)	196 (100)	50 (25.5)	114 (58.2)	32 (16.3)	*P*=	122
Total IgE (IU/ml)		13598	3705	3959	<0.001	3686
Specific IgE (U_A/ml)						
Anti-*Ascaris* IgE	30.8	62.5	20.3	24.8	<0.001	14.9
Anti-Dp IgE	4.1	7.8	1.8	2.7	<0.001	1.8
Anticockroach IgE	4.2	8.1	2.3	4.0	<0.001	2.8
Helminth infection	199					
Ascaris egg (+) (%)	152 (76.4)	39 (78.0)	88 (77.2)	23 (71.9)	0.789	78 (71.6)
(+++) (%)	71 (35.7)	21 (42.0)	43 (37.7)	7 (21.9)	0.158	32 (29.4)
Trichuris (+) (%)	100 (50.3)	22 (44.0)	56 (49.1)	20 (62.5)	0.252	66 (60.6)
Pneumonia history (+) *n* (%)						
At 0 years	56 (25.6)	6 (12.0)	31 (27.2)	12 (37.5)	0.024	16 (13.1)
1 year	44 (20.1)	2 (4.0)	21 (18.4)	18 (56.3)	<0.001	4 (3.3)
2 years	38 (16.4)	2 (4.0)	0 (0.0)	32 (100)	<0.001	2 (2.0)

IgE: immunoglobulin E; Dp: *Dermatophagoides pteronyssinus*.

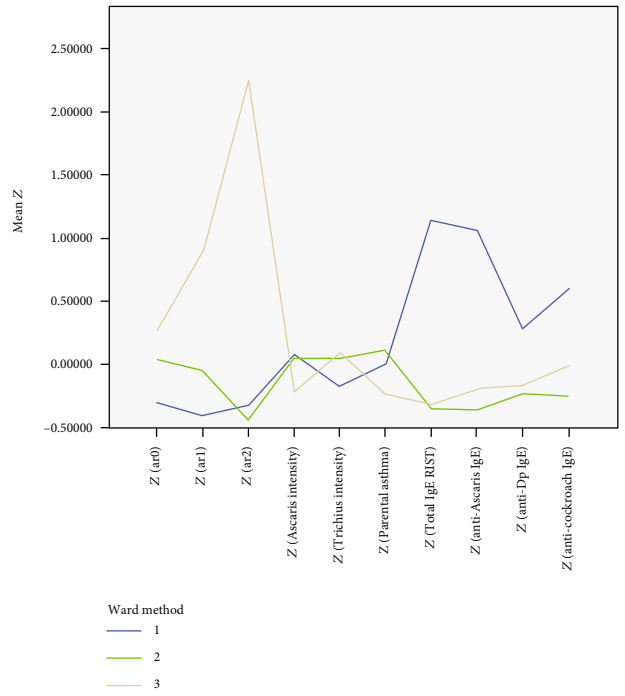

Figure 2: Graph of the three clusters. Three clusters were identified. This polygonal line graph shows the standardized value of the variables regarding the number of the history of pneumonia at 0, 1, and 2 years of age, *Ascaris* infection intensity, *Trichuris* infection intensity, parental asthma, and total and specific IgE levels.

clusters (78%, 77.2%, and 72%), and it was higher in Clusters 1 and 2 than in Cluster 3, although the differences were not significant.

The children in Cluster 1 had higher titers of the total and anti-*Ascaris* IgE and slightly elevated anti-Dp and anticockroach IgE levels. We reported that in 2005, elevated serum anti-*Ascaris* IgE was associated with BHR in children in rural Bangladesh [20]. This finding was supported by a subsequent study, which was conducted in the same region of Bangladesh in 2008, when the infection prevalence was 17.4%. That study reported that anti-*Ascaris* IgE was associated with an increased risk of ever having asthma among 5-year-old children [24]. Studies conducted in Latin America have also reported similar results [25–27]. The fact that children in Cluster 1 had higher titers of anti-Dp and anticockroach IgE may be explained by a predisposition to atopy among the children in this group. In other words, the children in Cluster 1 are likely to produce high titers of anti-*Ascaris* IgE when they were infected with *Ascaris* because they were atopic. This group may resemble to multisensitized atopic wheezing cluster in other studies [28]. However, neither the family history of asthma nor allergies were obvious in Cluster 1.

Another explanation for the elevated levels of anti-*Ascaris* and anti-Dp IgE is the cross-reactivity between the *Ascaris* and the house-dust mite antigens. The *Ascaris* antigen's cross-reactivity with that of the house-dust mite through tropomyosin might stimulate the production of elevated anti-Dp and anticockroach IgE [29]. Therefore, if *Dermatophagoides* antigen is abundant in the environment and is inhaled, it might join with anti-*Ascaris* IgE on the mast cell surface of the airway and result in wheezing [30, 31]. It is understandable that the group with a high level of anti-*Ascaris* IgE comprises one cluster, as anti-*Ascaris* IgE was an independent risk factor for wheezing [19]. In the study in 2001, whose participants are the target population of the present study, the odds ratios of anti-*Ascaris* IgE levels for current wheezing increased and *P* values decreased as the children expressed severer symptoms. This association was not found in total, anti-DP, or anticockroach IgEs.

The children in Cluster 2 experienced relatively few episodes of pneumonia and had the lowest titers of the total and anti-*Ascaris* IgE and the lowest anti-Dp IgE level. Before the analysis, we expected to find an association of family history of asthma and allergies with a high titer of anti-Dp IgE in

this group or with *Ascaris* infection intensity as measured by *Ascaris* egg count in the stool. Therefore, we analyzed *Ascaris* infection intensity and family history asthma and allergies by the demographic and health-related characteristics of the three groups: sex; history of diarrhea; physical status; number of family members; number of older or younger children; number of rooms in the house; duration of exclusive breast feeding; coverage for the diphtheria, pertussis, and tetanus vaccine and the measles and bacillus Calmette-Guerin vaccines; eczema; allergic rhinitis; household smoking; water supply; and parental education. However, no specific characteristics of the children were found to be significant in the analysis, except for a higher level of maternal education. Then, what factor contributed to wheezing in Cluster 2? This group and Cluster 1 had a higher prevalence of *Ascaris* infection than did Cluster 3, although the difference was not significant. The main difference between Clusters 1 and 2 was the serum levels of IgE, indicating that children in Cluster 1 had the capacity to produce high titers of IgE than Cluster 2. In 2015, we conducted an epidemiological study, which found concurrent decreases in the prevalence of wheezing and *Ascaris* infection among 5-year-old children in rural Bangladesh [15]. The study also showed that wheezing children had a significantly higher rate of *Ascaris* infection compared to never-wheezing children, although *Ascaris* infection was not a risk factor for wheezing. However, it was evident that wheezing and the prevalence of *Ascaris* infection decreased simultaneously.

In animal models, worms have been linked to type 2 immune responses through ILC2s in the lungs, including airway hyperresponsiveness which resembles an extreme form of allergic airway disease [4–7]. Although the function of human ILC2s in *Ascaris* infection should be investigated epidemiologically and experimentally in future studies, it has been reported that *Ascaris* induces an inflammatory response in the lungs independent of its effect on IgE production, which may explain some of the contradictory findings of studies examining the association between geohelminth infection, atopy, and asthma [18]. As anti-*Ascaris* IgE increases only in individuals with current or past *Ascaris* infections, the notion that childhood wheezing in rural Bangladesh might be attributable to *Ascaris* infection is reasonable. These findings indicate that the high prevalence of *Ascaris* infection in Clusters 1 (78%) and 2 (77.2%) might be a contributing factor to the wheezing of the children in these groups.

Cluster 3 ($n = 32$) consisted of children with a higher frequency of pneumonia episodes and lower titers of the total and specific IgEs. In the present study, information about pneumonia episodes was obtained from the record-keeping system of the HDSS of the icddr,b. In 2001, pneumonia was recorded by community health research workers every two weeks. This surveillance was based on the mother's report of the child's increased respiratory rates with or without chest indrawing, following the World Health Organization's guidelines [32]. *Haemophilus influenzae*, *Streptococcus pneumoniae*, *Branhamella catarrhalis*, and Gram-negative bacilli were the predominant causative bacteria of pneumonia in 157 patients who were admitted to a pediatric hospital for treatment of pneumonia, as reported in a 1998 study conducted in Dhaka, Bangladesh [33]. Respiratory syncytial virus, which is known to cause recurrent wheezing and BHR in later life [34, 35], was the most common virus detected in children less than 2 years old who were hospitalized due to severe lower respiratory tract infections. Rhinovirus, a causative agent of the common cold, is also related to exacerbations of asthma attacks in 80% of children and might have been present in 50% of adults [36, 37]. Although we did not examine the etiologic agents of pneumonia in our study, we speculate that the majority of episodes might have been due to these pathogens.

Acute lower respiratory infections (ALRI) have been major causes of morbidity and mortality in Bangladesh; however, improvements in the management of childhood illnesses have successfully decreased deaths caused by ALRI among young children [38]. Thus, it is understandable that these children had a higher risk of developing asthma in subsequent years. The symptoms of children in Cluster 3 were compatible with these observations, indicating the need for attention to wheezing post-ALRI in order to stem the increase in asthma in rural Bangladeshi children. This group might be comparable to the nonatopic postviral bronchial hyperresponsiveness group of Tucson Study [39].

We found 3 clusters as predictive index for asthma in infants and preschoolers in rural Bangladesh. Anti-*Ascaris* IgE was an independent risk factor for wheezing against the fact that anti-DP IgE was not a risk factor for wheezing. However, children with high anti-*Ascaris* IgE and anti-Dp IgE seem to comprise 1 group, which indicates that the children with high anti-*Ascaris* IgE might emerge as children who have high anti-Dp IgE with the development of the society in the future. Since the children in this group might develop persistent wheezing in the future through early sensitization by any antigen, early sensitization with *Ascaris* antigen by *Ascaris* infection should absolutely be prevented. Therefore, we think children with high anti-*Ascaris* IgE might need to be followed up carefully, before the development of the future atopic type to curb the increase of persistent asthma.

5. Conclusion

In conclusion, data on childhood wheezing from a study conducted in 2001 was classified into three distinct categories; 26% of the wheezing was attributable to anti-*Ascaris* IgE, 16% to the history of pneumonia during early childhood, and the remaining 58% might have been due to *Ascaris* infection. Although we could not find any specific characteristics in Cluster 2, we speculate that the high prevalence of *Ascaris* infection might have been a contributing factor to wheezing. Childhood wheezing caused by *Ascaris* infection might be induced through the complex interplay between innate, acquired, and regulatory immunity, although the underlying mechanism for such wheezing remains unclear. As *Ascaris* infection remains a major public health problem in this rural area of Bangladesh, despite its dramatic decrease in prevalence, the role of ILC2s, anti-*Ascaris* IgE, and Tregs in *Ascaris* infection on childhood wheezing merits further investigation.

Data Availability

The numeric-type data used to support the findings of the current study are available from the corresponding author upon reasonable request.

Conflicts of Interest

All the authors confirm that there are no conflicts of interest to disclose.

Acknowledgments

The authors thank the participants for giving their precious time and samples. We also thank the study physician, nurse, and the field research assistants. We thank Prof. Masamine Jimba, the professor and the chair of the Department of Community and Global Health of The University of Tokyo, for critically writing the manuscript and the overall help to the research project. The study was funded by the ICH Research Fund of the Department Community and Global Health, Graduate School of Medicine, The University of Tokyo.

References

[1] "Soil-transmitted helminth infections," July 2019, https://www.who.int/news-room/fact-sheets/detail/soil-transmitted-helminth-infections.

[2] GBD 2017 Disease and Injury Incidence and Prevalence Collaborators, "Global, regional, and national incidence, prevalence, and years lived with disability for 354 diseases and injuries for 195 countries and territories, 1990-2017: a systematic analysis for the Global Burden of Disease Study 2017," *The Lancet*, vol. 392, no. 10159, pp. 1789–1858, 2018.

[3] R. K. Spillman, "Pulmonary Ascariasis in Tropical Communities," *The American Journal of Tropical Medicine and Hygiene*, vol. 24, no. 5, pp. 791–800, 1975.

[4] C. Schwartz, E. Hams, and P. G. Fallon, "Helminth modulation of lung inflammation," *Trends in Parasitology*, vol. 34, no. 5, pp. 388–403, 2018.

[5] F. Chen, Z. Liu, W. Wu et al., "An essential role for T_H2-type responses in limiting acute tissue damage during experimental helminth infection," *Nature Medicine*, vol. 18, no. 2, pp. 260–266, 2012.

[6] J. E. Allen and T. E. Sutherland, "Host protective roles of type 2 immunity: parasite killing and tissue repair, flip sides of the same coin," *Seminars in Immunology*, vol. 26, no. 4, pp. 329–340, 2014.

[7] J. E. Weatherhead, P. Porter, A. Coffey et al., "AscarisLarval infection and lung invasion directly induce severe allergic airway disease in mice," *Infection and Immunity*, vol. 86, no. 12, 2018.

[8] The International Study of Asthma and Allergies in Childhood (ISAAC) Steering Committee, "Worldwide variation in prevalence of symptoms of asthma, allergic rhinoconjunctivitis, and atopic eczema: ISAAC," *The Lancet*, vol. 351, no. 9111, pp. 1225–1232, 1998.

[9] M. R. Sears, "Descriptive epidemiology of asthma," *The Lancet*, vol. 350, pp. S1–S4, 1997.

[10] E. von Mutius, F. D. Martinez, C. Fritzsch, T. Nicolai, G. Roell, and H. H. Thiemann, "Prevalence of asthma and atopy in two areas of West and East Germany," *American Journal of Respiratory and Critical Care Medicine*, vol. 149, no. 2, pp. 358–364, 1994.

[11] E. O. Addo Yobo, A. Custovic, S. C. Taggart, A. P. Asafo-Agyei, and A. Woodcock, "Exercise induced bronchospasm in Ghana: differences in prevalence between urban and rural schoolchildren," *Thorax*, vol. 52, no. 2, pp. 161–165, 1997.

[12] N. Pearce, N. Aït-Khaled, R. Beasley et al., "Worldwide trends in the prevalence of asthma symptoms: phase III of the International Study of Asthma and Allergies in Childhood (ISAAC)," *Thorax*, vol. 62, no. 9, pp. 758–766, 2007.

[13] A. H. van den Biggelaar, R. van Ree, L. C. Rodrigues et al., "Decreased atopy in children infected with *Schistosoma haematobium*: a role for parasite-induced interleukin-10," *The Lancet*, vol. 356, no. 9243, pp. 1723–1727, 2000.

[14] M. Medeiros Jr., J. P. Figueiredo, M. C. Almeida et al., "*Schistosoma mansoni* infection is associated with a reduced course of asthma," *The Journal of Allergy and Clinical Immunology*, vol. 111, no. 5, pp. 947–951, 2003.

[15] H. Takeuchi, A. F. Khan, S. M. Ahmad et al., "Concurrent decreases in the prevalence of wheezing and Ascaris infection among 5-year-old children in rural Bangladesh and their regulatory T cell immunity after the implementation of a national deworming program," *Immunity, Inflammation and Disease*, vol. 7, no. 3, pp. 160–169, 2019.

[16] J. Leonardi-Bee, D. Pritchard, J. Britton, and the Parasites in Asthma Collaboration, "Asthma and Current Intestinal Parasite Infection," *American Journal of Respiratory and Critical Care Medicine*, vol. 174, no. 5, pp. 514–523, 2006.

[17] C. Ardura-Garcia, P. Garner, and P. J. Cooper, "Is childhood wheeze and asthma in Latin America associated with poor hygiene and infection? A systematic review," *BMJ Open Respiratory Research*, vol. 5, no. 1, article e000249, 13 pages, 2018.

[18] J. Calvert and P. Burney, "Ascaris, atopy, and exercise-induced bronchoconstriction in rural and urban South African children," *Journal of Allergy and Clinical Immunology*, vol. 125, no. 1, article 105.e5, pp. 100–105.e5, 2010.

[19] H. Takeuchi, K. Zaman, J. Takahashi et al., "High titre of anti-*Ascaris* immunoglobulin E associated with bronchial asthma symptoms in 5-year-old rural Bangladeshi children," *Clinical and Experimental Allergy*, vol. 38, no. 2, pp. 276–282, 2008.

[20] H. Takeuchi, A. F. Khan, M. Yunus et al., "Anti-*Ascaris* immunoglobulin E associated with bronchial hyper-reactivity in 9-year-old rural Bangladeshi children," *Allergology International*, vol. 65, no. 2, pp. 141–146, 2016.

[21] N. Nieuwenhuizen, A. L. Lopata, M. F. Jeebhay, D. R. Herbert, T. G. Robins, and F. Brombacher, "Exposure to the fish parasite *Anisakis* causes allergic airway hyperreactivity and dermatitis," *The Journal of Allergy and Clinical Immunology*, vol. 117, no. 5, pp. 1098–1105, 2006.

[22] M. I. Asher, U. Keil, H. R. Anderson et al., "International Study of Asthma and Allergies in Childhood (ISAAC): rationale and methods," *The European Respiratory Journal*, vol. 8, no. 3, pp. 483–491, 1995.

[23] International Centre for Diarrhoeal Disease Research Bangladesh (ICDDR,B), *Demographic surveillance system-Matlab Vol. 1, methods and procedures*, Initiative for Climate Change and Health (ICCH), Health System and Population Studies Division, icddr,b, 1978.

[24] M. D. Hawlader, E. Ma, E. Noguchi et al., "Ascaris lumbricoids infection as a risk factor for asthma and atopy in rural Bangladeshi children," *Tropical Medicine and Health*, vol. 42, no. 2, pp. 77–85, 2014.

[25] A. L. Moncayo, M. Vaca, G. Oviedo et al., "Effects of geohelminth infection and age on the associations between allergen-specific IgE, skin test reactivity and wheeze: a case-control study," *Clinical and Experimental Allergy*, vol. 43, no. 1, pp. 60–72, 2013.

[26] P. Endara, M. Vaca, T. A. Platts-Mills et al., "Effect of urban vs. rural residence on the association between atopy and wheeze in Latin America: findings from a case-control analysis," *Clinical and Experimental Allergy*, vol. 45, no. 2, pp. 438–447, 2015.

[27] N. M. Alcântara-Neves, S. J. Badaró, M. C. dos Santos, L. Pontes-de-Carvalho, and M. L. Barreto, "The presence of serum anti-*Ascaris lumbricoides* IgE antibodies and of *Trichuris trichiura* infection are risk factors for wheezing and/or atopy in preschool-aged Brazilian children," *Respiratory Research*, vol. 11, no. 1, p. 114, 2010.

[28] O. E. Savenije, R. Granell, D. Caudri et al., "Comparison of childhood wheezing phenotypes in 2 birth cohorts: ALSPAC and PIAMA," *Journal of Allergy and Clinical Immunology*, vol. 127, no. 6, pp. 1505–1512.e14, 2011.

[29] A. B. Santos, G. M. Rocha, C. Oliver et al., "Cross-reactive IgE antibody responses to tropomyosins from Ascaris lumbricoides and cockroach," *Journal of Allergy and Clinical Immunology*, vol. 121, no. 4, pp. 1040–1046.e1, 2008.

[30] N. Acevedo, A. Erler, P. Briza, F. Puccio, F. Ferreira, and L. Caraballo, "Allergenicity of Ascaris lumbricoides tropomyosin and IgE sensitization among asthmatic patients in a tropical environment," *International Archives of Allergy and Immunology*, vol. 154, no. 3, pp. 195–206, 2011.

[31] V. Ahumada, E. García, R. Dennis et al., "IgE responses to *Ascaris* and mite tropomyosins are risk factors for asthma," *Clinical and Experimental Allergy*, vol. 45, no. 7, pp. 1189–1200, 2015.

[32] S. H. Factor, J. A. Schillinger, H. D. Kalter et al., "Diagnosis and management of febrile children using the WHO/UNICEF guidelines for IMCI in Dhaka, Bangladesh," *Bulletin of the World Health Organization*, vol. 79, no. 12, pp. 1096–1105, 2001.

[33] Y. Utsunomiya, K. Ahmed, N. Rikitomi et al., "Isolation of pathogenic bacteria from induced sputum from hospitalized children with pneumonia in Bangladesh," *Journal of Tropical Pediatrics*, vol. 44, no. 6, pp. 338–342, 1998.

[34] F. Huq, M. Rahman, N. Nahar et al., "Acute lower respiratory Thact infection due to virus among hospitalized children in Dhaka, Bangladesh," *Clinical Infectious Diseases*, vol. 12, Supplement_8, pp. S982–S987, 1990.

[35] N. Sigurs, R. Bjarnason, F. Sigurbergsson, and B. Kjellman, "Respiratory syncytial virus bronchiolitis in infancy is an important risk factor for asthma and allergy at age 7," *American Journal of Respiratory and Critical Care Medicine*, vol. 161, no. 5, pp. 1501–1507, 2000.

[36] R. F. Lemanske Jr., D. J. Jackson, R. E. Gangnon et al., "Rhinovirus illnesses during infancy predict subsequent childhood wheezing," *The Journal of Allergy and Clinical Immunology*, vol. 116, no. 3, pp. 571–577, 2005.

[37] T. Jartti and J. E. Gern, "Role of viral infections in the development and exacerbation of asthma in children," *The Journal of Allergy and Clinical Immunology*, vol. 140, no. 4, pp. 895–906, 2017.

[38] A. H. Baqui, A. A. Sabir, N. Begum, S. E. Arifeen, S. N. Mitra, and R. E. Black, "Causes of childhood deaths in Bangladesh: an update," *Acta Paediatrica*, vol. 90, no. 6, pp. 682–690, 2001.

[39] R. T. Stein, D. Sherrill, W. J. Morgan et al., "Respiratory syncytial virus in early life and risk of wheeze and allergy by age 13 years," *Lancet*, vol. 354, no. 9178, pp. 541–545, 1999.

Hindawi
Journal of Immunology Research
Volume 2019, Article ID 6793596, 16 pages
https://doi.org/10.1155/2019/6793596

Research Article

Sm16, A *Schistosoma mansoni* Immunomodulatory Protein, Fails to Elicit a Protective Immune Response and Does Not Have an Essential Role in Parasite Survival in the Definitive Host

Wilma Patrícia de Oliveira Santos Bernardes,[1] **Juliano Michel de Araújo**,[2] **Gardênia Braz Carvalho**,[1] **Clarice Carvalho Alves**,[1] **Aline Thaynara de Moura Coelho**,[3] **Isabela Thamara Sabino Dutra**,[2] **Sueleny Silva Ferreira Teixeira**,[4] **Rosy Iara Maciel de Azambuja Ribeiro**,[3] **Marina de Moraes Mourão**,[2] **Rosiane Aparecida da Silva-Pereira**,[1] **and Cristina Toscano Fonseca**[1]

[1]*Laboratório de Biologia e Imunologia de Doenças Infeciosas e Parasitárias, Instituto René Rachou, Fiocruz-MG, Belo Horizonte, Minas Gerais 30190009, Brazil*
[2]*Laboratório de Helmintologia e Malacologia Médica, Instituto René Rachou, Fiocruz-MG, Belo Horizonte, Minas Gerais 30190009, Brazil*
[3]*Laboratório de Patologia Experimental, Universidade Federal De São João Del Rei-Campus Divinópolis, Minas Gerais 35501-296, Brazil*
[4]*Laboratório de Diagnóstico e Terapia de Doenças Infecciosas e Oncológicas, Instituto René Rachou, Fiocruz-MG, Belo Horizonte, Minas Gerais 30190009, Brazil*

Correspondence should be addressed to Cristina Toscano Fonseca; cristina.toscano@fiocruz.br

Received 7 June 2019; Accepted 11 September 2019; Published 1 December 2019

Guest Editor: Barbara C. Figueiredo

Sm16 is an immunomodulatory protein that seems to play a key role in the suppression of the cutaneous inflammatory response during *Schistosoma mansoni* penetration of the skin of definitive hosts. Therefore, Sm16 represents a potential target for protective immune responses induced by vaccination. In this work, we generated the recombinant protein rSm16 and produced polyclonal antibodies against this protein to evaluate its expression during different parasite life-cycle stages and its location on the surface of the parasite. In addition, we analyzed the immune responses elicited by immunization with rSm16 using two different vaccine formulations, as well as its ability to induce protection in Balb/c mice. In order to explore the biological function of Sm16 during the course of experimental infection, RNA interference was also employed. Our results demonstrated that Sm16 is expressed in cercaria and schistosomula and is located in the schistosomula surface. Despite humoral and cellular immune responses triggered by vaccination using rSm16 associated with either Freund's or alum adjuvants, immunized mice presented no reduction in either parasite burden or parasite egg laying. Knockdown of *Sm16* gene expression in schistosomula resulted in decreased parasite size *in vitro* but had no effect on parasite survival or egg production *in vivo*. Thus, our findings demonstrate that although the vaccine formulations used in this study succeeded in activating immune responses, these failed to promote parasite elimination. Finally, we have shown that Sm16 is not vital for parasite survival in the definitive host and hence may not represent a suitable target for vaccine development.

1. Introduction

Schistosomiasis is a neglected tropical disease with an important impact on public health [1]. The development of an effective vaccine formulation against the disease would help to control its transmission [2, 3]. However, this is hampered by the complexity of both the parasite and its life cycle [4, 5], as well as by the poor knowledge regarding the biological

function of vaccine target antigens, and the mechanisms and components of the host's immune system involved in parasite elimination [6].

The skin is the first barrier confronted by schistosome parasites during infection of the definitive host. In fact, how parasites deal with immune factors in the skin dictates their survival in the host [7, 8]. Though the host's skin contains many cells that can respond upon parasite activation, schistosomes have evolved several mechanisms to evade host immune responses. The secretion of immunomodulatory molecules by the parasite's acetabular gland, resulting in increased IL-10, IL-1ra, and PGE production by host cells, is one of such mechanisms [9–11]. Therefore, immune modulatory proteins secreted by the parasite represent an interesting target for the hosts' protective immune response induced by immunization.

Sm16, also known as SPO-1 or SmSLP, is one of the most abundant components of *S. mansoni* cercarial excretion/secretion product [12]. This 16 kDa protein, which is secreted by the parasite during penetration of the mammalian host, shares 100% identity with its ortholog in *S. japonicum* [13]. Both orthologs are believed to play an important role in the suppression of cutaneous inflammatory responses during parasite penetration of the host skin [10, 13], thus facilitating parasite survival. Among the modulatory mechanisms induced by Sm16, inhibition of IL-2 production by lymph node cells from *S. mansoni* infected mice and increased production of IL-1ra by human keratinocytes have been described [10]. Additionally, Sm16 inhibits macrophage activation (due to retention of internalized antigen in early endosomes, causing a delay in antigen processing and presentation), consequently inhibiting the activation of the host adaptive immune response [14]. Sm16 also inhibits TLR-3 and TLR-4 signaling in human monocytic cell lines [15] and exerts an immunodulatory function even under LPS stimulation, inhibiting neutrophil infiltration to the site of LPS inoculation [16].

Although several studies have shown that Sm16 and its *S. japonicum* ortholog modulate inflammation *in vitro* and *in vivo* [10, 13–15, 17], the exact function of these proteins in the establishment of parasitism in the host is still not well understood. Herein, we expressed a recombinant form of Sm16 (rSm16) and raised polyclonal antibodies against it. We then evaluated the expression of Sm16 during the different parasite life-cycle stages associated with the definitive host and also evaluated the presence of this antigen on the parasite surface. The effect of the immune response triggered against Sm16 on parasite reproduction and survival was evaluated. Moreover, we explored the biological function of this protein during the course of experimental infection using RNA interference- (RNAi-) based gene knockdown. We observed that Sm16 is mainly expressed in the schistosomula life-cycle stage and is located on the external surface of the parasite. Although immunization of mice with different vaccine formulations was able to activate both cellular and humoral arms of the immune response, both formulations failed to induce protective immunity. Finally, knocking down the expression of Sm16 resulted in a decreased schistosomula size until day 4 of parasite culture *in vitro*, but the lack of Sm16 expression had no effect on parasite survival or egg production *in vivo*.

2. Methods

2.1. Mice and Parasites. Balb/c male and female mice (*Mus musculus*) aged 6-8 weeks were obtained from the Institute René Rachou (CPqRR)/FIOCRUZ (Fundação Oswaldo Cruz) animal facility. The *Schistosoma mansoni* LE strain is routinely maintained in the Mollusk Room "Lobato Paraense" at Instituto René Rachou (FIOCUZ/MG). *Schistosoma mansoni* cercariae were obtained by exposing infected *Biomphalaria glabrata* snails to light for 1-2 hours to induce shedding. For RNAi assays, and western blotting analysis, cercariae were mechanically transformed into schistosomula of cercariae [18] and were cultured in Glasgow Mem (GMEM) (Sigma-Aldrich, Germany) supplemented as previously described [19]. Infected mice were perfused and adult worms were recovered from the hepatic portal system, while the livers of the same animals were removed for egg recovery. Protocols using animals were licensed by the Ethics Committee of Animal Use (CEUA) of FIOCRUZ under licenses LW25/15 and LW22/16.

2.2. Recombinant Antigen Preparation. The fragment of the DNA sequence corresponding to the region encoding amino acids 23 to 90 of the *S. mansoni* Sm16 protein (GenBank: AAD26122.1 and WormBase ParaSite: Smp341790) was used to construct a synthetic gene for expression in *Escherichia coli*. According to Holmfeldt and colleagues [20], this sequence results in a recombinant protein, which is less prone to aggregation and is highly expressed in *E. coli*. A bacterial codon-optimized synthetic *Sm16* gene containing the restriction sites for the enzyme *BamH*I and *Xho*I at the 5′ and 3′ ends, respectively, was obtained from a commercial supplier (GenScript, Piscataway, NJ, USA) inserted into a pUC57 vector. An initiation codon ATG was inserted between the *BamH*I restriction site and the codon corresponding to the first amino acid of rSm16. This construct was subcloned into the *BamH*I/*Xho*I sites of the pET21a plasmid (Novagen) and transfected into *E. coli* BL21 (DE3).

In order to express and obtain rSm16, transformed cells were cultured overnight at 37°C in liquid LB medium (Kasvi) supplemented with 100 μg/ml ampicillin (Sigma-Aldrich). A volume of 10 ml of this overnight starter culture was used to inoculate 1000 ml of fresh LB medium containing 100 μg/ml ampicillin. When the OD_{600} reached approximately 0.6, protein expression was induced by the addition of 1 mM IPTG (Promega) and allowed to proceed for 4 hours at 37°C. Cells were harvested by centrifugation at 5000 × g for 20 minutes and the supernatant was discarded. The cell pellet was resuspended in lysis buffer (50 mM Tris (GE-Healthcare), 500 mM NaCl (Êxodo Científica), 0.2 mM EDTA (Química Moderna), 3% sucrose (Synth), and 1% TritonX-100 (Sigma-Aldrich)), containing 200 μg/ml lysozyme (Sigma-Aldrich), 1 mM phenylmethylsulfonyl fluoride (PMSF) (GE Healthcare), and 20 μg/ml deoxyribonuclease I from bovine pancreas type IV (DNase) (Sigma-Aldrich). Proteins were extracted by sonication in an ultrasonic processor (VC 750

Vibra-Cell™) by 5 cycles of a 30 sec pulse using 30% output followed by 1 min on ice. The lysate was clarified by centrifugation at 15000 × g for 30 minutes and the supernatant collected for His-tag protein purification by affinity chromatography using a nickel column QIAexpress Ni-NTA Fast Start Kit (Qiagen) under denaturing conditions. The purified protein was dialyzed against PBS at pH 7.2 using the Mini Dialysis Kit 1 kDa cut-off (GE HealthCare) and quantified using the BCA Protein Assay Kit (Thermo Scientific Pierce, Rockford, IL, USA).

The expression and purification of rSm16 were analyzed by 15% SDS-PAGE, as described by Laemmli [21]. The protein was blotted onto nitrocellulose membrane (GE Healthcare) as described by Towbin et al. [22], followed by blocking with 5% dry milk at 4°C for 16 hr. After washing, the membrane was incubated with monoclonal 6x-His-tag antibody (1 : 3,000) (GE Healthcare) for 1 hr at room temperature, and after three washes in 0.05% Tween 20 in TBS (TBS-T) (LCG Biotecnologia), the membrane was incubated for 1 hr with horseradish peroxidase- (HRP-) conjugated goat anti-mouse IgG antibody (SouthernBiotech) (1 : 5,000). The reaction was developed using 3-3′-diaminobenzidine tetrahydrochloride substrate (Sigma-Aldrich).

2.3. Production of Anti-Sm16 Polyclonal Antibodies. In order to obtain Sm16-specific polyclonal antibodies, female Balb/c mice (six to eight weeks) were inoculated subcutaneously with 25 μg of rSm16 plus Freund's complete adjuvant in the first dose and Freund's incomplete adjuvant in the two subsequent doses (with a 15-day interval between each dose). The control group was inoculated with saline plus Freund's adjuvant. Serum samples were obtained every 15 days after the first immunization and titrated by enzyme-linked immunosorbent assay (ELISA).

2.4. Western Blotting Analysis. Protein extracts from different stages of the *S. mansoni* life cycle, cercariae, 3-hour cultured schistosomula, 7-day cultured schistosomula, adult worms, and eggs, were obtained by lysis of the parasites in lysis buffer (8 M urea, 2 M thiourea, 4% CHAPS, 20 mM Tris, 500 mM DTT, and protease inhibitor (GE Healthcare)). After homogenization under continuous agitation for 2 hrs at room temperature, followed by 10 repeated passages through a 31G hypodermic needle, the homogenate obtained was centrifuged at 20,000 × g for 30 min at 25°C and the supernatant was collected. Protein extraction from eggs was improved by crushing eggs with a pestle. After protein quantification using the Bradford protein assay, 10 μg of protein extract from each stage was loaded into two identical 15% SDS-PAGE gels. One gel was stained by Coomassie Blue R-250, and the other gel was blotted onto the nitrocellulose membrane, as described above. The membrane was blocked for 16 hours at 4°C and incubated with hyperimmune serum against rSm16 (1 : 200) for 1 hr. After the washing step, the membrane was incubated for 1 hr with a horseradish peroxidase- (HRP-) conjugated goat anti-mouse IgG antibody (Amersham ECL Anti-Mouse IgG) diluted 1 : 5,000. After a further washing step, protein expression was detected with a chemiluminescent substrate using the ECL Prime Western Blotting Detection Reagent (GE Healthcare) using an ImageQuant LAS 4000 (GE Healthcare). The quantification of protein expression was performed by densitometric analysis using the ImageJ software (version 1.51p), and the Coomassie Blue-stained SDS-PAGE gel was used to normalize protein loading.

2.5. Immunolocalization of Sm16. Schistosomula were incubated for either 90 min or 3 hrs in supplemented RPMI medium (3% streptomycin/penicillin and 5% FBS) or seven days in GMEM supplemented medium. Approximately 1,000 schistosomula were fixed with 1% formaldehyde in PBS for 1 hr at 4°C. The schistosomula were then incubated in blocking solution (1% BSA in PBS) for 30 min and then incubated with agitation with either anti-Sm16 hyperimmune or control serum diluted 1 : 100 in blocking solution for approximately 16 hrs. After a washing step, the schistosomula were incubated for 2 hrs at room temperature with PE-conjugated rat anti-mouse IgG1 antibody (BD Pharmingen) diluted 1 : 80 in blocking solution. As a specificity control, some schistosomula were incubated with only the secondary antibody. The parasites were washed with PBS, mounted in antifading medium, and examined using a fluorescence microscope (LSM 510 Carl Zeiss).

2.6. Vaccination Protocol. Female six-eight-week-old Balb/c mice were immunized by subcutaneous route (12 animals/group) with rSm16 (25 μg/animal/dose) plus alum adjuvant (1 mg/animal/dose), or Freund's adjuvant (100 μl/animal/dose). In the first dose, mice were immunized with complete Freund's adjuvant (CFA), and in the subsequent boosters, incomplete Freund's adjuvant (IFA) was used. The control groups were inoculated with saline plus alum or saline plus Freund's adjuvant. Mice received three doses in a fifteen-day interval regimen. Animals were challenged through percutaneous infection with 100 cercariae (LE Strain) 15 days after the last dose. Fifty days after infection, animals were perfused by portal veins and adult worms were obtained as previously reported [23, 24] (SFig1). Briefly, animals were euthanized; a solution containing saline plus 500 units/l of heparin was pumped into the aortic artery and worms were collected from the hepatic portal vein. The number of worms was counted using a stereomicroscope. The protection levels were calculated by comparing the number of worms recovered from the immunized group with its respective control group using the following formula:

$$\mathrm{PL} = \frac{\mathrm{BCG} - \mathrm{BIG}}{\mathrm{BCG}} \times 100, \quad (1)$$

where PL is the protection level, BCG is the parasite burden of the control group, and BIG is the parasite burden of the immunized group. The results were analyzed using unpaired Student's t-test with 95% confidence level.

2.7. Histopathological Analysis and Egg Counts from the Gut and Liver. The gut and liver from each mouse from both the control and rSm16-immunized groups were removed after perfusion. These organs were weighed and digested with 10% KOH for 16 hrs at 4°C and for 30 min at 37°C. The eggs

were obtained by centrifugation at 900 × g for 10 min and resuspended in 1 ml of saline. The number of eggs was counted using a light microscope. The results were analyzed using either the unpaired Student's *t*-test or the Mann-Whitney test for parametric and nonparametric data. For both tests, a 95% confidence level was used.

In order to evaluate the effect of immunization on granuloma formation, a section of the left lateral lobe of the liver of control and rSm16-immunized mice were collected and fixed in 4% buffered formaldehyde in PBS. Histological sections were performed using a microtome and the slides were stained with Gomory trichrome. The granuloma area was determined as described by Alves and collaborators [25]. Briefly, approximately 100 granulomas were evaluated for each group. Only granulomas at the exudative-productive stage with a well-defined egg were evaluated using a 10x objective lens. The granuloma area was calculated using the AxioVision version 4.8 image analysis software (Carl Zeiss MicroImaging GmbH, Germany) and expressed in square micrometers (μm^2). The results were analyzed using either the unpaired Student's *t*-test or the Mann-Whitney test for parametric and nonparametric data. For both tests, a 95% confidence level was used.

2.8. Antibody Assessment. Individual sera from the mice in each immunized group were obtained 15 days after each immunization dose. ELISA was performed to evaluate the production of specific anti-rSm16 IgG, IgG1, and IgG2a antibodies. Briefly, MaxiSorp 96-well microtiter plates (Nunc, USA) were coated with 5 μg/ml rSm16 in carbonate-bicarbonate buffer (pH 9.6) for 16 hrs at 4°C. The plates were blocked with 300 μl/well of 0.05% Tween-20 in phosphate-buffered saline (pH 7.2) (PBST) plus 10% FBS for 2 hrs at room temperature. One hundred microliters of each serum sample, diluted 1 : 800 in PBST to evaluate IgG and IgG1, or 1 : 400 for IgG2a, were added to the plates and incubated for 1 hr at room temperature (RT). After six washes with PBST, HRP-conjugated goat anti-mouse IgG (1 : 10,000), IgG1, (1 : 10,000), and IgG2a (1 : 12,000) (Southern Biotech, USA) were added and incubated for 1 hr at RT. The color reaction was obtained by addition of TMB substrate (Microwell Peroxidase Substrate System, Bio-Rad, USA) and stopped with 5% sulfuric acid. The absorbance was detected at 450 nm using an ELISA plate reader (Bio-Rad, USA), and the data were analyzed using a two-way ANOVA ($P < 0.05$) followed by Tukey's multiple comparison test with a 95% confidence level. Endpoint antibody titers were determined using a pool of sera samples from each group. The pool of sera from each group was serially diluted in PBST from 1 : 50 to 1 : 1,638,400. The cut-off point for seropositivity was determined using the mean absorbance observed in blank wells plus two standard deviations. The endpoint titer was determined as the last dilution in which the observed absorbance was above the cut-off point.

2.9. Immunophenotypic Analysis. Analysis of the cellular immune response was performed using blood samples from mice, collected 15 days after the third vaccine dose. Red cells were lysed using ACK lysing buffer, washed twice with apyrogenic saline, and adjusted to 1×10^6 cells/well. Thereafter, cells were incubated with anti-CD16/CD32 antibodies (clone 2.4G2, BD Bioscience, USA) to block antibody binding to FcγR. Surface molecules were labeled by incubating the cells for 30 min with monoclonal antibodies using one of the following two combinations: (i) anti-CD19 conjugated to PE-Cy7 (clone IM7, BD Pharmingen), anti-CD3 conjugated to FITC (clone BM8, eBioscience), and anti-CD27 conjugated to biotin (clone LG.7F9, eBioscience) or (ii) anti-CD4 conjugated to FITC (clone GK1.5, BD Pharmingen) and anti-CD44 conjugated to APC (clone IM7, BD Pharmingen). Then, the cells were washed, and those of the first combination were incubated for 20 min with streptavidin APC-Cy7 (1 : 1000) for 15 min at 4°C. After a washing step, cells were acquired using a LSRFortessa flow cytometer (Becton Dickinson, San Jose, CA). Data were analyzed using FlowJo software 10.0 (Tree Star, Ashland). The results were analyzed using one-way ANOVA or Kruskal-Wallis test followed by Holm-Sidak's or Dunn's multiple comparison tests for parametric and nonparametric data, respectively. For both tests, a 95% confidence level was used. Samples that had a reduced number of acquired events, interruption of the flow during acquisition, or an excessive number of doublets were excluded from the analysis.

2.10. Cytokine Analysis. To assess cytokine production, plasma obtained 15 days after the last immunization dose was used in CBA-based flow cytometry. For this, the anti-mouse Cytometric Bead Array (CBA) Th1/Th2/Th17 Kit (BD Pharmingen, USA) was used according to the manufacturer's protocol. Data acquisition was performed in a FACS-Verse flow cytometer (BD, USA) and analyzed using FCAP Array Software (Becton Dickinson). The results were analyzed using either one-way ANOVA or the Kruskal-Wallis test, followed by either Holm-Sidak's or Dunn's multiple comparison tests, for parametric and nonparametric data, respectively. For both tests, a 95% confidence level was used.

2.11. Double-Stranded RNA Synthesis and Parasite Exposure. The sequences of the primers used to amplify the fragments for double-stranded RNA (dsRNA) synthesis and quantitative real-time PCR (RT-qPCR) were designed using the Primer 3 program (v.0.4.0) (bioinfo.ut.ee/primer3-0.4.0) and purchased from Integrated DNA Technologies Inc. (Coralville, IA). A T7 promoter sequence was added to the 5′-end of the dsRNA's designed primers. A 248 bp fragment of *Sm16* gene was amplified by PCR using the following primers: forward 5′aatacgactcactatagggCCTCACCCGAG TGAAAAAGA3′ and reverse 5′taatacgactcactatagggAATC CTTGGAAGACGCATTG3′. Total RNA from schistosomula was used for cDNA synthesis, and the latter as a template for *Sm16* amplification. Thereafter, the amplicon was Sanger sequenced to confirm the *Sm16* fragment identity using the BigDye™ Terminator v3.1 Cycle Sequencing Kit and an ABI 3730 DNA Analyzer**.** As a RNAi nonspecific control, a 360 bp fragment of the green-fluorescent protein (GFP) gene was amplified from the pCRII-GFP plasmid vector (Thermo Fisher Scientific, USA) using the primers GFP_

dsRNA_Forward 5′taatacgactcactatagggGTGTTCAATGC TTTGCGAGA3′ and GFP_dsRNA_Reverse 5′taatacgactcactatagggCTTTTCGTTGGGATCTTTCG3′.

The dsRNAs were synthesized using the PCR products and the T7 RiboMAX™ Express RNAi System Kit (Promega, USA), according to the manufacturer instructions. The syntheses were performed overnight at 37°C. Sample concentration was determined using a Nanodrop Spectrophotometer ND-1000 (Thermo Fischer Scientific, USA), and the integrity of the dsRNA was assessed by 1% agarose gel electrophoresis.

Mechanically transformed schistosomula were exposed to 200 nM of dsRNA (*Sm16* or *GFP*) in 6-well plates containing approximately 12,000 parasites in supplemented GMEM medium (3,000/ml). The same number of parasites was incubated in supplemented GMEM only. The cultures were maintained at 37°C, 5% CO_2, and 95% humidity for up to seven days after dsRNA exposure.

2.12. Gene Expression Analyses. Each day, 4,000 schistosomula were removed from the cultures used for RNAi for the analysis of relative gene expression using quantitative real-time PCR (RT-qPCR). The RNA extractions were carried out using TRIzol Reagent (Thermo Fisher Scientific, USA), as recommended by the manufacturer. Residual DNA was removed by DNase digestion using Turbo DNase (2 U/μl) (Thermo Fisher Scientific, USA). RNA was quantified using the Qubit 2.0 Fluorometer (Thermo Fischer Scientific, USA), and cDNA was synthesized using the ImProm-II™ Reverse Transcription System (Promega), according to manufacturer instructions. The RT-qPCR experiments were carried out in technical triplicates in the ViiA7 System (Thermo Fischer Scientific, USA) using Power SYBR® Green Master mix (Applied Biosystems, USA) and primers to amplify a 72 pb *Sm16* fragment (forward 5′ACGCCAATT ATCTTCGCTGT3′ and reverse 5′TTGCTCTAACGTTG TAGCTGTGA3′). A fragment of 53 pb from *Smgapdh* (Smp-056970) was used as endogenous normalization control (forward 5′TCGTTGAGTCTACTGGAGTCTTTA CG3′ and reverse 5′AATATGAGCCTGAGCTTTATC AATGG3′). The reactions were performed in a 20 μl final volume and after performing a concentration curve following the MIQE guideline recommendations [26]. The optimal concentration of primers was established 1500 nM for the *Sm16* and 900 nM for the *gapdh*. Post-RNAi *Sm16* transcript levels were assessed using the relative $2^{-\Delta\Delta Ct}$ method [27] and calculated as a percentage of difference compared to the *GFP* unspecific control. Experiments were conducted at a Real-Time PCR Facility/RPT09D PDTIS/René Rachou Institute/FIOCRUZ MG.

2.13. In Vitro and In Vivo RNAi Experiments. Schistosomula exposed to medium only, or *Sm16* or *GFP* dsRNA, were examined every two days for evaluation of phenotypic alterations using an inverted fluorescence microscope (Axio Observer, Carl Zeiss). Characteristics, such as parasite surface area, color, motility, and viability, were evaluated. Images of two fields from each sample, containing approximately 100 schistosomula, were captured, and the area (μm^2) of each schistosomulum was determined using AxioVision version 4.8 software. Four independent experiments were performed to generate the data that was analyzed using a Kruskal-Wallis test followed by Dunn's multiple comparison test at a 95% confidence level.

To monitor parasite viability, 5 μg/ml propidium iodide (Sigma-Aldrich) was added to approximately 100 schistosomula, and the stained parasites were observed using a fluorescence microscope with a 544 nm filter (Carl Zeiss). The results from four biological replicates were analyzed using two-way ANOVA followed by Tukey's multiple comparison test at a 95% confidence level.

After parasite exposure to *Sm16* or *GFP*-dsRNA for 2 days, approximately 270 schistosomula were subcutaneously inoculated into 6-to-8-week-old Balb/c male mice. Untreated schistosomula were also inoculated as a control. Overall, 12 mice were used for each of the 3 treatment groups, per each of the two independent biological replicates performed. After 50 days, adult worms were recovered by perfusion of the hepatic portal system from mice. The liver and gut from mice were also obtained, weighed, and digested with 10% KOH solution for subsequent determination of the egg number. The data were analyzed using either one-way ANOVA or the Kruskal-Wallis test, followed by either Holm-Sidak's or Dunn's multiple comparison tests, for parametric and nonparametric data, respectively. For both tests, a 95% confidence level was used.

3. Results

3.1. Expression and Purification of the rSm16 Protein. In order to obtain rSm16, we choose to express the fragment of the Sm16 protein corresponding to amino acids 23-90 in an *E. coli* system (Figure 1(a)). The DNA sequence of the synthetic gene was optimized for expression in prokaryotic systems through changing the native codons to those preferentially used by *E. coli*, as represented in Figure 1(b). A protein of approximately 15 kDa, corresponding to expected molecular weight of rSm16, was purified from the bacterial lysate after 4 hours of IPTG induction, using nickel-affinity purification. A high purity fraction of rSm16 was observed in a Coomassie Blue-stained SDS-PAGE (Figure 1(c)). The His-tag fused to rSm16 was recognized by a monoclonal 6x-His-tag antibody, indicating the correct expression of 15 kDa recombinant protein from the designed gene sequence (Figure 1(c)).

3.2. Sm16 Is Present in the Schistosomula Tegument and Is More Expressed in Cercariae and Early Transformed Larval Stages. Sm16 has previously been shown to have low immunogenicity in mice immunized with either the *Sm16* gene or recombinant protein [17]. Here, to test the immunogenicity of rSm16 (23-90), mice were immunized with three doses of recombinant antigen combined with Freund's adjuvant. Significant production of specific antibodies was observed in immunized mice after both the second and the third immunizations (SFig.2). The endpoint antibody titer observed after two immunization doses was 1 : 51,200, and

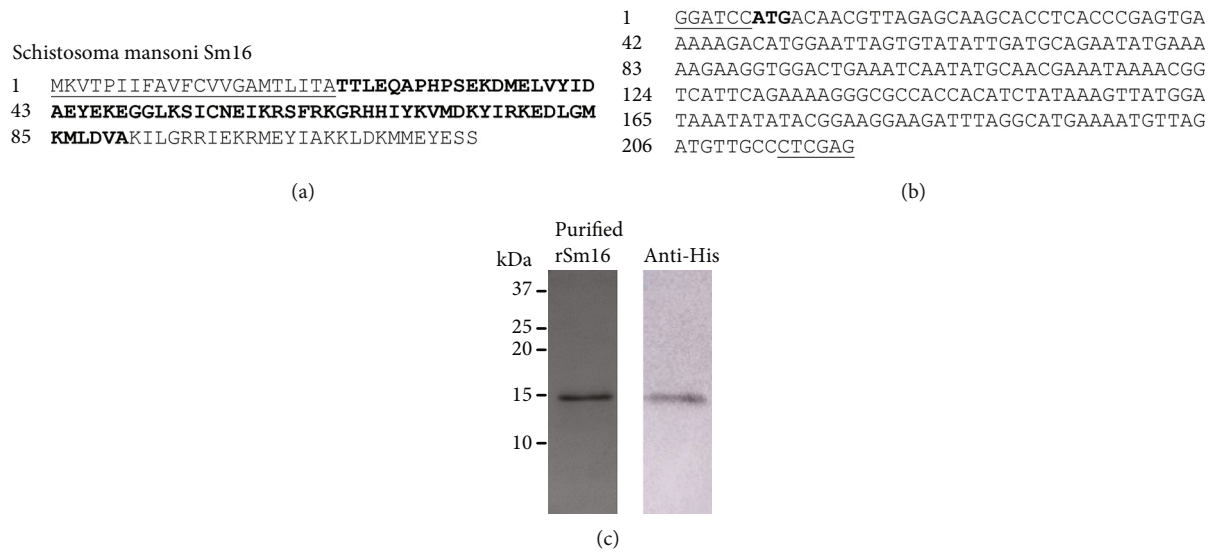

Figure 1: Purification of recombinant Sm16. (a) Amino acid sequence of *Schistosoma mansoni* Sm16 (GenBank: AAD26122.1 and WormBase ParaSite: Smp_341790). The signal peptide is underlined and the sequence in bold corresponds to amino acids 23 to 90. (b) Synthetic gene construction containing the DNA sequence corresponding to the region encoding the amino acids 23 to 90 with restriction enzyme sites *BamH*I and *Xho*I at the 5′ and 3′ ends, respectively, and the initiation codon ATG in bold. (c) 15% SDS-PAGE of purified rSm16 stained by Coomassie Blue R-250 and Western blot using monoclonal 6x-His-tag antibody. Molecular weight markers Dual Color (Bio-Rad) are indicated in kDa.

30 days after the third immunization, there was an increase of eightfold in the antibody's endpoint titer against rSm16.

The polyclonal antibodies obtained after the third immunization dose were used to assess the Sm16 expression throughout the parasite stages associated with the vertebrate host (cercaria, schistosomulum, adult worms, and eggs). Densitometric analysis demonstrated that cercariae and recently transformed schistosomula (3 hours) express approximately 2-fold higher levels of Sm16 than 7-day-old schistosomula. In adult worms and egg extract, no protein expression of Sm16 could be detected (Figure 2(a)). By immunofluorescence of whole fixed schistosomula, we detected Sm16 on the parasite surface. Antibodies against rSm16 specifically recognized the native form of this protein on the surface of schistosomula at 90 min, 3 h, and 7 days after transformation (Figure 2(b)). Neither the control serum (Figure 2(b)), nor the secondary antibody recognized Sm16 (data not shown).

3.3. rSm16/Alum Vaccine Formulation Induced a Stronger Humoral Immune Response than rSm16/Freund's. The ability of the Sm16 recombinant protein to elicit an immune response in the vertebrate host was evaluated using two distinct vaccine formulations: rSm16 administered with either Freund's adjuvant or alum. Immunophenotyping was performed using the blood from mice 15 days after their third immunization. The strategy used to analyze the data is presented in Figure 3(a). The rSm16/alum formulation induced a higher proportion of circulating B cells ($CD3^-CD19^+$) and a lower proportion of circulating T $CD4^+$ cells ($CD3^+CD4^+$) (Figures 3(b) and 3(c)) than either alum alone or Sm16/Freund's formulations. Mice immunized with Sm16/Freund's formulation showed a higher proportion of memory B cells compared to either Freund's alone or rSm16/alum formulations (Figure 3(d)). A higher proportion of $CD4^+$ effector cells was also observed with the Sm16/Freund's formulation compared to Sm16/alum (Figure 3(e)).

The levels of circulating cytokines in the plasma of mice inoculated with the different vaccine formulations or their respective controls were also determined. No differences in cytokine production were observed between the plasma from animals immunized with rSm16/alum in comparison with the alum-only control group (Figure 4). In contrast, mouse immunization with rSm16 plus Freund's adjuvant produced an increased level of IL-2 compared to animals inoculated with saline plus Freund's adjuvant (Figure 4(e)). In the absence of the recombinant antigen, alum and Freund's adjuvants induced different patterns of circulating cytokines. Freund's adjuvant induced higher levels of circulating IL-17, TNF-α, IFN- , IL-6, and IL-4 than alum (Figures 4(a)–4(f), respectively). Decreased levels of IL-17 and IL-6 cytokines were also observed in the plasma from mice that were immunized with Sm16/alum formulation compared to the levels of these cytokines observed in sera from Sm16/Freund's immunized mice (Figures 4(a) and 4(d), respectively). IL-10 levels were below the CBA detection limit and, therefore, could not be determined.

Mouse immunization with rSm16 administered with either Freund's or alum adjuvant induced a significant production of specific anti-rSm16 IgG, IgG1, and IgG2a antibodies compared with their respective controls, as early as fifteen days after the first immunization dose for IgG and IgG1, and fifteen days after the second dose for IgG2a (Figure 5(a)–5(c),

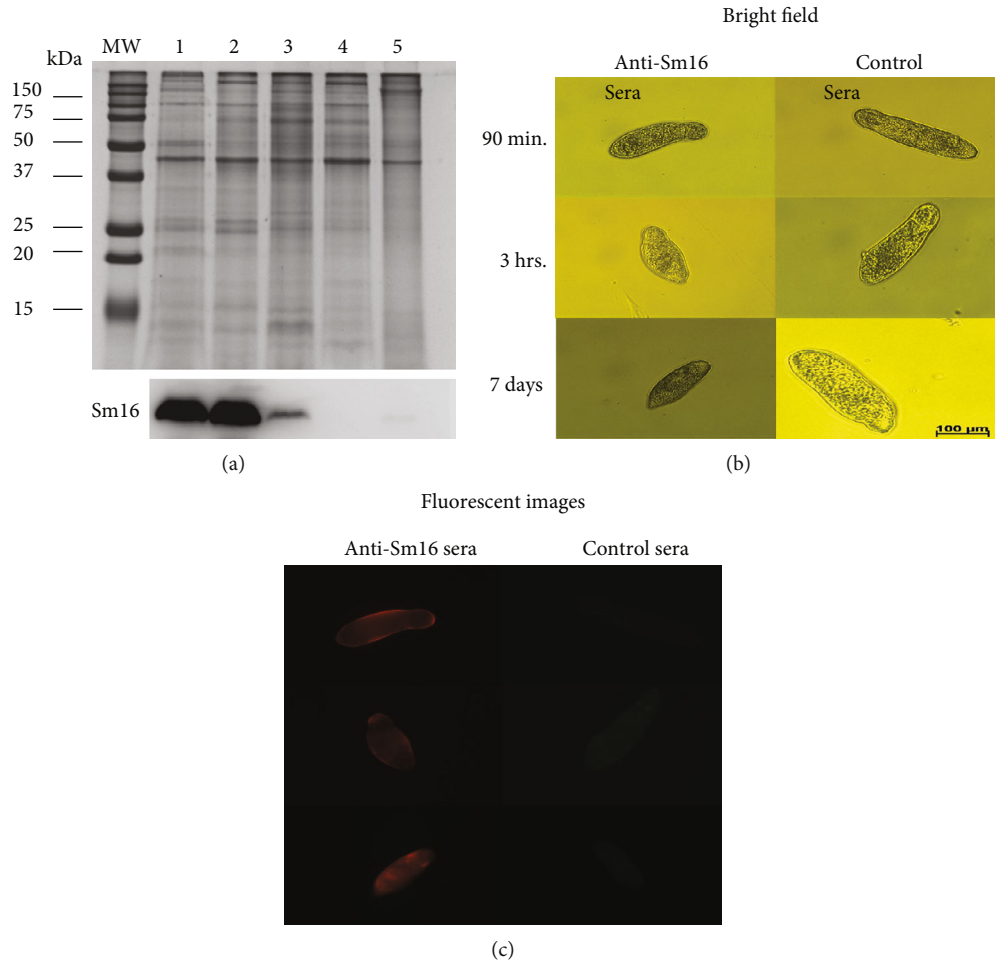

Figure 2: Expression and location of native *Schistosoma mansoni* Sm16. (a) 10 μg of total protein extract from *S. mansoni* cercariae (1), 3-hour schistosomula (2), 7-day schistosomula (3), adult worms (4), and eggs (5) were electrophoresed in a 15% SDS-PAGE and stained by Coomassie Brilliant Blue R-250 or blotted onto nitrocellulose membranes for Western blot analysis using serum from mice immunized with the recombinant Sm16 protein. Densitometric analysis was performed using the ImageJ software, and the Coomassie Blue-stained SDS-PAGE gel was used to normalize protein loading. (b) Transformed schistosomula were maintained in culture for 90 min, 3 hrs, or 7 days and were incubated with control serum, from mice inoculated with saline+CFA/IFA, or with serum from mice immunized with rSm16+CFA/IFA. Antibody reactivity to Sm16 was detected by a PE-conjugated rat anti-mouse IgG1 antibody. The schistosomula were observed by fluorescence microscopy using a LSM 510 Carl Zeiss microscope.

respectively). The levels of these antibodies, after the second and third immunization doses, increased with both formulations, in comparison to the levels observed fifteen days after the first immunization dose (Figure 5(a)–5(c)). After the second immunization dose, higher levels of anti-rSm16 IgG1 antibodies were observed in the rSm16/alum group compared to rSm16/Freund's group (Figure 5(b)). In contrast, mice immunized with rSm16/Freund's produced significantly higher levels of specific IgG2a than rSm16/alum immunized mice, after the second and third doses (Figure 5(c)). Also, after the first, second, and third immunization doses, the endpoint titer of anti-rSm16 IgG was 4-, 2-, and 2-folds higher, respectively, in mice that received the rSm16/alum formulation than those immunized with rSm16/Freund's (Table 1). Differences were also observed in the endpoint titer of rSm16-specific IgG1. Mice immunized with rSm16/alum produced 8-, 4-, and 2-folds more antibodies than the rSm16/Freund's group after the first, second, and third doses, respectively (Table 1). Both vaccine formulations produced similar titers of IgG2a against rSm16 throughout the immunization scheme.

3.4. Regardless of the Immune Response Elicited, Both rSm16 Vaccine Formulations Failed to Induce Protection against Challenge Infection. To evaluate the impact of the immune response elicited by immunization of mice with rSm16 on the parasite survival, after receiving three doses of the vaccine, mice were challenged with *S. mansoni* cercariae, and fifty days postchallenge, the parasite burden was determined. Mouse immunization with rSm16 formulated with either Freund's or alum did not result in significant reduction in parasite burden or in the number of eggs per gram of liver or gut, in both immunization trials (Table 2). Liver pathology was also not affected by immunization with the rSm16/alum formulation. However, when the rSm16/Freund's formulation was used, an increase in granuloma size was observed

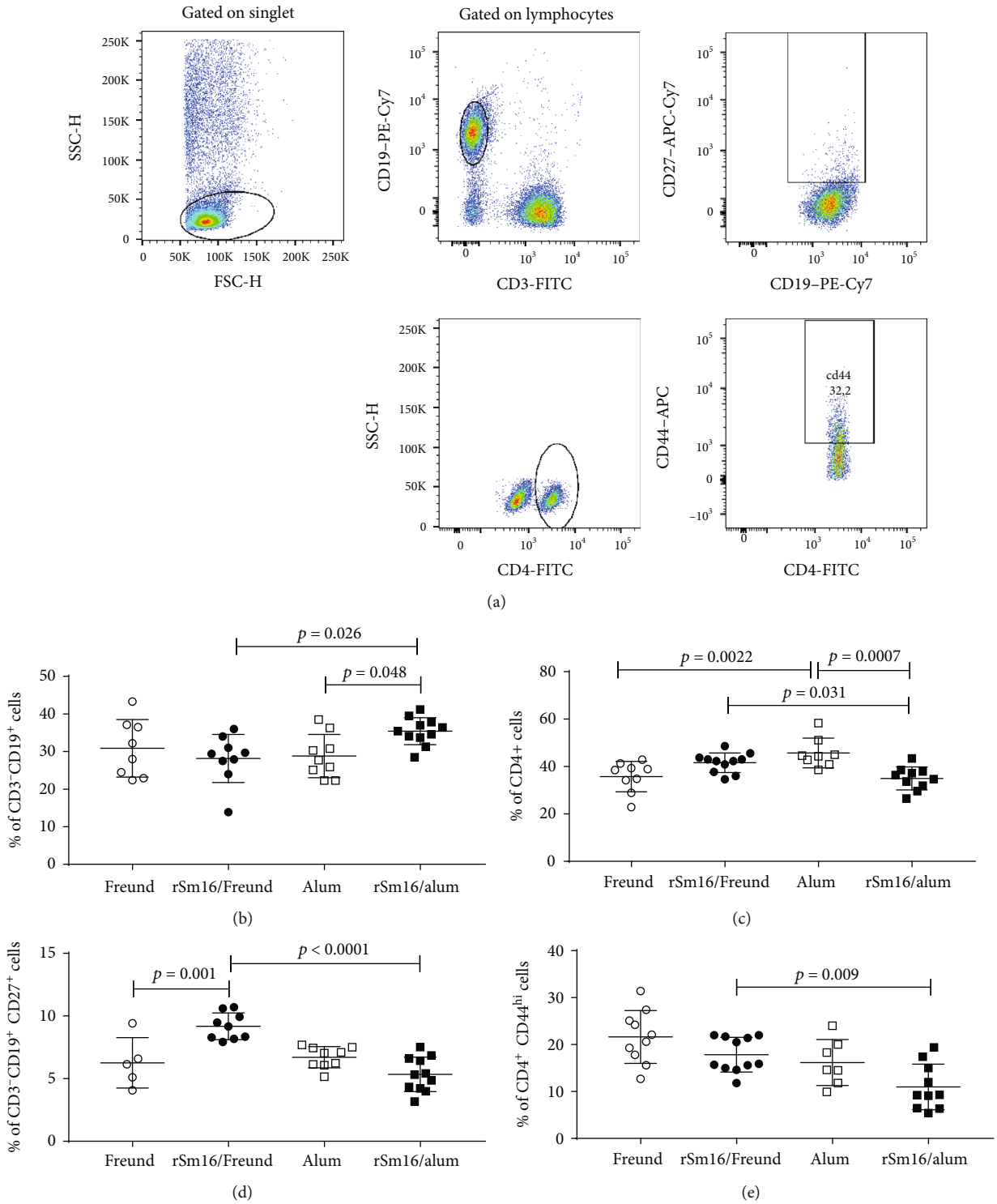

Figure 3: Immunophenotyping of blood cells from rSm16-immunized mice. Blood samples were obtained from 12 mice for each group to determine the frequency of total and memory B cells and total and effector T CD4$^+$ cells. Data analysis was carried out as demonstrated in (a). Within the singlet cells/lymphocyte population, CD3$^-$CD19$^+$ B cells were selected and the percentage of total B cells was evaluated. Within the population of CD3$^-$CD19$^+$ double-positive cells, the percentage of CD19$^+$CD27$^+$ (memory B cells) was determined. Within the singlet cell/lymphocyte population, total T CD4$^+$ were assessed and the frequencies were defined. Within that population, the percentage CD4$^+$CD44$^+$ representing CD4$^+$ T effector cells was determined. Data represents percentage of CD3$^-$CD19$^+$ B Cells (b), CD4$^+$ T cells (c), CD19$^+$CD27$^+$ memory B cells (d), and CD4$^+$CD44$^+$ effector T cells (e) in mice immunized with Freund's adjuvant only (closed circles), rSm16/Freund's (black circles), alum only (open squares), and rSm16/alum (black squares). Mean ± SD is presented in each graph. Significant differences which were observed using one-way ANOVA (c–e) or Kruskal-Wallis tests (b) followed by Holm-Sidak's (c–e) or Dunn's (b) multiple comparison tests, using a correction for multiple comparison analysis, are shown in the figures.

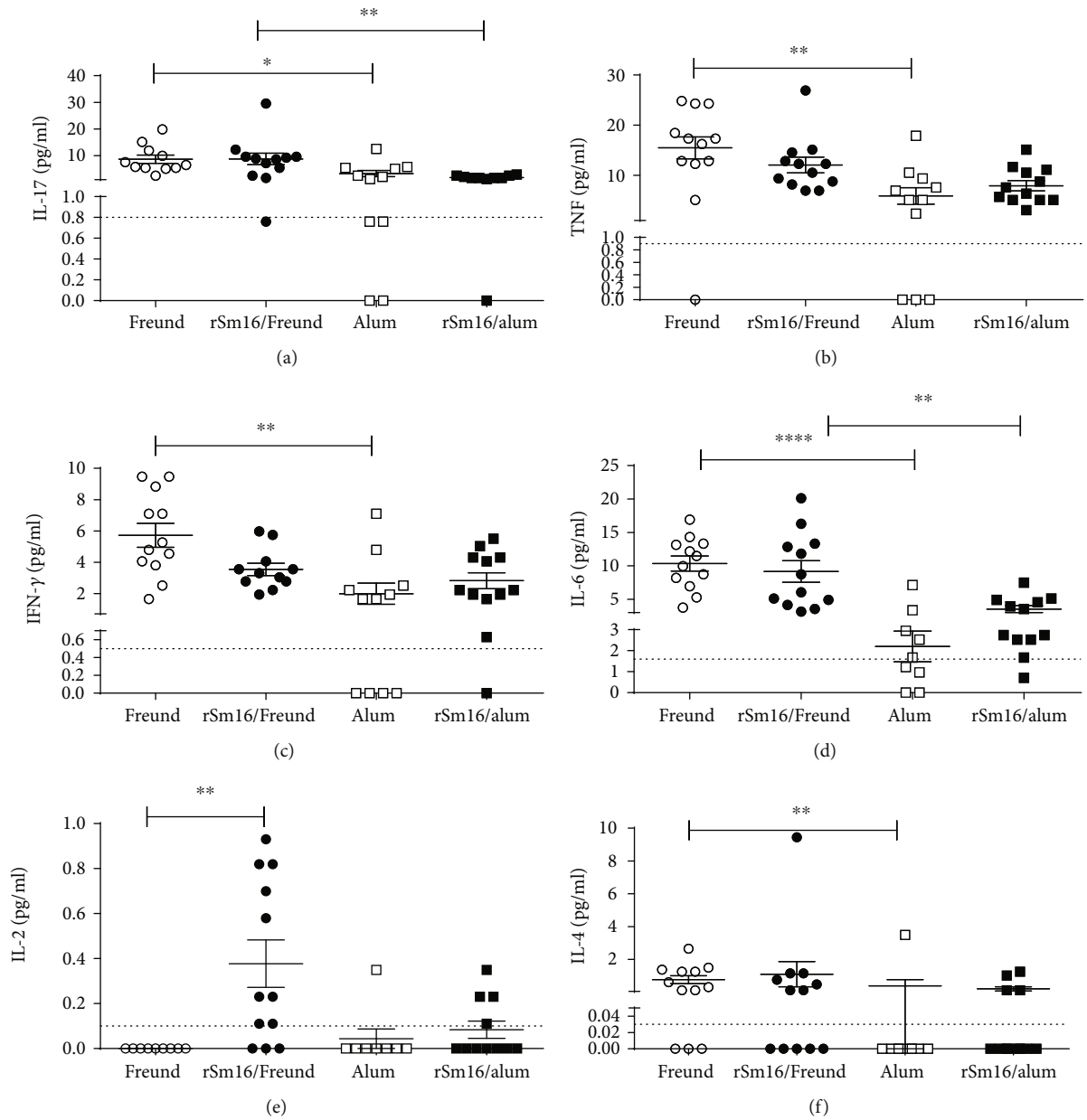

Figure 4: Cytokine profile induced in Balb/c mice immunized with rSm16. Plasma from mice immunized with different vaccine formulations was obtained fifteen days after the third immunization for cytokine measurement. (a) IL-17, (b) TNF-α, (c) IFN-γ, (d) IL-6, (e) IL-2, and (f) IL-4 production in response to immunization with Freund's adjuvant only (open circles), alum only (open squares), rSm16/Freund's (black circles), or rSm16/alum (black squares). Cytokine levels were measured using the CBA Th1/Th2/Th17 kit. Mean ± SEM is presented in the graph. Significant differences observed using one-way ANOVA (d) or Kruskal-Wallis test (a–c,e, f) followed by Holm-Sidak's (d) or Dunn's (a–c,e, f) multiple comparison tests, using a correction for multiple comparison analysis, are shown in the figures. Statistically significant differences are denoted in each graph.

in immunized mice compared to the control group (Figure 6).

3.5. Knockdown of Sm16 in Schistosomula Did Not Impair Parasite Survival in the Vertebrate Host. The use of rSm16 in vaccine formulations had no effect on parasite elimination, although an immune response was elicited by vaccination. Therefore, to further evaluate the role of Sm16 in parasite biology, we knocked down *Sm16* expression in schistosomula using RNAi methodology. Using specific *Sm16* dsRNA, the levels of *Sm16* transcripts were significantly reduced (96%) as early as 24 hours after schistosomula treatment (Figure 7(a)). The *Sm16* transcript level remained reduced (98%) until the 7^{th} day post-dsRNA treatment (Figure 7(a)). Parasite survival after reduction of the *Sm16* transcript levels was evaluated *in vitro* for 10 days. When parasites treated with *Sm16* dsRNA were compared to untreated control or to parasites treated with *GFP* dsRNA, no increment in the percentage of dead schistosomula was observed (Figure 7(b)). With regard to the impact of *Sm16* knockdown

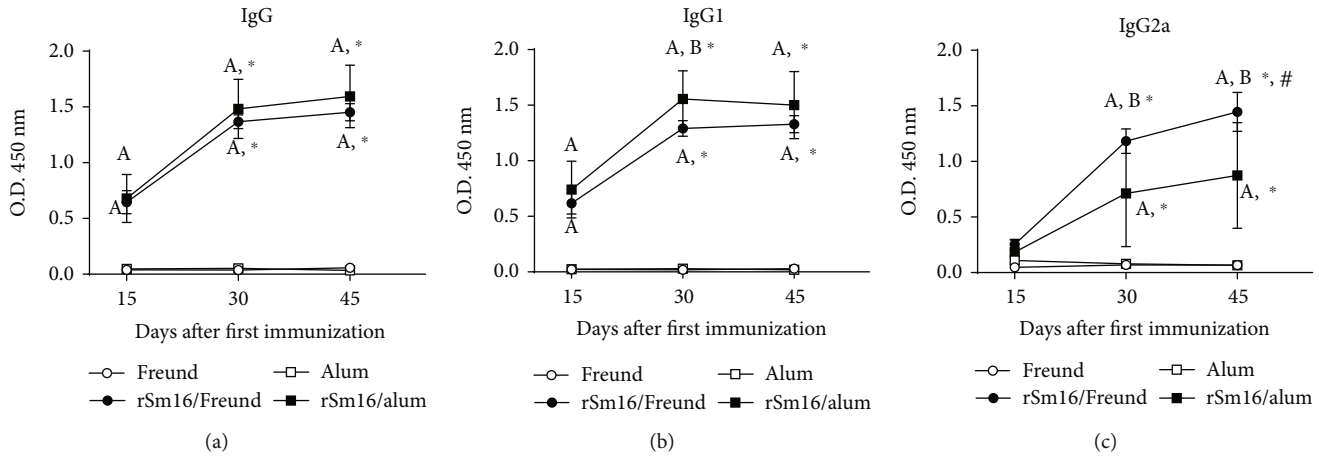

Figure 5: Production of Sm16-specific antibodies in immunized mice. Sera from mice were obtained 15 days after each immunization dose and were assessed to determine the levels of IgG (a), IgG1 (b), and IgG2a (c) antibodies against rSm16 in mice inoculated with Freund's adjuvant only (open circles), alum only (open squares), rSm16/Freund's (black circles), or rSm16/alum (black squares). Mean ± SD is presented in the graphs. Two-way ANOVA followed by Tukey's multiple comparison test was performed using a correction for multiple comparison analysis. Significant differences related to the first dose are indicated by an asterisk ($P < 0.05$) and to the second dose are denoted by symbol # ($P < 0.05$). Significant differences between the Freund's only and the alum-only control groups are denoted by the letter "A" ($P < 0.05$). Significant differences between rSm16/Freund and rSm16/alum are indicated by the letter "B" ($P < 0.05$).

Table 1: Endpoint titers of specific IgG antibodies against rSm16 in immunized mice.

	1st dose			2nd dose			3rd dose		
	IgG	IgG1	IgG2a	IgG	IgG1	IgG2a	IgG	IgG1	IgG2a
rSm16/Freund's	6,400	1,600	200	51,200	25,600	1,600	204,800	102,400	3,200
rSm16/alum	25,600	12,800	200	102,400	102,400	3,200	408,600	204,800	3,200

on parasite morphology, exposure to *Sm16* dsRNA resulted in a reduction of schistosomula size at days 2 (4.07%) and 4 (5.11%) after dsRNA treatment in comparison to the untreated group (Figures 7(c) and 7(d)), but by the sixth day postexposure to dsRNA, no significant differences in parasite morphology were observed among groups (Figure 7(e)). In order to evaluate the impact of reduced expression of the *Sm16* transcript on the establishment of infection *in vivo*, mice were subcutaneously infected with untreated schistosomula or with schistosomula treated with specific *Sm16* dsRNA or nonspecific *GFP* dsRNA. Fifty days after schistosomula inoculation, no differences in parasite burden or in the number of eggs trapped in the liver or intestine were observed (Table 3).

4. Discussion

In order to survive in the definitive host, schistosomes have evolved several immune evasion mechanisms [5]. In the skin, where the parasite first faces the host immune system, an inflammatory response is rapidly regulated by molecules secreted by the parasite [7]. Among these molecules, Sm16, also named SPO-1 or SmSLP, has been described as the major immune modulatory molecule secreted by the parasite during its penetration into the host skin [10]. Due to its potential role in parasite establishment in the host, Sm16 represents a potential target for immunization-based therapies that are aimed at eliminating the parasite.

Therefore, in this study, we produced a recombinant form of Sm16 to be used as an antigen in vaccine formulations against schistosomiasis. Sm16 has been described in the literature as a difficult protein to express in heterologous systems [15, 16, 20]. The first 22 amino acids in the N-terminal of the protein correspond to a signal peptide that drives the protein to a secretory pathway [20]. The C-terminal peptide sequence from Lys^{91} to Gly^{94} of Sm16 has also been described to promote protein aggregation, and a high yield of recombinant protein could only be obtained when the coding region for the amino acids 23-90 of Sm16 was used [15]. So, in order to obtain high yield of rSm16, we choose to express the protein region containing amino acids 23-90. The predicted molecular weight of this Sm16 recombinant protein was 11.5 kDa, but the recombinant protein showed a slow migration pattern in SDS-PAGE, as already observed for other recombinant Sm16 described by other groups [16]. Western blotting analysis of protein extracts from different parasite life-cycle stages demonstrated that Sm16 is not expressed in the adult worm or eggs, but it is more expressed in cercariae and recently transformed schistosomula, consistent with its potential biological function of modulating host immune response during skin migration [10]. Interestingly, Sm16 expression was also detected in 7-day schistosomula. Our results on Sm16 expression in parasite life-cycle stages in the vertebrate host differed from those published by Rao and Ramaswamy [16], which demonstrated Sm16 expression in adult

Table 2: Protection induced by rSm16 immunization in mice.

	Worm burden			Protection (%)	Eggs/gram of liver (mean ± SD)	Egg/gram of intestine (mean ± SD)
	Male	Female	Total			
Trial 1						
Freund's	24 ± 6	21 ± 3.4	45 ± 8.1		10,604 ± 4,197	nd
rSm16/Freund's	23 ± 4	22 ± 5.5	46 ± 9.8	0%	20,151 ± 9,698	nd
Alum	25 ± 7.6	23 ± 7.5	43 ± 13		27,796 ± 18,446	22,176 ± 8,138
rSm16/alum	20 ± 6.5	18 ± 5.7	40 ± 10	7.0%	14,870 ± 10,373	16,353 ± 4,229
Trial 2						
Freund's	24 ± 8.6	22 ± 8	46 ± 18		40,088 ± 13,835	25,451 ± 11,114
rSm16/Freund's	26 ± 6.4	21 ± 6	47 ± 14	0%	56,091 ± 21,221	39,673 ± 23,297
Alum	21 ± 6.8	18 ± 6	39 ± 11		22,019 ± 6,143	16,009 + 6,931
rSm16/alum	25 ± 6.5	21 ± 6.1	46 ± 12	0%	23,806 ± 9,331	14,111 + 2,009

nd: not determined.

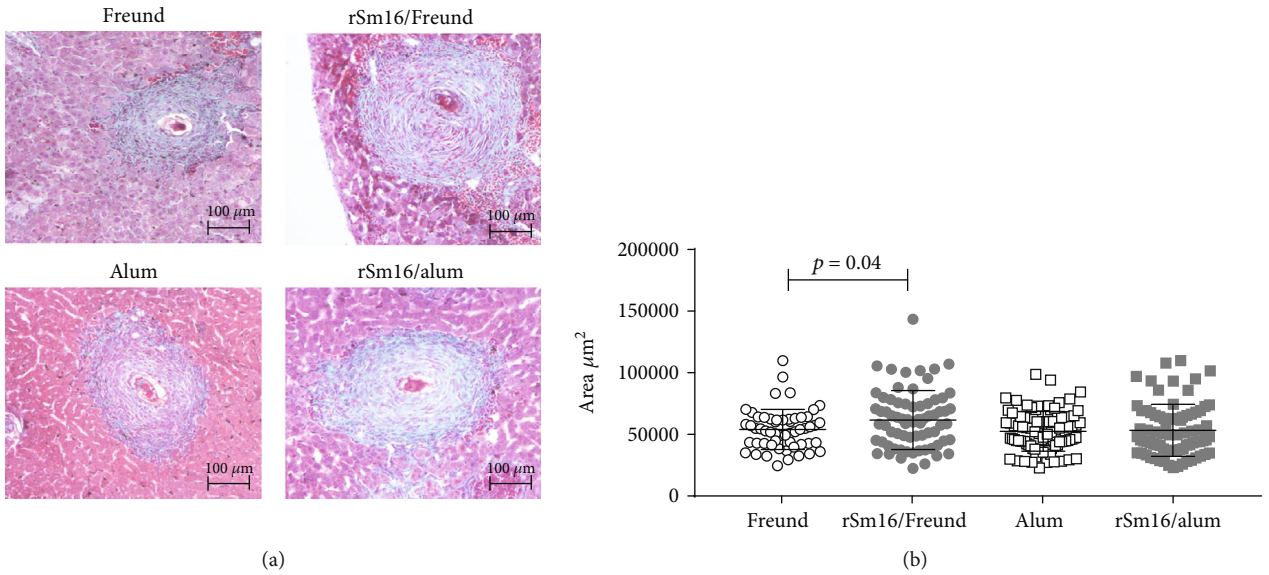

Figure 6: Hepatic granuloma area in mice immunized with rSm16. (a) Representative histological sections of liver granulomas from each immunized group. Scale bar = 100 μm (100x). (b) Approximately 100 granulomas from rSm16/Freund's (gray circles) and its Freund's only control group (open circles) and from rSm16/alum (gray squares) and its alum-only control group (open squares) with a single well-defined egg at the exudative-productive stage were randomly selected and measured. Total area of the granulomas was expressed in square micrometers (μm^2). Mean ± SD is presented in the graphs. Unpaired Student's t-test was used to analyze data from Freund's only and rSm16/Freund's groups, and the Mann-Whitney test was used to analyze data from alum-only and rSm16/alum groups. Statistically significant difference is denoted in the graph.

worms. Unlike Rao and Ramaswamy [16], who raised their polyclonal anti-Sm16 antibody using purified native Sm16 as the antigen, in our study, we used polyclonal antibodies produced against recombinant Sm16, which guarantees the specific recognition of this protein in parasite extract.

Staining of whole fixed parasites with polyclonal antibodies against rSm16 demonstrated that a considerable amount of this protein is located on the parasite surface. Sm16 is secreted by the acetabular gland during skin penetration [11] and is described as being able to interact with plasma membrane lipids, in a non-cell-specific manner [20]. This ability to interact with plasma membrane lipids may explain the location of Sm16 at the schistosomula surface, but if this interaction plays any specific role in parasite development or is only a consequence of the ability of Sm16 to interact with lipids still needs further investigation. However, it is worth noting that schistosomula which had Sm16 expression knocked down by RNAi showed reduced parasite size after two and four days in culture, suggesting that Sm16 may interact with a signaling pathway involved in parasite morphology and growth.

Sm16 is the major component of the excretory/secretory products involved in modulating the host immune response

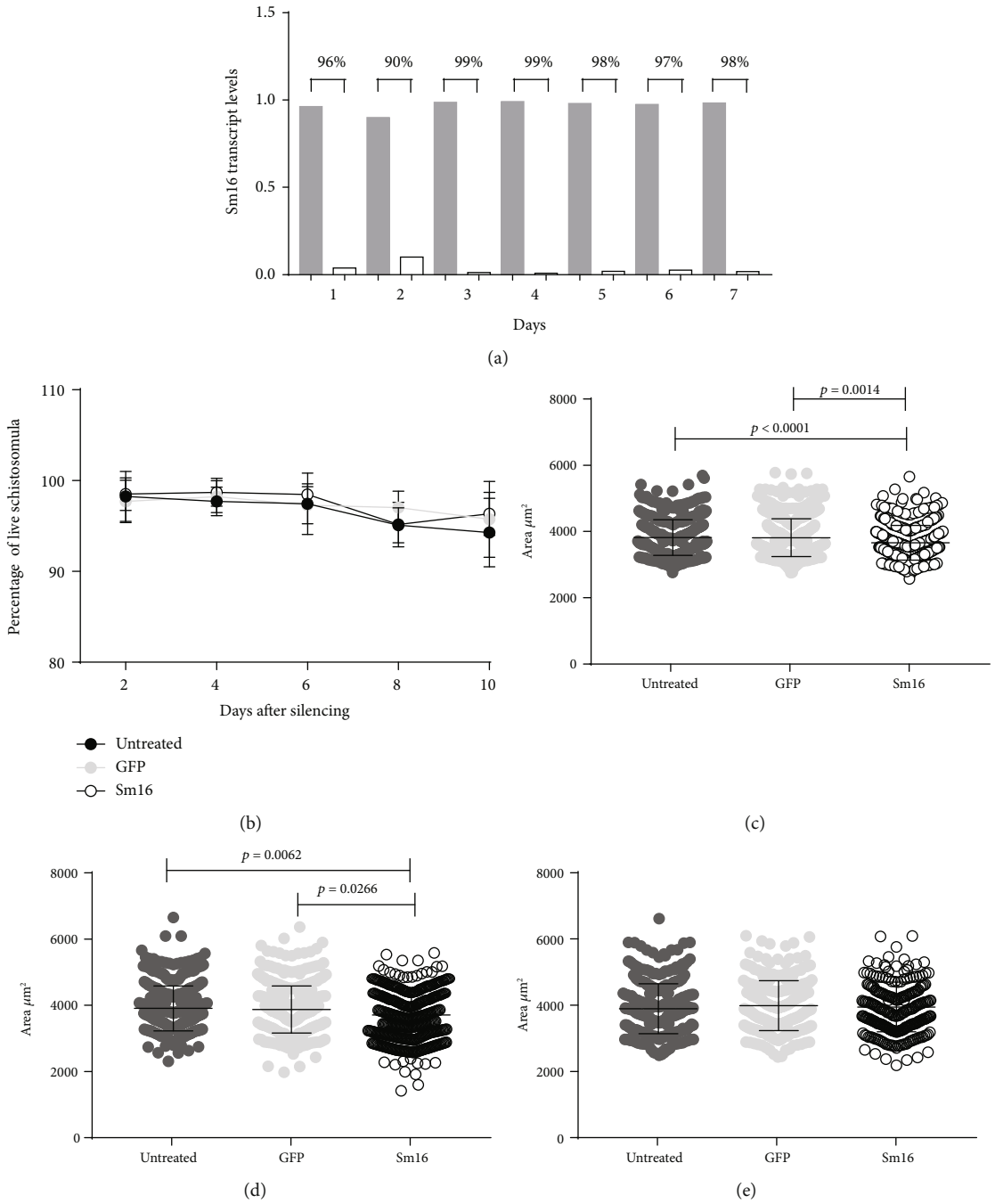

Figure 7: *In vitro* analyses of parasite development following *Sm16* knockdown. (a) Schistosomula were exposed to specific *Sm16* dsRNA and unrelated *GFP* dsRNA for seven days. The level of the *Sm16* transcript was assessed daily by RT-qPCR. Gray bars represent the expression of the Sm16 transcript on schistosomula exposed to *GFP* dsRNA and white bars to *Sm16* dsRNA. The percentage numbers represent the reduction of the *Sm16* transcript levels in schistosomula exposed to *Sm16* dsRNA relative to those exposed to *GFP* dsRNA. (b) Parasite survival after *Sm16* knockdown was evaluated *in vitro* every 2 days for 10 days. Approximately 100 schistosomula were labeled with 5 μg/μl propidium iodide and observed by fluorescence microscopy. The area of the schistosomula was evaluated two (c), four (d), and six (e) days after treatment with the dsRNA. Images of approximately 100 schistosomula were captured, and the area of each schistosomulum (μm^2) was measured using AxioVision version 4.8 software. Untreated parasites are denoted by dark gray circles. Light gray circles correspond to the control *GFP* dsRNA-treated schistosomula and open circles to specific *Sm16* dsRNA-treated schistosomula. Mean ± SD is presented in the graph. The data were generated from four independent experiments and analyzed using a two-way ANOVA followed by Tukey's multiple comparison test (b) or Kruskal-Wallis test followed by Dunn's multiple comparison test (c–e) using a correction for multiple comparison analysis. Statistically significant differences are shown in the figures.

Table 3: Reduction in the parasite burden from mice infected with *Sm16*-silenced schistosomula.

	Worm burden recovery (mean ± SD)	% reduction*	Eggs/gram of liver (mean ± SD)	% reduction#	Eggs/gram of intestine (mean ± SD)	% reduction#
Trial 1						
Control	25 ± 17		10,336 ± 4,813		3,673 ± 1,569	
GFP	30 +/-14	NS	10,274 ± 5,153	NS	6,928 ± 4,290	NS
Sm16	23 ± 13	8% (NS)	9,445 ± 4,413	8.6% (NS)	4,595 ± 2,934	NS
Trial 2						
Control	19 ± 17		10,435 ± 9,528		3,156 ± 3,575	
GFP	18 ± 10	5.3% (NS)	10,388 ± 6,407	0.5% (NS)	2,195 ± 1,460	30% (NS)
Sm16	25 ± 20	NS	12,941 ± 6,536	NS	4,679 ± 4,305	NS

*Reduction of total worms compared to control group. #Reduction of eggs in tissue (liver and intestine) compared to the control group. NS: not significant.

in order to promote parasite survival in the skin [10]. Therefore, blocking the biological function of Sm16 could result in protection of the vertebrate host against parasite infection, and antibodies against this antigen could be important factors that block the interaction of this protein with its target in the host or directly neutralize its function. On the other hand, as Sm16 was observed at the parasite surface, an ADCC mechanism could also promote parasite death. This mechanism of death has been previously described to be involved in the protective immunity induced by Smp-80 and GST immunization [28–30]. Thus, to test the ability of vaccine formulations containing rSm16 to induce protection in mice, two different adjuvants were evaluated: Freund's and alum. Freund's adjuvant has been described to induce a Th1 type of immune response, while alum induces a Th2 immune profile [31]. Indeed, we found that mouse immunization with these adjuvants in the absence of antigen induced different immunological profiles. Freund's adjuvant induced significantly higher levels of circulating cytokines (IL-17, TNF-α, IFN- , IL-6, and IL-4) than alum. The addition of the rSm16 to Freund's formulation induced a significant increase in the concentration of circulating IL-2 cytokine, whereas the Sm16/alum formulation did not induce change in the levels of any circulating cytokines evaluated. The cellular profile induced in mice by immunization was also different between the two vaccine formulations. The proportion of circulating B cells induced by the Sm16/alum formulation was higher than that by the Sm16/Freund's formulation. Nevertheless, the opposite was observed with regard to the proportion of memory B cells. The proportion of circulating $CD4^+$ T cells and $CD4^+$ effector T cells was also lower using the Sm16/alum formulation in comparison with the Sm16/Freund formulation.

Regarding specific antibody production, both vaccine formulations induced significant production of IgG, IgG1, and IgG2a anti-Sm16 antibodies, while the Sm16/alum formulation also induced the production of at least two-fold higher titers of specific IgG and IgG1 antibodies than the Sm16/Freund's formulation. Overall, these results demonstrate that the use of adjuvants in association with rSm16 was able to circumvent the immunosuppressive properties previously demonstrated for the native parasite protein, activating both cellular and humoral immune responses in vaccinated animals.

Neither the immune response triggered by Sm16/alum nor the one triggered by Sm16/Freund formulation was able to induce significant levels of protection in mice. This lack of protection cannot be attributed to the production of nonfunctional antibodies against the native form of the protein, since antibodies produced after immunization recognized the native form of the protein in protein extracts from different parasite stages, and on the schistosomula surface. But, as the C-terminal of Sm16 is lacking in our recombinant protein and since this terminal portion had been described to interact with host immune cells [15, 20], the lack of antibodies against the epitopes from this region of the protein could explain the lack of protection observed in our study. However, this hypothesis still needs to be investigated.

Analysis of the granuloma area in the liver of immunized mice demonstrated that larger granuloma sizes could be observed in mice immunized with Sm16/Freund's. Since Sm16 was not detected in the egg protein extract, this increase in the granuloma area could not be directly attributed to a response against this antigen, but rather to the immune profile observed in animals that received this formulation. Many cytokines have been described to be involved in granuloma formation and modulation. Type-2 cytokines, such as IL-5, IL-4, and IL-13, are responsible for the recruitment and activation of immune cells involved in granuloma formation, whereas IL-10 has been related to the granuloma modulation [32–34]. Another important cytokine involved in the genesis of granuloma is IL-2. Studies have shown that the blockage of this cytokine by neutralizing antibodies results in a reduction of the granuloma area associated with a decrease in IL-5 secretion by T cells [35]. The significantly greater amounts of IL-2 detected in the blood of mice immunized with Sm16/Freund's may be associated with the increased granuloma area observed in animals receiving this vaccine formulation.

Since the immune response triggered by Sm16 immunization did not successfully reduce *S. mansoni* infection, we choose to evaluate the role of this protein in parasite survival during the course of infection. The use of RNAi technology significantly reduced the levels of Sm16 transcripts in

schistosomula in comparison to the untreated group from day 1 until day 7 post-dsRNA exposure. Despite having analyzed the levels of RNA, this result is in agreement with the observation that this protein is expressed even in 7-day schistosomula, as observed in the Western blotting and immunofluorescence assays, suggesting that Sm16 expression still occurs in lung-stage parasites. Sm16 knockdown resulted in a reduction of schistosomula size *in vitro* but had no effect on *in vivo* parasite survival or egg production. Besides Sm16, other molecules secreted by the parasite during skin migration have also been described as potential immune modulators of the host immune response [12, 36], including prostaglandin E_2 (PGE2), SmGST-28 kDa, cyclophilin, and paramyosin [9, 37–40]. In the absence of the Sm16 expression, these proteins may modulate the host immune system to guarantee successful migration of schistosomula through the host skin.

In conclusion, although Sm16 could be detected on the parasite surface by antibodies produced in response to immunization using rSm16, neither the humoral nor the cellular immune responses induced by the rSm16 antigen promoted protection against infection in mice. However, since the recombinant protein used in the vaccine formulations tested in this study did not express the C-terminal part of Sm16, additional studies evaluating the Sm16 C-terminal part are still required before ruling out Sm16 as a vaccine candidate. Our study also demonstrated that decreased Sm16 gene expression in schistosomula had no significant impact in parasite survival and egg laying, suggesting that this protein is not essential for parasite survival or reproduction.

Overall, our results suggest that due to the redundancy of parasite immunosuppressive molecules in the evasion process, a vaccine that seeks to neutralize the effect of these molecules should include several vaccine targets in its formulation.

Data Availability

The data used to support the findings of this study are included within the article.

Conflicts of Interest

The authors declare no conflict of interest.

Acknowledgments

The authors thank the Program for Technological Development in Tools for Health-RPT-FIOCRUZ for use of its facilities. We also thank Dr. Alice Fusaro Faioli for proofreading this manuscript. This work was supported by Fundação de Amparo à Pesquisa do Estado de Minas Gerais/Programa de Pesquisa para o SUS-PPSUS APQ-003478-13), Fundação de Amparo à Pesquisa do Estado de Minas Gerais/Rede mineira de Imunobiológicos (RED00140-16), CNPq-Brasil (303711/2015-9 and 303131/2018-7), Coordenação de Aperfeiçoamento de Pessoal de Nível Superior-Brasil (CAPES) Finance Code 001, Programa Print-Fiocruz-Capes, and Instituto René Rachou-Fiocruz-MG. The following fellowships were also received: IRR (WPOSB); CAPES (JMA); FAPEMIG (CCA, GBC); CNPq (ITSD); Pq-CNPq (CTF, MMM).

Supplementary Materials

Supplementary Figure 1: immunization protocol. Supplementary Figure 2: Sm16-specific antibody titer endpoints in immunized mouse serum. Pools of sera from mice immunized with rSm16 plus Freund's adjuvant obtained 15 days after the second dose (black circles) or 30 days after the third dose (black square) were serially diluted, beginning at 1 : 50, and used in an ELISA assay. The threshold was calculated using the mean absorbance value of the blank wells plus two standard deviations. The arrows indicate antibody titer endpoints observed after two and three immunization doses. *(Supplementary Materials)*

References

[1] World Health Organization, *Global health estimates 2016: disease burden by cause, age, sex, by country and by region, 2000-2016*, World Health Organization, Geneva, 2018, November 2018, https://www.who.int/healthinfo/global_burden_disease/.

[2] A. Stylianou, C. Hadjichrysanthou, J. E. Truscott, and R. M. Anderson, "Developing a mathematical model for the evaluation of the potential impact of a partially efficacious vaccine on the transmission dynamics of Schistosoma mansoni in human communities," *Parasites & Vectors*, vol. 10, no. 1, p. 294, 2017.

[3] R. A. Alsallaq, D. Gurarie, M. Ndeffo Mbah, A. Galvani, and C. King, "Quantitative assessment of the impact of partially protective anti-schistosomiasis vaccines," *PLoS Neglected Tropical Diseases*, vol. 11, no. 4, article e0005544, 2017.

[4] B. Gryseels, "Schistosomiasis," *Infectious Disease Clinics of North America*, vol. 26, no. 2, pp. 383–397, 2012.

[5] P. Cai, G. N. Gobert, H. You, and D. P. McManus, "The Tao survivorship of schistosomes: implications for schistosomiasis control," *International Journal for Parasitology*, vol. 46, no. 7, pp. 453–463, 2016.

[6] C. T. Fonseca, S. C. Oliveira, and C. C. Alves, "Eliminating schistosomes through vaccination: what are the best immune weapons?," *Frontiers in Immunology*, vol. 6, no. 6, p. 95, 2015.

[7] S. J. Jenkins, J. P. Hewitson, G. R. Jenkins, and A. P. Mountford, "Modulation of the host's immune response by schistosome larvae," *Parasite Immunology*, vol. 27, no. 10-11, pp. 385–393, 2005.

[8] R. A. Paveley, S. A. Aynsley, P. C. Cook, J. D. Turner, and A. P. Mountford, "Fluorescent imaging of antigen released by a skin-invading helminth reveals differential uptake and activation profiles by antigen presenting cells," *PLoS Neglected Tropical Diseases*, vol. 3, no. 10, p. e528, 2009.

[9] A. C. Fusco, B. Salafsky, and T. Shibuya, "Cytokine and eicosanoid regulation by Schistosoma mansoniduring LSE penetration," *Mediators of Inflammation*, vol. 2, no. 1, 77 pages, 1993.

[10] K. Ramaswamy, B. Salafsky, S. Potluri, Y. X. He, J. W. Li, and T. Shibuya, "Secretion of an anti-inflammatory, immunomodulatory factor by Schistosomulae of Schistosoma mansoni," *Journal of inflammation*, vol. 46, no. 1, pp. 13–22, 1995.

[11] K. Ramaswamy, B. Salafsky, M. Lykken, and T. Shibuya, "Modulation of IL-1a, IL-1b and IL-1ra production in human keratinocytes by schistosomulae of Schistosoma mansoni," *Immunology and Infectious Diseases*, vol. 5, pp. 100–107, 1996.

[12] R. S. Curwen, P. D. Ashton, S. Sundaralingam, and R. A. Wilson, "Identification of novel proteases and immunomodulators in the secretions of schistosome cercariae that facilitate host entry," *Molecular & Cellular Proteomics*, vol. 5, no. 5, pp. 835–844, 2006.

[13] S. Hu, Z. Wu, L. Yang, and M. C. Fung, "Molecular cloning and expression of a functional anti-inflammatory protein, Sj16, of Schistosoma japonicum," *International journal for parasitology*, vol. 39, no. 2, pp. 191–200, 2009.

[14] D. E. Sanin and A. P. Mountford, "Sm16, a major component of Schistosoma mansoni cercarial excretory/secretory products, prevents macrophage classical activation and delays antigen processing," *Parasites & Vectors*, vol. 8, no. 1, p. 1, 2015.

[15] K. Brännström, M. E. Sellin, P. Holmfeldt, M. Brattsand, and M. Gullberg, "The Schistosoma mansoni protein Sm16/SmSLP/SmSPO-1 assembles into a nine-subunit oligomer with potential to inhibit toll-like receptor signaling," *Infection and Immunity*, vol. 77, no. 3, pp. 1144–1154, 2009.

[16] K. V. Rao and K. Ramaswamy, "Cloning and expression of a gene encoding Sm16, an anti-inflammatory protein from _Schistosoma mansoni_," *Molecular and Biochemical Parasitology*, vol. 108, no. 1, pp. 101–108, 2000.

[17] K. V. Rao, Y. X. He, and K. Ramaswamy, "Suppression of cutaneous inflammation by intradermal gene delivery," *Gene Therapy*, vol. 9, no. 1, pp. 38–45, 2002.

[18] F. J. Ramalho-Pinto, G. Gazzinelli, R. E. Howells, T. A. Mota-Santos, E. A. Figueiredo, and J. Pellegrino, "Schistosoma mansoni: Defined system for stepwise transformation of cercaria to schistosomule in vitro," *Experimental Parasitology*, vol. 36, no. 3, pp. 360–372, 1974.

[19] L. D. G. A. Avelar, S. G. Gava, R. H. Neves et al., "Smp38 MAP kinase regulation in *Schistosoma mansoni*: roles in survival, oviposition, and protection against oxidative stress," *Frontiers in Immunology*, vol. 10, no. 21, pp. 1–16, 2019.

[20] P. Holmfeldt, K. Brännström, M. E. Sellin, B. Segerman, S. R. Carlsson, and M. Gullberg, "The Schistosoma mansoni protein Sm16/SmSLP/SmSPO-1 is a membrane-binding protein that lacks the proposed microtubule-regulatory activity," *Molecular and Biochemical Parasitology*, vol. 156, no. 2, pp. 225–234, 2007.

[21] U. K. LAEMMLI, "Cleavage of Structural Proteins during the Assembly of the Head of Bacteriophage T4," *Nature*, vol. 227, no. 5259, pp. 680–685, 1970.

[22] H. Towbin, T. Staehelin, and J. Gordon, "Electrophoretic transfer of proteins from polyacrylamide gels to nitrocellulose sheets: procedure and some applications," *Proceedings of the National Academy of Sciences of the United States of America*, vol. 76, no. 9, pp. 4350–4354, 1979.

[23] J. Pellegrino and A. F. Siqueira, "A perfusion technic for recovery of *Schistosoma mansoni* from experimentally infected guinea pigs," *Revista brasileira de malariologia e doenças tropicais. Publicações avulsas*, vol. 8, no. 4, pp. 589–597, 1956.

[24] H. K. Rofatto, B. O. Araujo-Montoya, P. A. Miyasato et al., "Immunization with tegument nucleotidases associated with a subcurative praziquantel treatment reduces worm burden following *Schistosoma mansoni* challenge," *PeerJ*, vol. 1, no. 1, article e58, 2013.

[25] C. C. Alves, N. Araujo, V. C. F. dos Santos et al., "Sm29, but not Sm22.6 retains its ability to induce a protective immune response in mice previously exposed to a Schistosoma mansoni infection," *PLOS Neglected Tropical Diseases*, vol. 9, no. 2, article e0003537, 2015.

[26] S. A. Bustin, V. Benes, J. A. Garson et al., "The MIQE guidelines: minimum information for publication of quantitative real-time PCR experiments," *Clinical Chemistry*, vol. 55, no. 4, pp. 611–622, 2009.

[27] K. J. Livak and T. D. Schmittgen, "Analysis of relative gene expression data using real-time quantitative PCR and the 2(-Delta Delta C(T)) Method," *Methods*, vol. 25, no. 4, pp. 402–408, 2001.

[28] J. M. Balloul, R. J. Pierce, J. M. Grzych, and A. Capron, "In vitro synthesis of a 28 kilodalton antigen present on the surface of the schistosomulum of Schistosoma mansoni," *Molecular and Biochemical Parasitology*, vol. 17, no. 1, pp. 105–114, 1985.

[29] J. M. Balloul, J. M. Grzych, R. J. Pierce, and A. Capron, "A purified 28,000 dalton protein from *Schistosoma mansoni* adult worms protects rats and mice against experimental schistosomiasis," *TheJournal of Immunology*, vol. 138, no. 10, pp. 3448–3453, 1987.

[30] W. Torben, G. Ahmad, W. Zhang et al., "Role of antibody dependent cell mediated cytotoxicity (ADCC) in Sm-p80-mediated protection against Schistosoma mansoni," *Vaccine*, vol. 30, no. 48, pp. 6753–6758, 2012.

[31] S. Apostólico Jde, V. A. Lunardelli, F. C. Coirada, S. B. Boscardin, and D. S. Rosa, "Adjuvants: Classification, Modus Operandi, and Licensing," *Journal of Immunology Research*, vol. 2016, Article ID 1459394, 16 pages, 2016.

[32] D. L. Boros and J. R. Whitfield, "Endogenous IL-10 regulates IFN-γ and IL-5 cytokine production and the granulomatous response in Schistosomiasis mansoni-infected mice," *Immunology*, vol. 94, no. 4, pp. 481–487, 1998.

[33] P. G. Fallon, E. J. Richardson, G. J. McKenzie, and A. N. McKenzie, "Schistosome Infection of Transgenic Mice Defines Distinct and Contrasting Pathogenic Roles for IL-4 and IL-13: IL-13 Is a Profibrotic Agent," *The Journal of Immunology*, vol. 164, no. 5, pp. 2585–2591, 2000.

[34] K. F. Hoffmann, A. W. Cheever, and T. A. Wynn, "IL-10 and the Dangers of Immune Polarization: Excessive Type 1 and Type 2 Cytokine Responses Induce Distinct Forms of Lethal Immunopathology in Murine Schistosomiasis," *The Journal of Immunology*, vol. 164, no. 12, pp. 6406–6416, 2000.

[35] A. W. Cheever, F. D. Finkelman, P. Caspar, S. Heiny, J. G. Macedonia, and A. Sher, "Treatment with anti-IL-2 antibodies reduces hepatic pathology and eosinophilia in Schistosoma mansoni-infected mice while selectively inhibiting T cell IL-5 production," *The Journal of immunology*, vol. 148, no. 10, pp. 3244–3248, 1992.

[36] G. M. Knudsen, K. F. Medzihradszky, K. C. Lim, E. Hansell, and J. H. McKerrow, "Proteomic analysis of Schistosoma mansoni cercarial secretions," *Molecular & Cellular Proteomics*, vol. 4, no. 12, pp. 1862–1875, 2005.

[37] K. Ramaswamy, P. Kumar, and Y. X. He, "A role for parasite-induced PGE2 in IL-10-mediated host immunoregulation by skin stage schistosomula of Schistosoma mansoni," *Journal of Immunology*, vol. 165, no. 8, pp. 4567–4574, 2000.

[38] M. Hervé, V. Angeli, E. Pinzar et al., "Pivotal roles of the parasite PGD2 synthase and of the host D prostanoid receptor 1 in schistosome immune evasion," *European Journal of Immunology*, vol. 33, no. 10, pp. 2764–2772, 2003.

[39] J. Deng, D. Gold, P. T. LoVerde, and Z. Fishelson, "Inhibition of the complement membrane attack complex by Schistosoma mansoni paramyosin," *Infection and Immunity*, vol. 71, no. 11, pp. 6402–6410, 2003.

[40] A. Floudas, C. D. Cluxton, J. Fahel et al., "Composition of the Schistosoma mansoni worm secretome: identification of immune modulatory cyclophilin A," *PLoS neglected tropical diseases*, vol. 11, no. 10, article e0006012, 2017.

Hindawi
Journal of Immunology Research
Volume 2019, Article ID 5148575, 13 pages
https://doi.org/10.1155/2019/5148575

Research Article

C/EBP Homologous Protein (CHOP) Activates Macrophages and Promotes Liver Fibrosis in *Schistosoma japonicum*-Infected Mice

Mengyun Duan,[1] **Yuan Yang**,[2] **Shuang Peng**,[1] **Xiaoqin Liu**,[1] **Jixin Zhong**,[3] **Yurong Guo**,[1] **Min Lu**,[1] **Hao Nie**,[4,5] **Boxu Ren**,[1] **Xiangzhi Zhang**,[6] **and Lian Liu**[6]

[1]*Department of Medical Imaging, Medical School of Yangtze University, Jingzhou 434023, China*
[2]*Department of Radiology, Renmin Hospital of Wuhan University, Wuhan 430060, China*
[3]*Cardiovascular Research Institute, Case Western Reserve University, Cleveland, OH 44106, USA*
[4]*Department of Pathogenic Biology, Medical School of Yangtze University, Jingzhou 434023, China*
[5]*Clinical Molecular Immunology Center, Medical School of Yangtze University, Jingzhou 434023, China*
[6]*Department of Pharmacology, Medical School of Yangtze University, Jingzhou 434023, China*

Correspondence should be addressed to Boxu Ren; boxuren188@163.com, Xiangzhi Zhang; xiangzhizhang188@163.com, and Lian Liu; liulian@yangtzeu.edu.cn

Received 19 July 2019; Revised 29 September 2019; Accepted 9 October 2019; Published 1 December 2019

Guest Editor: Carina S. Pinheiro

CCAAT/enhancer-binding homologous protein (CHOP), a transcriptional regulator induced by endoplasmic reticulum stress (ER stress) is a pivotal factor in the ER stress-mediated apoptosis pathway. Previous studies have shown that CHOP is involved in the formation of fibrosis in a variety of tissues and is associated with alternative macrophage activation. The role of CHOP in the pathologic effects of liver fibrosis in schistosomiasis has not been reported, and underlying mechanisms remain unclear. This study is aimed at understanding the effect of CHOP on liver fibrosis induced by *Schistosoma japonicum* (*S. japonicum*) in vivo and clarifying its mechanism. C57BL/6 mice were infected with cercariae of *S. japonicum* through the abdominal skin. The liver fibrosis was examined. The level of IL-13 was observed. The expressions of CHOP, Krüppel-like factor 4 (KLF4), signal transducer and activator of transcription 6 (STAT6), phosphorylation STAT6, interleukin-13 receptor alpha 1 (IL-13Rα1), and interleukin-4 receptor alpha (IL-4Rα) were analysed. The eosinophilic granuloma and collagen deposition were found around the eggs in mice infected for 6 and 10 weeks. IL-13 in plasma and IL-13Rα1 and IL-4Rα in liver tissue were significantly increased. The phosphorylated STAT6 was enhanced while Krüppel-like factor 4 (KLF4) was decreased in liver tissue. The expression of CHOP and colocalization of CHOP and CD206 were increased. Overall, these results suggest that CHOP plays a critical role in hepatic fibrosis induced by *S. japonicum*, likely through promoting alternative activation of macrophages.

1. Introduction

Schistosomiasis, a common parasitic disease caused by parasitic flatworms called schistosomes, is mainly prevalent in developing countries and is severely impacting people's health, causing enormous health and socioeconomic burdens to mankind. 200 million people worldwide are still under threat from schistosomiasis in 2016 [1]. Epidemiological surveys show that schistosomiasis endemic areas are distributed in 178 counties in 11 provinces in China's mountain areas [2]. China is one of the primary epidemic areas of *S. japonicum*. There are still 37,601 cases of schistosomiasis in China, and 259 million people are threatened by schistosomiasis in 2016 [3].

Hepatic fibrosis is a significant hallmark during the progression from *S. japonicum* infection-induced schistosomiasis to the end-stage liver disease [4–6]. Macrophages play an indispensable role in the fibrosis process of different tissues or organs, which not only participates in early inflammatory reactions but also secretes various inflammatory factors to participate in the body's immune response [7–12]. At present, the mainstream view is that macrophages can be divided into classically activated macrophages mainly stimulated by LPS or IFN-γ and an alternatively activated phenotype mainly

stimulated by IL-4 or IL-13 [13]. These classically activated macrophages are also known as M1 macrophages, and the alternatively activated macrophages are also known as M2 macrophages [10]. A large number of M2 macrophages infiltrate in the liver during the course of *S. japonicum* infection, and animal studies have shown that M2 macrophages may exhibit as a novel target for the prevention and treatment of fibrosis [14]. M2 macrophages produce various factors during the development of fibrosis such as arg-1 and FIZZ1, which aggravate Th2 immunity [15]. Furthermore, arg-1 can hydrolyze l-arginine into proline and polyamine, promoting the synthesis of collagen and the occurrence of fibrosis [16].

CHOP is also known as CHOP 10, DDIT 3, or GADD153; its promotion in the process of fibrosis is increasingly confirmed, despite the well-recognized role of CHOP in facilitating apoptosis, unfolded protein response (UPR), and integrated stress response (ISR). Moreover, CHOP deficiency can alleviate pulmonary fibrosis [17], renal fibrosis [18], and liver fibrosis [19], accompanied by a decreased polarization of M2 macrophages. However, it is not clear if CHOP is involved in liver fibrosis during schistosomiasis. We noted that CHOP and the M2 macrophage marker CD206 were spatially colocalized in the liver tissue of mice infected with schistosomiasis. Therefore, we hypothesized that CHOP mediates the production of M2 macrophages to promote pathological changes associated with fibrotic development. To validate this hypothesis, we established a C57BL/6 mouse as an experimental schistosomiasis model for *S. japonicum* to analyse how CHOP is associated with liver fibrosis formation and possible underlying mechanisms.

2. Materials and Methods

2.1. Animal and S. japonicum Infections. Eight-week-old C57BL/6 mice, weighting 22 ± 2 g, were purchased from the Hubei Provincial Center for Disease Control and Prevention (Wuhan, Hubei Province, China), and cercariae of *S. japonicum* were bought from Jiangsu Provincial Center for Disease Control and Prevention (Nanjing, Jiangsu Province, China). 100 mice were randomly divided into the control group and the infection group, of which 30 were in the control group and 70 in the infection group. Mice were infected with cercariae of *Schistosoma japonicum* to establish a hepatic fibrosis model. When the room temperature is 26°C, the *Oncomelania hupensis* were placed in purified water, and then a microscope (DM 1000, Leica, Germany) was used to count the number of cercariae. We used the abdominal patch method to infect mice. The abdomen hairless skin was exposed to the cercariae for 15-20 minutes under natural light (50 ± 2). The mice were euthanized 6 or 10 weeks after infection, and liver specimens were collected.

2.2. Liver Index. Mice were euthanized 6 and 10 weeks after undergoing infection of cercariae of *S. japonicum* and the weight of wet liver (A) and body weight (B) were recorded. The acquired data were expressed as the wet liver weight divided by the total body weight times 100. Liver/body weight ratio = $A/B \times 100\%$.

2.3. Histology. Liver tissues were fixed in 4% formalin and embedded in paraffin. Then, these histological sections were cut at 5 μm. Hematoxylin-eosin (HE) staining was used to analyse the area of granuloma. Masson staining was used to analyse the degree of collagen deposition. Images of six random microscopic fields of blue-stained collagen fibres in the liver section of each mouse were recorded using an inverted microscope (Olympus, Olympus DP27, Japan) and then digitized and analysed on Image-Pro Plus software 6.0 as previously described. A Masson Stain Kit was offered by Wuhan Servicebio Technology Company (BA-4079A, BASO, Zhuhai, China).

2.4. Immunohistochemistry. For immunostaining, the slices were placed in an EDTA pH 9.0 buffer and microwaved for antigen repair, with medium heat for 8 minutes, and low heat for 8 minutes before power failure. After natural cooling, wash the slices with PBS 3 times for 5 minutes each. Nonspecific proteins were blocked with 3% BSA for 30 minutes. The sections were then probed with a mouse-derived anti-CHOP antibody (Santa Cruz, United States; 1 : 50) and a rabbit-derived anti-fibronectin antibody (Abcam, the United Kingdom; 1 : 500) at 4°C overnight, followed by incubation with an HRP-labeled anti-mouse-IgG and an HRP-labeled anti-rabbit-IgG secondary antibody (SeraCare, United States; 1 : 100) at room temperature for 50 minutes.

2.5. Immunofluorescence. Procedures for liver tissue fixation, dehydration, and embedding were described above. For immunofluorescence, the slices were placed in an EDTA pH 8.0 buffer for microwave repair, and power was cut off after 8 minutes of low heat. The washing and nonspecific protein blocking steps are as described above. The sections were then probed with a rabbit-derived anti-CHOP antibody (Bioss, Beijing, China; 1 : 200) and a rabbit-derived anti-CD206 antibody (Proteintech, Wuhan, China; 1 : 200) at 4°C overnight, followed by incubation with an FITC-labeled anti-rabbit-IgG and an CY3-labeled anti-rabbit-IgG secondary antibody (Hundred Thousand Biological Technology, Wuhan, China; 1 : 100) at room temperature for 50 minutes. Sections incubated with normal IgG were used as a negative control. Immunofluorescence images were acquired using a scanning sequential mode to avoid bleed-through effects with a fluorescence microscope (Eclipse CI, Nikon, Japan), and images were processed using the MicroPublisher (Q-IMAGING, Canada).

2.6. RNA Isolation and RT-qPCR. Total RNA was extracted from mice liver tissue homogenate with TRIzol (Invitrogen, USA) and quantified by NanoPhotometer® NP80 (Implen, Germany). The total RNA (1 μg) was reverse transcribed to cDNA with a PrimeSecript™ RT reagent kit (Takara RR047A, Japan) and incubated at 42°C for 2 min to remove genomic DNA then incubated at 37°C for 15 min and 85°C for 5 s. Real-time quantitative PCR (RT-qPCR) was carried out using a three-step approach at 95°C for 30 s, followed by 95°C for 5 s, 60°C for 30 s, and 72°C for 30 s according to the specification for the SYBR® Premix Ex Taq™ (Tli RNaseH Plus, Takara, Japan) on an Applied Biosystems

Table 1: Sequences of real-time PCR primers used throughout.

Primer	Direction	Sequence	Temperature	Length
CHOP	Forward	5′-TATCTCATCCCCAGGAAACG-3′	60	219
	Reverse	5′-GGGCACTGACCACTCTGTTT-3′		
STAT6	Forward	5′-CTCTGTGGGGCCTAATTTCCA-3′	60	135
	Reverse	5′-CATCTGAACCGACCAGGAACT-3′		
IL-4 receptor α	Forward	5′-GCTGCTGACCTGGAATAACCT-3′	60	181
	Reverse	5′-CGCCGTATAGTAGACCCCTG-3′		
IL-13 receptor α1	Forward	5′-TCAGCCACCTGTGACGAATTT-3′	60	101
	Reverse	5′-TGAGAGTGCAATTTGGACTGG-3′		
GAPDH	Forward	5′-GGTTGTCTCCTGCGACTTCA-3′	60	183
	Reverse	5′-TGGTCCAGGGTTTCTTACTCC-3′		

Table 2: Effect of *S. japonicum* infection on the body weight, liver weight, and LBWR of mice.

Infection time (weeks)	Body weight (g)		Liver weight (g)		Liver/body weight ratio (g)	
	Control group	Model group	Control group	Model group	Control group	Model group
6	20.8 ± 1.1	25.3 ± 2.8	0.97 ± 0.11	1.92 ± 0.1	4.65 ± 0.61	7.68 ± 0.97
10	21.1 ± 0.9	26.1 ± 0.4	1.12 ± 0.07	2.32 ± 0.3	5.33 ± 0.48	9.27 ± 1.16

Changes of liver index (%) in control and infected mice at different time points after *S. japonicum* infection. Data were presented as mean ± SEM of 6-8 mice.

7500 Real-Time-PCR System (Life Technologies, USA). All the primers were synthesized by Sangon Biotech (Wuhan, China), and the primer sequence is listed in Table 1. Gene expression was normalized to GAPDH using the $^{\Delta\Delta}$Ct method.

2.7. Western Blot. Liver tissues were lysed in a RIPA lysis buffer (P0013b, Beyotime Biotechnology, China), and proteins were quantified by a BCA protein assay kit (Beyotime Biotechnology, China). Equivalent amounts (40 μg) of total protein were separated by 12% SDS-PAGE and transferred to a PVDF membrane (Immobilon-P, Germany). The membrane was subsequently blocked with 5% skim milk in TBST solution for 2 h at room temperature and incubated at 4°C overnight, using the following primary antibodies: KLF4 (1 : 500; Abcam, Cambridge, MA, USA), GAPDH (1 : 1000; CST, USA), and CHOP (1 : 500; Santa Cruz, United States). HRP-conjugated secondary antibodies (1 : 10000) were next applied for 1 h at room temperature. The antigen-antibody complexes were detected by a Pierce ECL substrate kit (MULTI SCIENCES, China). Specific bands were scanned and quantified by Quantity One software (Bio-Rad, USA). GAPDH was used as the loading control.

2.8. ELISA. The IL-13 levels in the serum of the mice were determined by ELISA. The sera were assayed for IL-13 with mouse IL-13 ELISA kits (Elabscience, Wuhan, China). The procedures were executed according to the instruction manuals for the kits. Sterile PBS was used as a control.

2.9. Statistical Analysis. All data are presented as mean ± standard error of mean (SEM). Two-way ANOVA was used for comparison of different treatment time groups, followed by Tukey's multiple comparison test or Sidak's multiple comparison test. All statistical tests were performed using GraphPad Prism 6.0 (GraphPad Software, Inc.). Data was considered statistically significant only when $P < 0.05$.

3. Results

3.1. S. japonicum Infection Caused Liver Fibrosis. Compared with the control group, the liver/body weight ratio (LBWR) of mice infected with *S. japonicum* was significantly increased (Table 2, Figure 1(e)). Liver weights, etc. were normalized by body weight. The normal mice liver was displayed as ruddy with a smooth surface and bright red, whereas the liver of the infected mice appeared as dark red and had many small white granulomatous nodules on the surface (Figure 1(a)).

To study the liver pathology of mice infected with *S. japonicum*, the fixed liver tissues were stained with HE or Masson's trichrome (Figures 1(b) and 1(d)). The deposition of *S. japonicum* eggs and granulomas in the hepatic tissue from *S. japonicum*-infected mice was significantly elevated compared with that from the control mice (Figures 1(b) and 1(f)). The results showed that the lobule structure was intact; radiated liver cell cords were visible in the normal group (Figure 1(b)). After 6 weeks of infection, a large number of granular immune cells (see black dotted arrows) infiltrated the area around the eggs (see the short black arrow), surrounded by fibrous vascular tissue bands (see black solid arrow). More eggs (see the short black arrow) were deposited in the liver at 10 weeks, surrounded by a large amount of granulomatous tissue (see black dotted arrows) and entangled by fibrous tissue (see black solid arrow). Compared with the control group, the average granuloma area

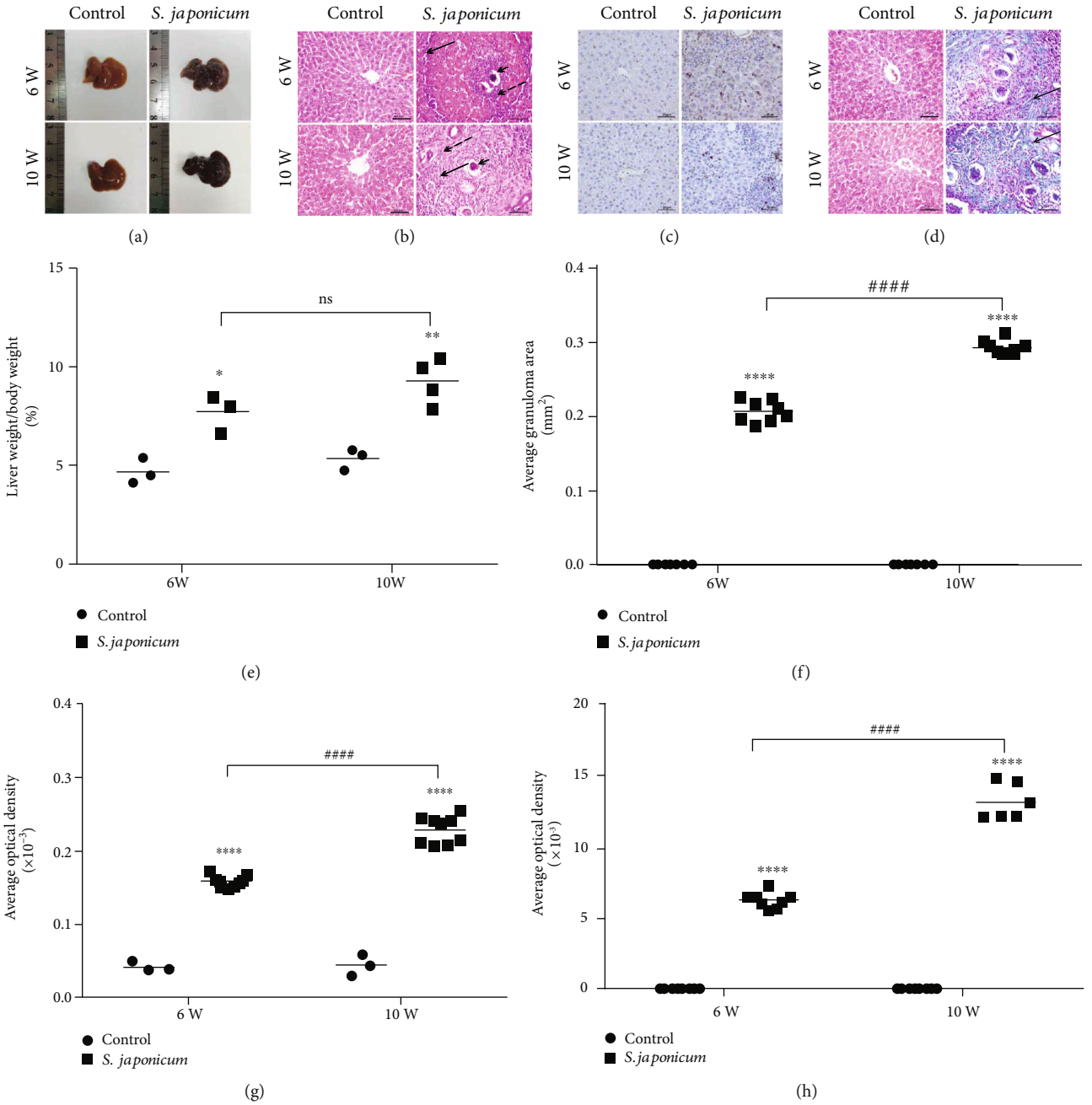

Figure 1: Liver fibrosis is aggravated by *S. japonicum* infection. The animals were infected with 50 ± 2*S. japonicum* cercariae. HE staining, Masson trichrome staining, and immunohistochemistry were used to observe the pathological changes and collagen deposition of liver tissue. (a) The morphology changes on the liver of *S. japonicum* infection in mice. (b) Liver tissues were stained with HE. Arrows indicate granulomatous lesions and arrowheads indicate schistosome eggs (magnified ×200). (c) The protein expression of fibronectin detected by immunohistochemistry (magnified ×400). (d) Liver tissues were stained with Masson's trichrome staining (magnified ×200). (e) Liver/body ratio of the infection group and the control group after *S. japonicum* cercariae. (f) Areas of single egg granulomas. (g) The quantitative analysis of fibronectin in liver tissues. (h) Average optical density of the collagen deposition in liver tissues. Data were presented as mean ± SEM of 6-8 mice. $^{*}P < 0.05$ and $^{**}P < 0.01$ vs. the control. $^{\#}P < 0.05$ and $^{\#\#}P < 0.01$ vs. the 6-week infection group.

increased significantly after 6 and 10 weeks after *S. japonicum* infection (Figure 1(f)).

Fibrotic collagen deposition, dyed blue, around the *S. japonicum* egg granulomas was evaluated by Masson's trichrome (Figure 1(d)). It showed no blue staining in the liver tissue of the control group, and a few fibres began to appear around the eggs after 6 weeks of infection (see black solid arrow). In addition, 10 weeks after infection, a large amount of fibres were deposited in the liver tissue (see black solid arrow), surrounding the egg deposition site (Figure 1(d)). We further analysed the average optical density (AOD) to reflect the expression level of collagen fibres. Compared with the control group, the expression of collagen fibres increased significantly after 6 and 10 weeks of *S. japonicum* infection

(Figure 1(h)). Besides, fibronectin, a marker of liver fibrosis, increased significantly after infection with *S. japonicum* compared to the uninfected group, and fibronectin deposition was aggravated with prolonged infection time (Figures 1(c) and 1(g)).

3.2. The Expression of CHOP in the Liver of Mice Increased in the Liver of S. japonicum-Infected Mice. Compared with the control group, the mRNA expression of CHOP increased by 1.5- and 3.5-folds after 6 and 10 weeks of infection with *S. japonicum*, respectively (Figure 2(b)). To further confirm subcellular localization of CHOP and protein level expression, immunohistochemistry and WB were performed to detect the CHOP expression. Consistent with the RT-qPCR results, WB and immunohistochemistry results showed that the CHOP expression increased after infection with *S. japonicum*, compared with the age-matched uninfected group, and the expression after 10 weeks of infection was higher than that after 6 weeks of infection (Figures 2(a) and 2(c)–2(e)).

3.3. The STAT6 Signal Pathway Is Activated and the KLF4 Expression Is Reduced following S. japonicum Infection. The phosphorylation of STAT6 approximately increased by 7- and 6-folds after 6 and 10 weeks of infection with *S. japonicum*, respectively, compared to the age-matched uninfected group (Figures 3(a) and 3(b)). At the same time, the expression of the KLF4 protein in the liver homogenate was also detected. The results showed that the expression of KLF4 approximately reduced by 4- and 7-folds after 6 and 10 weeks of infection with *S. japonicum*, respectively, compared to the age-matched uninfected group (Figures 3(a) and 3(d)). The mRNA expression of STAT6, IL-4Rα, and IL-13Rα1 increased approximately 1.5-3-folds after 10 weeks of infection with *S. japonicum*, and there were no obvious differences between the uninfected group and the infected group after 6 weeks of infection with *S. japonicum* except IL-13Rα1 (Figures 3(a) and 3(e)–3(g)). Coincidently, the results showed that the expression of IL-13 in the serum in the infected group was significantly increased compared with the uninfected group (Figure 3(b)). In general, our data indicate that *S. japonicum* infection increases pSTAT6, IL-4Rα, IL-13Rα1, and IL-13 expression and reduces KLF4.

3.4. The Expression of CHOP Increased Significantly in M2 Macrophages after S. japonicum Infection. To confirm the expression of CHOP in specific cell types, we used immunofluorescence to detect the cellular localization of CHOP in liver tissues. The results showed that CHOP was expressed in F4/80$^+$ macrophages. One or several eggs (see white dotted arrows) are surrounded by CHOP$^+$ and F4/80$^+$ macrophages (see white solid arrow), and the number of CHOP$^+$ and F4/80$^+$ coimmunostaining cells was significantly increased in a time-dependent manner (Figure 4(a)). CHOP and CD206 immunofluorescence assays showed that these macrophages were characterized by the M2 subtype. Eggs (see white dotted arrows) are surrounded by CHOP$^+$ and CD206$^+$ macrophages (see white solid arrow) (Figure 4(b)). The infiltration number of M2 macrophages in mice 10 weeks after infection was larger than that in mice 6 weeks after infection. In general, our results suggest that CHOP may be involved in the pathological process of fibrosis by regulating the activation of macrophages.

4. Discussion

S. japonicum infection often causes granulomatous inflammation at the site of egg deposition, leads to dysregulation of the immune system, activates hepatic stellate cells, and even causes persistent liver fibrosis [20]. The main pathological feature of liver fibrosis is the excessive deposition of ECM in tissues, which leads to excessive protein synthesis and disturbance of endoplasmic reticulum homeostasis [21–23]. CHOP is considered to be one of specific and convergent transcription factors of ER stress, and its activation is generally regulated at the transcriptional level [24]. Yu et al. [25] showed that taurine attenuating the hepatic pathologic features in mice infected with *S. japonicum* was related to the regulation of ERS. Recent studies have focused on the functions of CHOP on the formation of organ fibrosis in different disease models [17, 18, 26–31]. CHOP expression was significantly increased in many liver fibrosis models induced by different factors. These factors include drugs (such as carbon tetrachloride [32] and thioacetamide [33]), metabolic abnormalities (such as BDL [30, 34] and MCD diet [28, 35]), and alcohol [36–38]. Liver fibrosis is reduced and CHOP expression is reduced after treatment [19, 39]. Tauroursodeoxycholic acid (TUDCA), a hydrophilic bile acid, is a drug that inhibits the expression of CHOP, which alleviates liver fibrosis caused by cholestasis [22] and inhibits pulmonary fibrosis induced by bleomycin (BLM) [40]. In addition, the use of CHOP-deficient mice suggests that CHOP deficiency can reduce liver fibrosis caused by bile duct ligation [30, 34], cholestasis [30], or MCD diet [28] and retard renal fibrosis caused by diabetic nephropathy [21, 41]. Furthermore, in the human liver, the expression of CHOP is enhanced as the progression of nonalcoholic steatohepatitis to HCC [28]. However, the role of CHOP in liver fibrosis of *S. japonicum* is still not well understood. In the present study, the level of CHOP expression in infected mice was augmented compared to uninfected mice, suggesting that CHOP plays a critical role in hepatic fibrosis induced by *S. japonicum* [35].

Researchers found that glycoproteins such as IPSE (SmEP-25) [42], omega-1 [43], and kappa-5 [44] secreted by *S. mansoni* eggs and Sm29 [45] secreted by S. *haematobium*-stimulate Th2 cytokine production in mice. For *S. japonicum*, egg secretory proteins (ESP) instead of IPSE, omega-1, and kappa-5 played a central role in driving the development of the immune response to the Th2 pattern because it was predicted to stimulate the production of IL-1, IL-3, IL-5, IL-4, and IL-13 [46]. Th2 response is supported by alternatively activated antigen presenting cells (APCs). A growing number of researches payed attention to the role of M2 macrophages in the pathological process of schistosomiasis, especially liver fibrosis [47–50]. One or several eggs are surrounded by immune cells (mainly including alternately activated macrophages, Th2 cells, and eosinophils) and the extracellular matrix (ECM), protecting the host

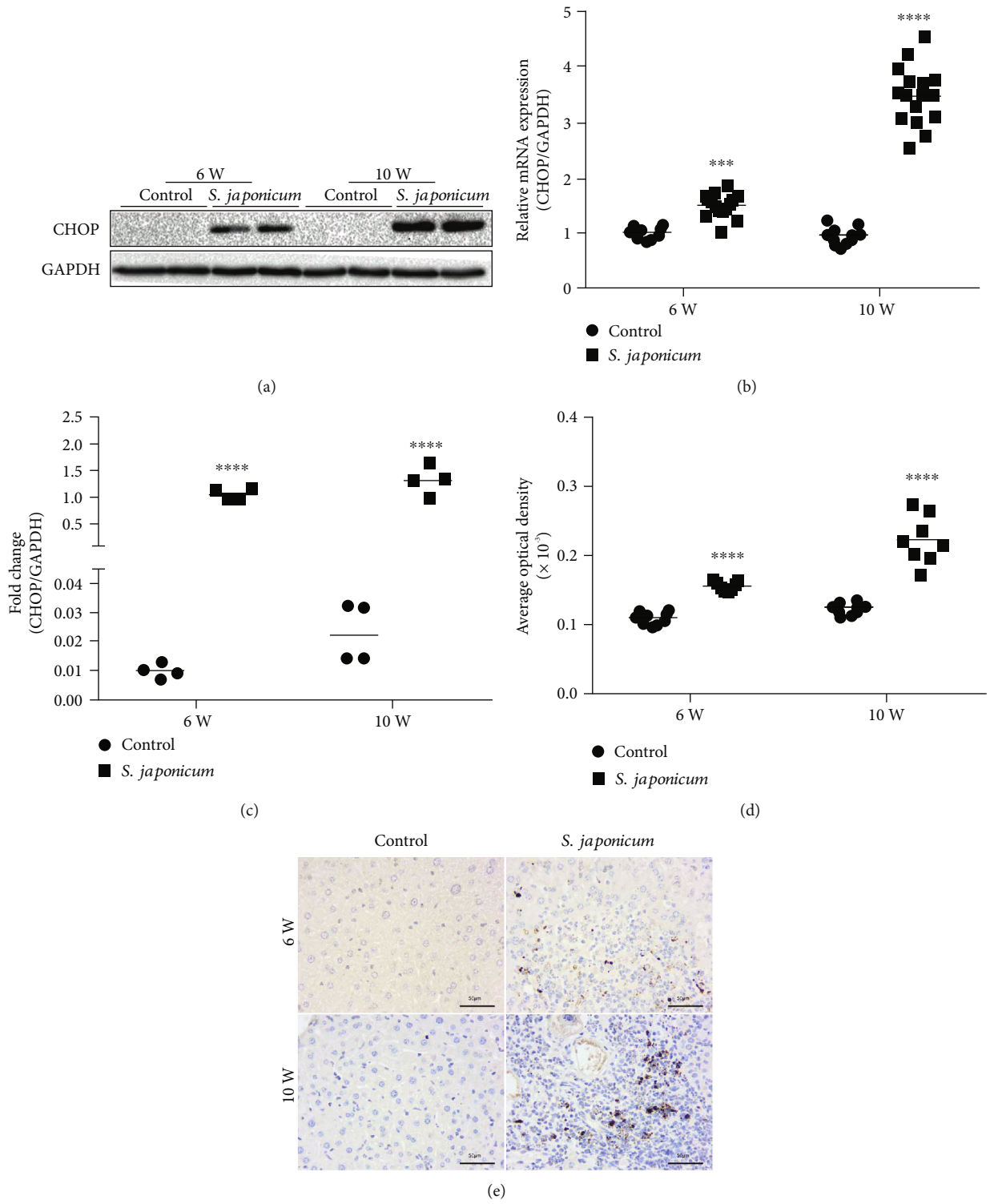

Figure 2: Expression of CHOP in transcription and protein levels increased after *S. japonicum* cercariae infection in murine liver homogenates. Mice were treated with *S. japonicum* cercariae or sterile 9% physiological saline; after being administrated for 6 and 10 weeks, 6-8 mice were euthanized. Real-time PCR, Western blot, and immunohistochemical assays were performed to detect the expression of CHOP in the liver homogenate. (a) The protein expression of CHOP detected by WB. (b) The mRNA expression quantitative analysis of CHOP in the liver homogenate. (c) The protein expression quantitative analysis of CHOP in the liver homogenate. (d) The quantitative analysis of CHOP in liver tissues. (e) The protein expression of CHOP detected by immunohistochemistry (magnified ×400). Data were presented as mean ± SEM of 6-8 mice. $^{*}P < 0.05$ and $^{**}P < 0.01$ vs. the control. $^{\#}P < 0.05$ and $^{\#\#}P < 0.01$ vs. the 6-week infection group.

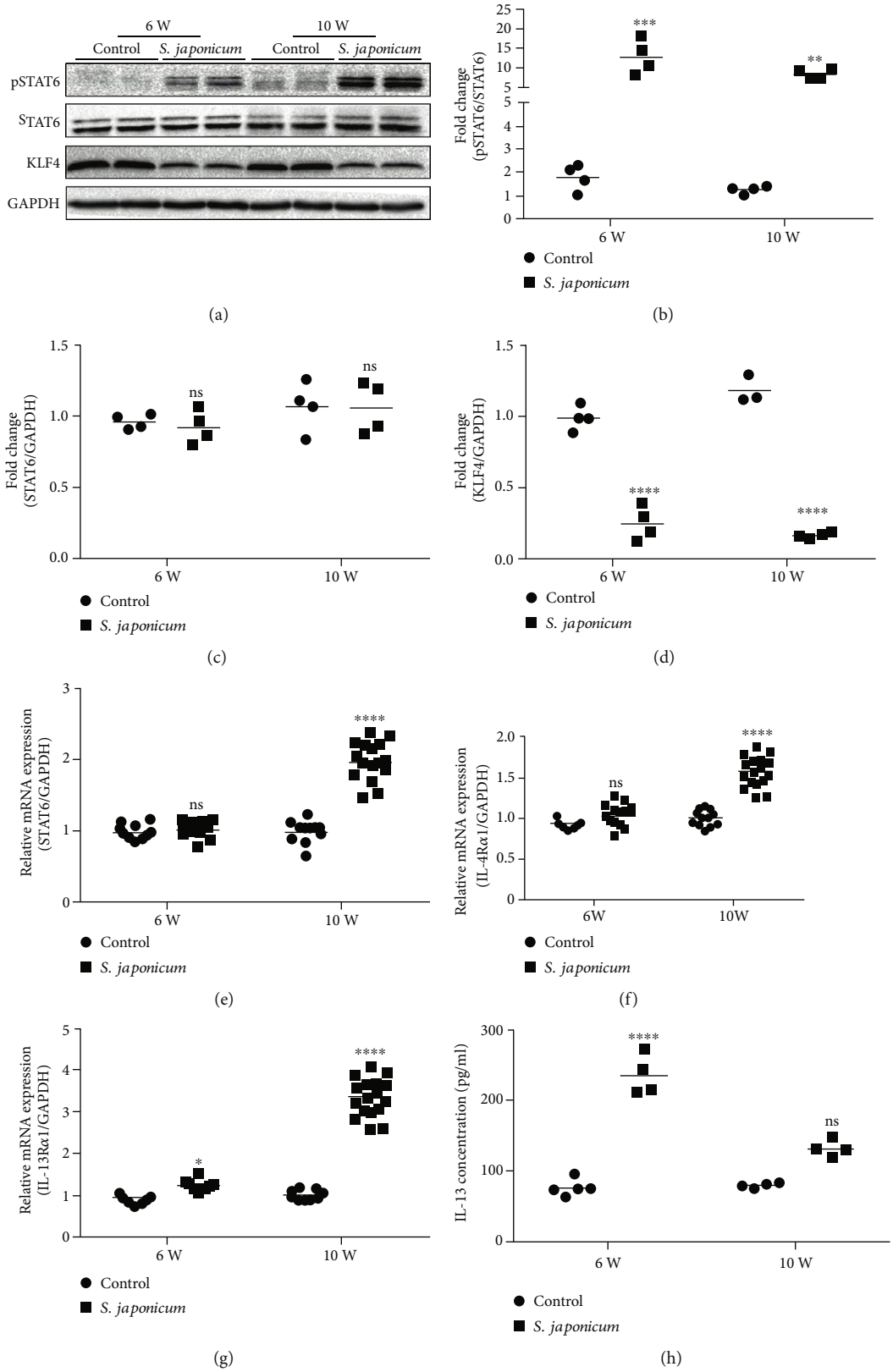

Figure 3: *S. japonicum* significantly increased the protein level of pSTAT6 and reduced the protein level of KLF4. (a) The protein expression of pSTAT6, STAT6, and KLF4 detected by Western blots. (b) Relative protein levels of pSTAT6/STAT6 were analysed. (c, d) Relative protein levels of STAT6 and KLF4 in the liver homogenate was analysed using GAPDH as a loading control. (e–g) Relative mRNA levels of STAT6, IL-4Rα, and IL-13Rα1 in the liver homogenate. (h) The IL-13 levels in the serum. Data are presented as mean ± SEM of 6-8 mice. $^{*}P < 0.05$ and $^{**}P < 0.01$ vs. the control. $^{\#}P < 0.05$ and $^{\#\#}P < 0.01$ vs. the 6-week infection group.

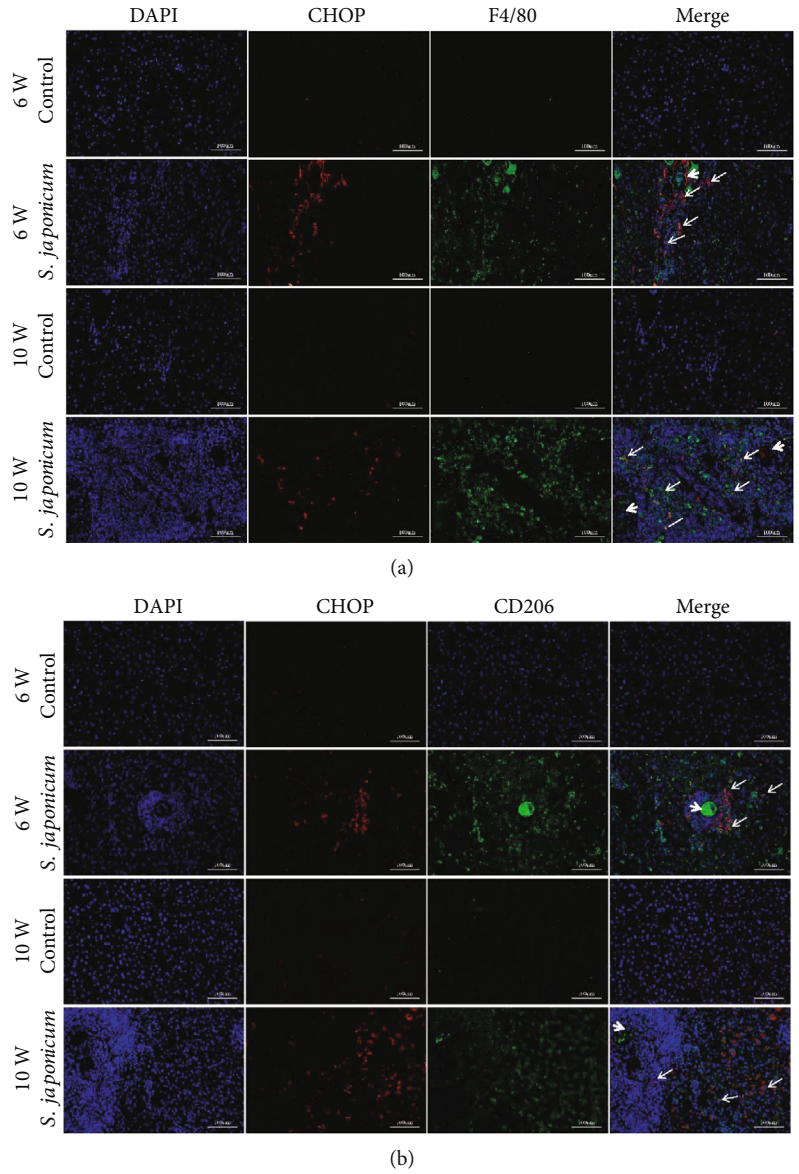

Figure 4: *S. japonicum* significantly increased the expression of CHOP in M2 macrophages. Immunofluorescence assays were performed to detect the colocalization of CD206 and CHOP. (a) Coimmunostaining of CHOP and F4/80 in liver tissues (magnified ×200). (b) Coimmunostaining of CHOP and CD206 in liver tissues (magnified ×200). Data were presented as mean ± SEM of 6-8 mice. $^{*}P < 0.05$ and $^{**}P < 0.01$ vs. the control. $^{\#}P < 0.05$ and $^{\#\#}P < 0.01$ vs. the 6-week infection group.

tissue from the toxins [51]. Gong and his team found that excretory secretion of antigen (ES) from *Schistosoma japonicum* eggs can activate macrophages to exhibit enhanced M2b polarization [47]. It has been reported that reducing or even eliminating mice macrophages can reduce organ fibrosis [52, 53], while M2 macrophage adoptive transplantation can aggravate organ fibrosis in mice [54, 55]. Moreover, the decrease in the infiltration of M2 macrophages can be observed in the $CHOP^{-/-}$ animal fibrosis model [18, 56, 57]. In our study, IL-13 in the serum was significantly increased in the infected group and immunofluorescence of the liver tissue showed a significant increase in the number of $CHOP^{+}$ $CD206^{+}$ macrophages in the infected group, compared with the uninfected group. Based on the above findings and previous work in our laboratory, we speculate that CHOP may mediate the polarization of M2 macrophages and participate in the formation of hepatic granuloma and fibrosis caused by *S. japonicum*. However, what molecular mechanisms are involved in M2 macrophage polarization?

STAT6 is an important regulatory transcription factor for M2 macrophage polarization [58]. Increasing evidence suggests that STAT6-mediated M2 macrophage polarization activation contributes to tissue fibrosis [59–62]. Corilagin reduces liver fibrosis induced by *S. japonicum* infection via reducing the expression of IL-13/STAT6 signal pathway-related molecules in alternative activated macrophages [48]. In our study, pSTAT6, IL-4Rα, and IL-13Rα1 were significantly increased following infection with *S. japonicum*. Research by Adedokun and his colleagues suggests that the

IL-4 promoter region is a predisposing factor for schistosomiasis and is critical in regulating the disease burden and that carriers of the rs2243250 T/T mutation are more severely affected. With the deletion of STAT6, the rs3024974T/T variant among infected children indicated the need for the STAT6 promoter gene in provoking schistosomiasis susceptibility in Nigeria [63]. With the application of mutant mice, the role of STAT6 activation in the study of fibrosis mechanisms is demonstrated. Moreover, a number of studies confirmed that STAT6 plays a role in different organs. STAT6 deficiency inhibits accumulation of bone marrow-derived fibroblasts, formation of myofibroblasts, expression of ECM proteins, and deposition of collagen in obstructed kidneys [64]. Compared with wild-type (WT) mice, the lungs from $STAT6^{-/-}$ mice show inhibition of acute inflammation and reduction of fibrotic diseases after administration of multiwalled carbon nanotubes (MWCNT) [65]. The study found that IL-4 interacts with type I and type II IL-4Rs to induce downstream signalling pathways, including the JAK3-STAT6 signalling pathway [66]. It indicates that the IL-4/IL-4Rα pathway is closely related to fibrotic diseases. Consistent with this, IL-4Rα deficiency inhibits STAT6 activation, monocyte to fibroblast transformation, and ECM protein production following IL-4 treatment [67]. In addition, IL-4Rα has profibrotic effects through activated macrophages during mouse skin repair [68]. Furthermore, CHOP deletion significantly reduced IL-4-induced STAT6 phosphorylation and IL-4Rα expression [69]. These data suggest that CHOP may regulate M2 macrophage polarization and mediated fibrosis via the IL-4/STAT6 signalling pathway.

It is reported that KLF4 is essential for IL-4-mediated macrophage M2 polarization and synergizes with STAT6 to promote M2 macrophage polarization [70]. We considered whether KLF4 is involved in the model of *S. japonicum* liver fibrosis. However, our results found that the KLF4 protein was reduced in liver homogenates in this model. Consistent with this, in the liver fibrosis model, KLF4 expression was decreased in hepatic stellate cells [71]. In addition, according to Men and his colleague's research, KLF4 was reduced in activated hepatic stellate cells (HSCs) and cirrhotic liver tissues and KLF4 deficiency promote HSC activation [72]. Another study suggests that other mechanisms independent of IL-4 may also regulate the M2 phenotype [73]. Therefore, whether KLF4 is involved in macrophage polarization in the *S. japonicum* model is an important issue that needs further study. At the same time, studies have found that KLF4 expression is decreased in patients with liver fibrosis and rat liver, and the results show that decreased expression of KLF4 can activate HSCs [74]. HSC activation is an important process of liver fibrosis, which can secrete a large amount of ECM and high expression of α-SMA and collagen to promote the development of fibrosis [75]. KLF4 overexpression inhibits the expression of α-SMA and collagen while inhibiting the proliferation of HSCs [71, 74]. In the early stage of liver fibrosis, the expression of KLF4 is higher to maintain the stability of activated HSCs [76] and inhibit the differentiation and activation of HSCs [71]. With the progression of liver fibrosis, the expression of KLF4 is gradually inhibited. It has also been reported that CHOP inhibits the expression of KLF4 at the transcriptional and translational levels by downregulating ATF4. When the CHOP gene is deleted, the expression of KLF4 is involved in the inhibition of cell proliferation [77]. In C57BL/6 mice, iron overload induced decreased KLF4 expression and liver fibrosis [78]. In summary, we speculate that KLF4 may play different roles in different disease models or organs, and KLF4 expression in different cell types may have different effects on the formation of liver fibrosis. Our study found that KLF4 reduction is involved in the process of liver fibrosis induced by *S. japonicum*. Combined with our observations, CHOP may promote liver fibrosis caused by *S. japonicum* by reducing the expression of KLF4 and activating M2 macrophages.

In conclusion, our results indicate that CHOP plays an important role in the progression of liver fibrosis caused by *S. japonicum*. We speculate that CHOP may be a key gene in the pathogenesis of *S. japonicum*-induced liver fibrosis because it has a wide range of effects in vivo. Further understanding of CHOP-mediated liver fibrosis and its regulation with hepatic macrophages may provide new ideas for the treatment of liver fibrosis in schistosomiasis. Next, we will further explore the regulatory mechanisms through gene knockout animals and cell experiments. Therefore, our future research focuses on testing the potential of CHOP antagonists to improve liver fibrosis induced by *S. japonicum*. In this case, the damaging effects of CHOP deficiency in the liver should be warily treated.

Abbreviations

CHOP:	C/EBP homologous protein
ER stress:	Endoplasmic reticulum stress
UPR:	Unfolded protein response
ISR:	Integrated stress response
S. *japonicum*:	*Schistosoma japonicum*
STAT6:	Signal transducer and activator of transcription 6
pSTAT6:	Phosphorylation signal transducer and activator of transcription 6
IL-4 Rα:	Interleukin-4 receptor alpha
IL-13Rα1:	Interleukin-13 receptor alpha 1
KLF4:	Krüppel-like factor 4
LBWR:	Liver/body weight ratio
APC:	Antigen presenting cells
ECM:	Extracellular matrix
AOD:	Average optical density
ES:	Excretory secretion
γT3:	Gamma-tocotrienol
UUO:	Unilateral ureteral obstruction
BDL:	Bile duct ligation
RT-qPCR:	Real-time quantitative PCR
WB:	Western blot
HE:	Hematoxylin-eosin
EDTA:	Ethylenediaminetetraacetic acid
BSA:	Bull serum albumin
PBS:	Phosphate buffer solution
TBST:	Tris-buffered saline Tween
HRP:	Horseradish peroxidase
WT:	Wild type

MWCNT: Multiwalled carbon nanotubes
ESP: Egg secretory proteins
HSCs: Hepatic stellate cells.

Data Availability

Our data used to support the findings of this study are all included within the article

Conflicts of Interest

All authors declare that there is no conflict of interests regarding the publication of this paper.

Authors' Contributions

Mengyun Duan, Yuan Yang, and Shuang Peng contributed equally to this article.

Acknowledgments

This work was supported by grants from the National Natural Science Foundation of China (No. 81772223), the Nature Science Foundation of Hubei Province (No. 2018CFB667), and the Yangtze Fund for Youth Teams of Science and Technology Innovation (No. 2016cqt04).

Supplementary Materials

Supplementary Figure 1: H&E staining and Masson staining of liver tissue of mice. (A) Liver tissues were stained with HE in uninfected group mice. (B) Liver tissues were stained with HE after 10 weeks of *S. japonicum* infection. (C) Liver tissues were stained with Masson's trichrome staining after 10 weeks of *S. japonicum* infection. The thin black arrow indicates fibres and the thick black arrow indicates schistosome eggs (magnified 50 times, 100 times, 200 times, and 400 times from left to right). Supplementary Figure 2: negative control for immunofluorescence. (A) Negative control of liver immunofluorescence in uninfected group mice. (B) Negative control of liver immunofluorescence after 10 weeks of *S. japonicum* infection (magnified by 200 times (left) and 400 times (right)). Supplementary Figure 3: negative control for immunohistochemistry. (A) Negative control of liver immunohistochemistry in uninfected group mice. (B) Negative control of liver immunohistochemistry after 10 weeks of *S. japonicum* infection (magnified by 200 times (left) and 400 times (right)). *(Supplementary Materials)*

References

[1] "Global, regional, and national incidence, prevalence, and years lived with disability for 328 diseases and injuries for 195 countries, 1990-2016: a systematic analysis for the Global Burden of Disease Study 2016," *The Lancet*, vol. 390, no. 10100, pp. 1211–1259, 2017.

[2] Y. Liu, Y.-B. Zhou, R.-Z. Li et al., "Schistosomiasis in The People's Republic of China - From Control to Elimination," *Advances in Parasitology*, X. N. Zhou, S. Z. Li, J. Utzinger, and R. Bergquist, Eds., vol. 92, pp. 73–95, 2016.

[3] Z. Li-Juan, X. Zhi-Min, D. Si-Min et al., "Endemic status of schistosomiasis in People's Republic of China in 2017," *Zhongguo xue xi chong bing fang zhi za zhi = Chinese journal of schistosomiasis control*, vol. 30, no. 5, pp. 481–488, 2018.

[4] S. D. Kamdem, R. Moyou-Somo, F. Brombacher, and J. K. Nono, "Host regulators of liver fibrosis during human schistosomiasis," *Frontiers in Immunology*, vol. 9, 2018.

[5] A. H. Aufses Jr., F. Schaffner, W. S. Rosenthal, and B. E. Herman, "Portal venous pressure in "pipestem" fibrosis of the liver due to schistosomiasis," *The American Journal of Medicine*, vol. 27, no. 5, pp. 807–810, 1959.

[6] Y. Liu, H. C. Yuan, D. D. Lin et al., "Studies on risk factors for liver fibrosis of Schistosomiasis japonica," *Zhongguo ji sheng chong xue yu ji sheng chong bing za zhi = Chinese journal of parasitology & parasitic diseases*, vol. 18, no. 1, pp. 18–20, 2000.

[7] Y. Feng, Y. Liang, J. Ren, and C. Dai, "Canonical Wnt signaling promotes macrophage proliferation during kidney fibrosis," *Kidney diseases*, vol. 4, no. 2, pp. 95–103, 2018.

[8] J. Hou, J. Shi, L. Chen et al., "M2 macrophages promote myofibroblast differentiation of LR-MSCs and are associated with pulmonary fibrogenesis," *Cell Communication and Signaling*, vol. 16, no. 1, p. 89, 2018.

[9] K. S. Smigiel and W. C. Parks, "Macrophages, wound healing, and fibrosis: recent insights," *Current Rheumatology Reports*, vol. 20, no. 4, 2018.

[10] F. Tacke and H. W. Zimmermann, "Macrophage heterogeneity in liver injury and fibrosis," *Journal of Hepatology*, vol. 60, no. 5, pp. 1090–1096, 2014.

[11] S.-Y. Weng, X. Wang, S. Vijayan et al., "IL-4 receptor alpha signaling through macrophages differentially regulates liver fibrosis progression and reversal," *eBioMedicine*, vol. 29, pp. 92–103, 2018.

[12] P. J. Wermuth and S. A. Jimenez, "The significance of macrophage polarization subtypes for animal models of tissue fibrosis and human fibrotic diseases," *Clinical and Translational Medicine*, vol. 4, no. 1, p. 2, 2015.

[13] F. O. Martinez, L. Helming, and S. Gordon, *Annual review of immunology*, vol. 27, Annual Reviews, 2009.

[14] A. V. Misharin, L. Morales-Nebreda, P. A. Reyfman et al., "Monocyte-derived alveolar macrophages drive lung fibrosis and persist in the lung over the life span," *Journal of Experimental Medicine*, vol. 214, no. 8, pp. 2387–2404, 2017.

[15] L. Ran, Q. Yu, S. Zhang et al., "Cx3cr1 deficiency in mice attenuates hepatic granuloma formation during acute schistosomiasis by enhancing the M2-type polarization of macrophages," *Disease Models & Mechanisms*, vol. 8, no. 7, pp. 691–700, 2015.

[16] R. W. Thompson, J. T. Pesce, T. Ramalingam et al., "Cationic amino acid transporter-2 regulates immunity by modulating arginase activity," *PLoS Pathogens*, vol. 4, no. 3, article e1000023, 2008.

[17] Y. Yao, Y. Wang, Z. Zhang et al., "Chop deficiency protects mice against bleomycin-induced pulmonary fibrosis by attenuating M2 macrophage production," *Molecular Therapy*, vol. 24, no. 5, pp. 915–925, 2016.

[18] S. H. Liu, C. T. Wu, K. H. Huang et al., "C/EBP homologous protein (CHOP) deficiency ameliorates renal fibrosis in unilateral ureteral obstructive kidney disease," *Oncotarget*, vol. 7, no. 16, pp. 21900–21912, 2016.

[19] D. DeZwaan-McCabe, J. D. Riordan, A. M. Arensdorf, M. S. Icardi, A. J. Dupuy, and D. T. Rutkowski, "The stress-regulated transcription factor CHOP promotes hepatic inflammatory gene expression, fibrosis, and oncogenesis," *Plos Genetics*, vol. 9, no. 12, p. e1003937, 2013.

[20] J. Luo, Y. Liang, F. Kong et al., "Vascular endothelial growth factor promotes the activation of hepatic stellate cells in chronic schistosomiasis," *Immunology and cell biology*, vol. 95, no. 4, pp. 399–407, 2017.

[21] S. Lenna and M. Trojanowska, "The role of endoplasmic reticulum stress and the unfolded protein response in fibrosis," *Current Opinion in Rheumatology*, vol. 24, no. 6, pp. 663–668, 2012.

[22] A. Paridaens, S. Raevens, L. Devisscher et al., "Modulation of the unfolded protein response by tauroursodeoxycholic acid counteracts apoptotic cell death and fibrosis in a mouse model for secondary biliary liver fibrosis," *International Journal of Molecular Sciences*, vol. 18, no. 1, p. 214, 2017.

[23] H. Tanjore, W. E. Lawson, and T. S. Blackwell, "Endoplasmic reticulum stress as a pro-fibrotic stimulus," *Biochimica et Biophysica Acta-Molecular Basis of Disease*, vol. 1832, no. 7, pp. 940–947, 2013.

[24] Y. Yang, L. Liu, I. Naik, Z. Braunstein, J. Zhong, and B. Ren, "Transcription factor C/EBP homologous protein in health and diseases," *Frontiers in Immunology*, vol. 8, p. 1612, 2017.

[25] Y. R. Yu, X. Q. Ni, J. Huang, Y. H. Zhu, and Y. F. Qi, "Taurine drinking ameliorates hepatic granuloma and fibrosis in mice infected with Schistosoma japonicum," *International Journal for Parasitology: Drugs and Drug Resistance*, vol. 6, no. 1, pp. 35–43, 2016.

[26] L. Zhang, Y. Wang, N. S. Pandupuspitasari et al., "Endoplasmic reticulum stress, a new wrestler, in the pathogenesis of idiopathic pulmonary fibrosis," *American Journal of Translational Research*, vol. 9, no. 2, pp. 722–735, 2017.

[27] A. Burman, W. E. Lawson, T. S. Blackwell, and H. Tanjore, "Hypoxia worsens pulmonary fibrosis through expression Of C/ebp homologous protein (chop)," *American Journal of Respiratory and Critical Care Medicine*, vol. 193, article A4136, 2016.

[28] K. Toriguchi, E. Hatano, K. Tanabe et al., "Attenuation of steatohepatitis, fibrosis, and carcinogenesis in mice fed a methionine-choline deficient diet by CCAAT/enhancer-binding protein homologous protein deficiency," *Journal of gastroenterology and hepatology*, vol. 29, no. 5, pp. 1109–1118, 2014.

[29] K. Taki, M. Ohmuraya, D. Hashimoto et al., "Abstract 897: CHOP-deficiency promotes chronic inflammation-induced pancreatic fibrosis," *Cancer Research*, vol. 75, 2015.

[30] N. Tamaki, E. Hatano, K. Taura et al., "CHOP deficiency attenuates cholestasis-induced liver fibrosis by reduction of hepatocyte injury," *American Journal of Physiology. Gastrointestinal and Liver Physiology*, vol. 294, no. 2, pp. G498–G505, 2008.

[31] N. Vij, M. O. Amoako, S. Mazur, and P. L. Zeitlin, "CHOP transcription factor mediates IL-8 signaling in cystic fibrosis bronchial epithelial cells," *American Journal of Respiratory Cell and Molecular Biology*, vol. 38, no. 2, pp. 176–184, 2008.

[32] B. San-Miguel, I. Crespo, D. I. Sanchez et al., "Melatonin inhibits autophagy and endoplasmic reticulum stress in mice with carbon tetrachloride-induced fibrosis," *Journal of Pineal Research*, vol. 59, no. 2, pp. 151–162, 2015.

[33] K. Mueller, Y. Sunami, M. Stuetzle et al., "CHOP-mediated hepcidin suppression modulates hepatic iron load," *Journal of Pathology*, vol. 231, no. 4, pp. 532–542, 2013.

[34] R. Liu, X. Li, Z. Huang et al., "C/EBP homologous protein-induced loss of intestinal epithelial stemness contributes to bile duct ligation-induced cholestatic liver injury in mice," *Hepatology*, vol. 67, no. 4, pp. 1441–1457, 2018.

[35] Y. Kim, S. K. Natarajan, and S. Chung, "Gamma-tocotrienol attenuates the hepatic inflammation and fibrosis by suppressing endoplasmic reticulum stress in mice," *Molecular Nutrition & Food Research*, vol. 62, no. 21, article 1800519, 2018.

[36] T. C. H. Tan, D. H. G. Crawford, L. A. Jaskowski et al., "Excess iron modulates endoplasmic reticulum stress-associated pathways in a mouse model of alcohol and high-fat diet-induced liver injury," *Laboratory Investigation*, vol. 93, no. 12, pp. 1295–1312, 2013.

[37] J. Xu, K. K. Y. Lai, A. Verlinsky et al., "Synergistic steatohepatitis by moderate obesity and alcohol in mice despite increased adiponectin and p-AMPK," *Journal of Hepatology*, vol. 55, no. 3, pp. 673–682, 2011.

[38] C. Ji, R. Mehrian-Shai, C. Chan, Y.-H. Hsu, and N. Kaplowitz, "Role of CHOP in hepatic apoptosis in the murine model of intragastric ethanol feeding," *Alcoholism, clinical and experimental research*, vol. 29, no. 8, pp. 1496–1503, 2005.

[39] D. Yuan, T. Xiang, Y. Huo et al., "Preventive effects of total saponins of Panax japonicus on fatty liver fibrosis in mice," *Archives of Medical Science*, vol. 14, no. 2, pp. 396–406, 2018.

[40] Y. Tanaka, Y. Ishitsuka, M. Hayasaka et al., "The exacerbating roles of CCAAT/enhancer-binding protein homologous protein (CHOP) in the development of bleomycin-induced pulmonary fibrosis and the preventive effects of tauroursodeoxycholic acid (TUDCA) against pulmonary fibrosis in mice," *Pharmacological research*, vol. 99, pp. 52–62, 2015.

[41] J. Wu, R. Zhang, M. Torreggiani et al., "Induction of Diabetes in Aged C57B6 Mice Results in Severe Nephropathy: An Association with Oxidative Stress, Endoplasmic Reticulum Stress, and Inflammation," *The American journal of pathology*, vol. 176, no. 5, pp. 2163–2176, 2010.

[42] G. Schramm, A. Gronow, J. Knobloch et al., "IPSE/alpha-1: A major immunogenic component secreted from Schistosoma mansoni eggs," *Molecular and biochemical parasitology*, vol. 147, no. 1, pp. 9–19, 2006.

[43] B. Everts, G. Perona-Wright, H. H. Smits et al., "Omega-1, a glycoprotein secreted by Schistosoma mansoni eggs, drives Th2 responses," *The Journal of experimental medicine*, vol. 206, no. 8, pp. 1673–1680, 2009.

[44] G. Schramm, J. V. Hamilton, C. I. A. Balog et al., "Molecular characterisation of kappa-5, a major antigenic glycoprotein from Schistosoma mansoni eggs," *Molecular and biochemical parasitology*, vol. 166, no. 1, pp. 4–14, 2009.

[45] J. Sotillo, M. S. Pearson, L. Becker et al., "In-depth proteomic characterization of Schistosoma haematobium: towards the development of new tools for elimination," *PLoS Neglected Tropical Diseases*, vol. 13, no. 5, article e0007362, 2019.

[46] C. De Marco Verissimo, J. Potriquet, H. You, D. P. McManus, J. Mulvenna, and M. K. Jones, "Qualitative and quantitative proteomic analyses of Schistosoma japonicum eggs and egg-derived secretory-excretory proteins," *Parasites & Vectors*, vol. 12, no. 1, p. 173, 2019.

[47] W. Gong, F. Huang, L. Sun et al., "Toll-like receptor-2 regulates macrophage polarization induced by excretory-secretory

antigens from Schistosoma japonicum eggs and promotes liver pathology in murine schistosomiasis," *PLoS neglected tropical diseases*, vol. 12, no. 12, article e0007000, 2018.

[48] P. Du, Q. Ma, Z.-D. Zhu et al., "Mechanism of Corilagin interference with IL-13/STAT6 signaling pathways in hepatic alternative activation macrophages in schistosomiasis-induced liver fibrosis in mouse model," *European journal of pharmacology*, vol. 793, pp. 119–126, 2016.

[49] X. He, R. Tang, Y. Sun et al., "MicroR-146 blocks the activation of M1 macrophage by targeting signal transducer and activator of transcription 1 in hepatic schistosomiasis," *EBioMedicine*, vol. 13, pp. 339–347, 2016.

[50] J. S. Duffield, M. Lupher, V. J. Thannickal, and T. A. Wynn, "Host responses in tissue repair and fibrosis," *Annual Review of Pathology: Mechanisms of Disease*, vol. 8, no. 1, pp. 241–276, 2013.

[51] E. Hams, G. Aviello, and P. G. Fallon, "The schistosoma granuloma: friend or foe?," *Frontiers in immunology*, vol. 4, p. 89, 2013.

[52] S. Joshi, A. R. Singh, S. S. Wong et al., "Rac2 is required for alternative macrophage activation and bleomycin induced pulmonary fibrosis; a macrophage autonomous phenotype," *PloS one*, vol. 12, no. 8, p. e0182851, 2017.

[53] B. Shen, X. Liu, Y. Fan, and J. Qiu, "Macrophages regulate renal fibrosis through modulating TGFβ superfamily signaling," *Inflammation*, vol. 37, no. 6, pp. 2076–2084, 2014.

[54] B. Pan, G. Liu, Z. Jiang, and D. Zheng, "Regulation of renal fibrosis by macrophage polarization," *Cellular Physiology and Biochemistry*, vol. 35, no. 3, pp. 1062–1069, 2015.

[55] S. A. Sung, S. K. Jo, W. Y. Cho, N. H. Won, and H. K. Kim, "Reduction of renal fibrosis as a result of liposome encapsulated clodronate induced macrophage depletion after unilateral ureteral obstruction in rats," *Nephron. Experimental Nephrology*, vol. 105, no. 1, pp. e1–e9, 2007.

[56] E. A. Ayaub, P. S. Kolb, Z. Mohammed-Ali et al., "GRP78 and CHOP modulate macrophage apoptosis and the development of bleomycin-induced pulmonary fibrosis," *Journal of Pathology*, vol. 239, no. 4, pp. 411–425, 2016.

[57] M. Zhang, Y. Guo, H. Fu et al., "Chop deficiency prevents UUO-induced renal fibrosis by attenuating fibrotic signals originated from Hmgb1/TLR4/NF κ B/IL-1 β signaling," *Cell Death & Disease*, vol. 6, no. 8, p. e1847, 2015.

[58] O. M. Rahal, A. R. Wolfe, P. K. Mandal et al., "Blocking interleukin (IL)4- and IL13-mediated phosphorylation of STAT6 (Tyr641) decreases M2 polarization of macrophages and protects against macrophage-mediated radioresistance of inflammatory breast cancer," *International Journal of Radiation Oncology, Biology, Physics*, vol. 100, no. 4, pp. 1034–1043, 2018.

[59] M. Gong, X. Zhuo, and A. Ma, "STAT6 upregulation promotes M2 macrophage polarization to suppress atherosclerosis," *Medical Science Monitor Basic Research*, vol. 23, pp. 240–249, 2017.

[60] J. L. Moreno, I. Mikhailenko, M. M. Tondravi, and A. D. Keegan, "IL-4 promotes the formation of multinucleated giant cells from macrophage precursors by a STAT6-dependent, homotypic mechanism: contribution of E-cadherin," *Journal of Leukocyte Biology*, vol. 82, no. 6, pp. 1542–1553, 2007.

[61] M. Sanson, E. Distel, and E. A. Fisher, "HDL induces the expression of the M2 macrophage markers arginase 1 and Fizz-1 in a STAT6-dependent process," *PloS one*, vol. 8, no. 8, p. e74676, 2013.

[62] K. Takeda, M. Kamanaka, T. Tanaka, T. Kishimoto, and S. Akira, "Impaired IL-13-mediated functions of macrophages in STAT6-deficient mice," *Journal of immunology*, vol. 157, pp. 3220–3222, 1996.

[63] S. A. Adedokun, B. N. Seamans, N. T. Cox et al., "Interleukin-4 and STAT6 promoter polymorphisms but not interleukin-10 or 13 are essential for schistosomiasis and associated disease burden among Nigerian children," *Infection Genetics and Evolution*, vol. 65, pp. 28–34, 2018.

[64] J. Yan, Z. Zhang, J. Yang, W. E. Mitch, and Y. Wang, "JAK3/-STAT6 stimulates bone marrow-derived fibroblast activation in renal fibrosis," *Journal of the American Society of Nephrology : JASN*, vol. 26, no. 12, pp. 3060–3071, 2015.

[65] J. Nikota, A. Banville, L. R. Goodwin et al., "Stat-6 signaling pathway and not Interleukin-1 mediates multi-walled carbon nanotube-induced lung fibrosis in mice: insights from an adverse outcome pathway framework," *Particle and fibre toxicology*, vol. 14, no. 1, p. 37, 2017.

[66] K. A. Shirey, L. M. Pletneva, A. C. Puche et al., "Control of RSV-induced lung injury by alternatively activated macrophages is IL-4Rα-, TLR4-, and IFN-β-dependent," *Mucosal Immunology*, vol. 3, no. 3, pp. 291–300, 2010.

[67] H. Liang, Z. Zhang, J. Yan et al., "The IL-4 receptor α has a critical role in bone marrow-derived fibroblast activation and renal fibrosis," *Kidney international*, vol. 92, no. 6, pp. 1433–1443, 2017.

[68] J. A. Knipper, S. Willenborg, J. Brinckmann et al., "Interleukin-4 receptor α signaling in myeloid cells controls collagen fibril assembly in skin repair," *Immunity*, vol. 43, no. 4, pp. 803–816, 2015.

[69] Y. Wang, J. Zhu, L. Zhang et al., "Role of C/EBP homologous protein and endoplasmic reticulum stress in asthma exacerbation by regulating the IL-4/signal transducer and activator of transcription 6/transcription factor EC/IL-4 receptor α positive feedback loop in M2 macrophages," *Journal of Allergy and Clinical Immunology*, vol. 140, no. 6, pp. 1550–1561.e8, 2017.

[70] X. Liao, N. Sharma, F. Kapadia et al., "Krüppel-like factor 4 regulates macrophage polarization," *The Journal of clinical investigation*, vol. 121, no. 7, pp. 2736–2749, 2011.

[71] Y.-k. Xue, J. Tan, D.-w. Dou et al., "Effect of Kruppel-like factor 4 on Notch pathway in hepatic stellate cells," *Journal of Huazhong University of Science and Technology [Medical Sciences]*, vol. 36, no. 6, pp. 811–816, 2016.

[72] R. Men, M. Wen, M. Zhao et al., "MircoRNA-145 promotes activation of hepatic stellate cells via targeting Kruppel-like factor 4," *Scientific Reports*, vol. 7, no. 1, article 40468, 2017.

[73] T. Satoh, O. Takeuchi, A. Vandenbon et al., "The Jmjd3-Irf4 axis regulates M2 macrophage polarization and host responses against helminth infection," *Nature immunology*, vol. 11, no. 10, pp. 936–944, 2010.

[74] S. Ge, L. Zhang, J. Xie et al., "MicroRNA-146b regulates hepatic stellate cell activation via targeting of KLF4," *Annals of hepatology*, vol. 15, no. 6, pp. 918–928, 2016.

[75] L. Tao, W. Ma, L. Wu et al., "Glial cell line-derived neurotrophic factor (GDNF) mediates hepatic stellate cell activation via ALK5/Smad signalling," *Gut*, vol. 68, no. 12, pp. 2214–2227, 2019.

[76] J. Han, X. Zhang, J. K. Lau et al., "Bone marrow-derived macrophage contributes to fibrosing steatohepatitis through

activating hepatic stellate cells," *The Journal of Pathology*, vol. 248, no. 4, pp. 488–500, 2019.

[77] A.-X. Zhou, X. Wang, C. S. Lin et al., "C/EBP-homologous protein (CHOP) in vascular smooth muscle cells regulates their proliferation in aortic explants and atherosclerotic lesions," *Circulation research*, vol. 116, no. 11, pp. 1736–1743, 2015.

[78] P. Handa, S. Thomas, V. Morgan-Stevenson et al., "Iron alters macrophage polarization status and leads to steatohepatitis and fibrogenesis," *Journal of Leukocyte Biology*, vol. 105, no. 5, pp. 1015–1026, 2019.

Hindawi
Journal of Immunology Research
Volume 2019, Article ID 9020519, 9 pages
https://doi.org/10.1155/2019/9020519

Research Article

Zika Virus Alters the Viscosity and Cytokines Profile in Human Colostrum

Ocilma B. de Quental,[1,2] Eduardo L. França,[2,3] Adenilda C. Honório-França,[2,3] Tassiane C. Morais,[2,4] Blanca E. G. Daboin,[2] Italla M. P. Bezerra,[2,5] Shirley V. Komninakis,[2] and Luiz C. de Abreu[2,4,5]

[1]*Department of Nursing, Faculty of Santa Maria (FSM), Cajazeiras 58900-000, Brazil*
[2]*Laboratory of Study Design and Scientific Writing, Department of Morphology and Physiology, Centro Universitário Saúde ABC (FMABC), Santo André, São Paulo 09060-870, Brazil*
[3]*Department of Biological and Health Science, Universidade Federal do Mato Grosso (UFMT), Barra do Garças 78600-000, Brazil*
[4]*Postgraduate Program in Public Health, School of Public Health, Universidade de São Paulo (USP), São Paulo 01246-904, Brazil*
[5]*Postgraduate Program in Public Policies and Local Development, Escola Superior de Ciências da Santa Casa de Misericórdia de Vitória (EMESCAM), Vitória 29027-502, Brazil*

Correspondence should be addressed to Eduardo L. França; dr.eduardo.franca@gmail.com

Received 9 August 2019; Accepted 14 October 2019; Published 15 November 2019

Guest Editor: Barbara C. Figueiredo

The resurgence of cases of Zika virus (ZIKV) infection, accompanied by epidemic of microcephaly in Brazil, has aroused worldwide interest in understanding the biological mechanisms of the virus that allow patient management and the viral dissemination control. Colostrum and human milk are possible sources of virus spread. Therefore, the objective of this study was to analyze the repercussions of ZIKV infection on rheological parameters and inflammatory cytokines of colostrum. The prospective cohort study included 40 puerperal donors of colostrum, divided into 2 groups: control (without ZIKV infection, $n = 20$) and a group infected with ZIKV during the gestational period ($n = 20$). Analyses were performed for the detection of ZIKV by polymerase chain reaction (PCR). In addition to obtaining the rheological parameters and quantification of IL-10 and IL-6 cytokines by flow cytometry, ZIKV and other flaviviruses were not detected in colostrum. However, maternal infection reflected increased viscosity, decreased levels of IL-10, and elevated levels of IL-6. The higher viscosity may represent a mechanical barrier that hinders the spread of the virus. The lower levels of anti-inflammatory mediators and higher inflammatory cytokines may possibly alter the viscosity, and it seems the higher viscosity represents a possible mechanism of adaptation of breastfeeding against a response to ZIKV.

1. Introduction

In recent years, Zika virus (ZIKV) infection has become a major public health problem due to the increased incidence of ZIKV contamination and its association with devastating adverse effects such as microcephaly and Guillain-Barré syndrome [1–7].

In 2015, Brazil suffered a large epidemic of microcephaly attributed to congenital infection by ZIKV [5, 8, 9]. It is believed that the virus had a rapid expansion in the country, due to the susceptibility of the population to its vector, the mosquito of the *Aedes* genus [10]. ZIKV infections were not restricted to Brazil; outbreaks and evidence of transmission have appeared in locations throughout the Americas, Africa, and other geographical regions. Around 86 countries and territories reported evidence of ZIKV infection, transmitted by the mosquito [5].

In addition to mosquito bites, it is interesting to note other risk factors that contribute to the increase of ZIKV dissemination potential, such as transmission through sexual relations

and maternal-fetal relationship [2, 3, 11] because the virus can be found in several biological fluids in infected individuals, such as in blood, urine, semen, and breast milk [3, 10, 12]. In this context of vertical transmission, questions are raised about the transference of ZIKV to the infant during breastfeeding; however, the data on this topic are still limited [3, 11].

It is known that the host immune response plays an important role in the clinical course of patients with viral infection. Particularly, cytokines may play an essential role in limiting viral spread [13]. Several cytokines that have been found in breast milk and contribute to the development of the child's immune system are related to inflammatory processes [14–16] and metabolic or infectious diseases [17–19], but the effects of maternal infection by ZIKV during gestation on the cytokines present in colostrum have not yet been elucidated.

Immunological and rheological alterations play an important role in some infectious diseases, being attributed an interaction of cytokines with the viscosity for the maintenance of the physicochemical properties of biological fluids [20]. The flow of human milk within the ductal system of the breast is essential to the health and well-being of both mother and child [21]. The viscosity of human milk has been examined in limited studies, but in colostrum from mothers with ZIKV, the rheological properties of human milk have not been studied yet.

It is possible that the ZIKV infections during the gestation could influence the soluble components of human milk impacting its viscosity as well as its proteins, such as cytokines which alters the immunological and rheological parameters of human milk. Thus, the aim of this study was to evaluate the effects of ZIKV infection on rheological parameters and inflammatory cytokines of colostrum during gestation.

2. Materials and Methods

2.1. Design and Samples. A prospective cohort study was carried out in 2016 and 2017, with 40 women (18-41 years old) who delivered in the public hospital of the State of Paraiba, Northeastern Brazil. Participants donated a colostrum sample, and they were interviewed again at 1 year postpartum by cell phone for data collection about possible child health complications. They were divided into 2 groups according to the presence or absence of infection by ZIKV during their gestational period. The control group ($n = 20$) was composed of women clinically healthy and the ZIKV group ($n = 20$) by puerperae that had ZIKV infection during pregnancy. These women had in their records the confirmation of the diagnosis of ZIKV infection by real-time PCR (polymerase chain reaction) performed by the Central Laboratory of Public Health of the State of Paraiba.

The inclusion criteria of the study were as follows: gestational age at delivery between 37 and 41 6/7 weeks; negative serological reactions for hepatitis, HIV, and syphilis; clinically healthy at delivery; and informed consent form signed. The exclusion criteria were as follows: twin pregnancy; delivery before the 36th week of gestation, and flavivirus or others infections in the postpartum period.

The women were informed about the purpose of the study, and the benefits of this research. The volunteers signed an informed consent form before entering the study, which was approved by the Institutional Committee for Ethics in Research (46643515.0.0000.5421).

2.2. Obtaining Colostrum. About 5 mL of colostrum from each woman were collected in sterile plastic tubes, between 48 and 72 hours postpartum. The samples were centrifuged (160xg, 4°C) for 10 minutes, which separated the colostrum into three different phases: cell pellet, an intermediate aqueous phase, and an upper fat layer. The aqueous supernatant (colostrum supernatant) was stored at -80°C for subsequent analysis.

The ZIKV group colostrum was analyzed by PCR to detect the presence of viral ribonucleic acid (RNA).

2.3. RNA Extraction in Colostrum from ZIKV Group. Viral RNA extraction from 1 mL of colostrum supernatant was performed using Qiamp™ Viral Blood Kit (Qiagen, Hilden, Germany) following the manufacturer's manual. The RNA was eluted in buffer, aliquoted for quantification in fluorimeter, and the remainder stored in -80°C freezer until be used.

2.4. Reverse Transcription Reaction. Purified RNA was used for reverse transcription reaction consisting of the transformation of RNA into complementary deoxyribonucleic acid. For this reaction, 5 μL RNA, 150 ng random primers (Invitrogen, Carlsbad, CA, USA), 0.5 mM deoxyribonucleotide triphosphates (dNTPs) (Invitrogen, Carlsbad, CA, USA), and 6 μL deionized water were used. The components were incubated for 5 minutes at 65°C, with subsequent thermal shock on ice. From this, it was added: 1x of First-Strand Buffer (Invitrogen, Carlsbad, CA, USA), 0.005 M DL-dithiothreitol (Invitrogen, Carlsbad, CA, USA), 40 U RNaseOUT™ (Invitrogen, Carlsbad, CA, USA), and 200 U Super Script™ III (Invitrogen, Carlsbad, CA, USA). The reaction was incubated in a thermocycler using the following cycling: 5 minutes at 25°C, 60 minutes at 50°C, and 15 minutes at 70°C.

2.5. Real-Time PCR for the Identification of Zika, Chikungunya, and Dengue Viruses "in House." RNA extracted from the colostrum supernatant was analyzed by real-time PCR (RT-qPCR) using the hydrolysable probes system (TaqMan™) for Zika, chikungunya, and dengue viruses [22, 23]. All RT-qPCR reactions of this research were performed on the 7500 Real-Time PCR system.

2.6. Real-Time PCR for the Identification of Zika, Chikungunya, and Dengue Viruses by RT-QPCR Multiplex. RNA extracted from colostrum supernatant was analyzed by Zika, dengue, and chikungunya (ZDC) multiplex RT-PCR assay (Bio-Rad Laboratories, Hercules, CA, USA), following the manufacturer's manual. This kit has all the required controls for a reliable result; in addition, the reverse transcription reaction and real-time PCR are performed in one step.

2.7. Real-Time PCR for Flavivirus Identification (Pan-Flavivirus). It used an RT-qPCR with a system of hydrolysable probes and primers designed to detect different viruses of the *Flavivirus* genus. This detection system was created for the epidemiological surveillance of flaviviruses with speed incessant accuracy [24].

2.8. Colostrum Supernatant Rheological Parameters. The rheological parameters were measured using the Modular Compact Rheometer—MCR 102 (Anton Paar™ GmbH, Ostfildern, Germany), according to França et al. [25]. In all experiments, 600 μL of samples were applied to the surface of the plate reader following the removal of excess sample. The readings were performed with a permanent control of gap measurements with TruGap™ in 0.099 mm increments and the measuring cell Toolmaster™ 50. The temperature control was achieved using T-Ready™ and the software Rheoplus V3.61. The graphics were obtained using Rheoplus. For the flow curves and viscosity, established parameters were based on the control of shear stress (τ) to 0-5 Pa for upsweep and 5-0 Pa for downward curves. The tests were conducted under isothermal conditions at 37°C, with 60 readings analyzed.

2.9. Quantification of Cytokines. The cytokines IL-6 and IL-10 were measured in colostrum supernatant by BD™ Cytometric Bead Array (BD Biosciences, San Jose, CA, USA) according to the manufacturer's manual. A flow cytometer was used for these analyses (BD FACS Calibur™, Biosciences, San Jose, CA, USA). The data were analyzed using the software FCAP Array™ 1.0 (BD Biosciences, San Jose, CA, USA).

2.10. Treatment of Colostrum Supernatant with IL-10. To investigate whether the inflammatory process influenced the viscosity of the human colostrum supernatant, the samples were incubated with IL-10, an important anti-inflammation mediator. In all experiments, 580 μL of samples was incubated with 20 μL of cytokine IL-10 (Sigma, St. Louis, USA; final concentration 100 pg/mL) for 1 h at 37°C [20]. This concentration was previously determined by dose-response curve. The colostrum supernatant was used immediately for the rheological analysis.

2.11. Statistical Analysis. Statistical analyses were performed with BioEstat® version 5.0 software (Mamirauá Institute, Belém, Brazil). The results were presented as mean (±standard deviation) or amostral number (%). The Shapiro-Wilk normality test was used. The two-way variance analysis (ANOVA) was used by rheological parameters analysis, and one-way variance analysis (ANOVA) was used by cytokines analysis, both followed by Tukey test. Pearson's test was used to describe the correlation between cytokine concentrations and viscosity. Significant differences were considered when $p < 0.05$.

3. Results

3.1. Subject Characteristics. Women in the control group were not diagnosed with ZIKV infection during pregnancy. While the mothers belonging to the ZIKV group had diagnosis confirmed by PCR test during gestation, but after delivery, no ZIKV was detected in colostrum. Of these, most had infection in the first trimester of gestation and only one case had infection during the third gestational trimester. Babies from both groups had no changes in the head circumference and there were no cases of microcephaly, but posteriorly, six women reported the development of infant health complications (convulsion, neuropsychomotor development delay, and hearing and vision impairment) (Table 1).

3.2. Rheological Parameters of the Colostrum Supernatant from Mothers with or without Gestational ZIKV Infection. There was no difference between the groups in the curve of colostrum supernatant flow. The flow curve for both groups started at source, ascended, and was nonlinear (Figure 1(a)).

Colostrum supernatant viscosity analyses at 37°C indicated viscosity was higher in the group of women who had ZIKV infection in the gestational period (Figure 1(b)).

3.3. Cytokine Concentrations and Correlations with the Viscosity of Colostrum Supernatant according to Maternal ZIKV Infection. Zika virus infection in the gestational period caused changes in the constituents of IL-10 and IL-6 cytokines in the colostrum supernatant since there was a significant reduction ($p < 0.05$) in IL-10 levels and elevation of IL-6 concentrations in colostrum of women who suffered from ZIKV infection in the gestational period (Figure 2(a)).

Cytokines IL-10 and IL-6 levels correlated with colostrum viscosity only for the control group ($p < 0.05$). IL-10 showed an inversely proportional correlation with the colostrum supernatant viscosity for the control group ($p < 0.05$). While IL-6 showed a correlation directly proportional to the colostrum supernatant viscosity ($p < 0.05$) (Figure 2(d)).

3.4. Cytokine Modulation in the Colostrum Supernatant Viscosity from Women with or without ZIKV Infection. In order to analyze whether the molecules with action of regulating inflammation cause the alterations in the viscosity, the colostrum supernatant was modulated with the exogenous cytokine IL-10. The results indicated that the exogenous stimulus of IL-10 increases the colostrum supernatant viscosity ($p < 0.05$) for both the control group (Figure 3(b)) and the ZIKV group (Figure 3(c)). However, the regulatory cytokine IL-10 was not enough to compensate the changes reflected in colostrum viscosity for the ZIKV group (Figure 3(a)) ($p > 0.05$).

4. Discussion

Human colostrum is a unique biofluid; its flow is essential for both mother and infant. It is composed of soluble and immunoprotective elements that protect the newborn from a variety of pathogenic microorganisms [19, 25–28].

In cases of ZIKV infection during the gestation, the mother develops milder symptoms, but in the fetus, the virus may cause growth restriction, a spectrum of central nervous system abnormalities, or even fetal death [10]. As a result, congenital infection may not be clinically detected during gestation, but adverse effects may appear in the postgestation

Table 1: Maternal and neonate parameters according to maternal gestational ZIKV infection.

Maternal and child parameters	Control ($n = 20$)	ZIKV ($n = 20$)
Age (years)	26.10 (±4.91)	25.95 (±7.24)
Signs and symptoms of gestational Zika	00 (0.00%)	20 (100.00%)
RT-PCR (serum) (%)—ZIKV+	—	20 (100.00%)
Gestational age at ZIKV infection (trimester)		
1 trimester	—	13 (65.00%)
2 trimester	—	6 (30.00%)
3 trimester	—	1 (5.00%)
Gestational age at delivery (weeks)	38.95 (±1.00)	39.65 (±0.99)
Infant sex		
Female (%)	11 (55.00%)	11 (55.00%)
Male (%)	9 (45.00%)	9 (45.00%)
Birth weight (g)	3375.50(±444.89)	3356.50 (±407.43)
Birth height (cm)	45.50 (±3.46)	48.00 (±3.52)
Brain perimeter (cm)	34.20(±0.89)	33.76 (±0.66)
Microcephaly	00 (0.00%)	00 (0.00%)
Infant health complications (outcomes at 1 year *postpartum)*	—	
Hearing impairment	—	2 (10.00%)
Vision impairment	—	1 (5.00%)
Convulsion	—	1 (5.00%)
Neuropsychomotor development delay	—	2 (10.00%)
ZIKA IgG/IgM (colostrum)—negative (%)	20 (100.00%)	—
PCR (colostrum)—ZIKV and flavivirus—(%)	—	20 (100.00%)

Maternal and neonatal data are shown as mean (±SD) or amostral number (%).

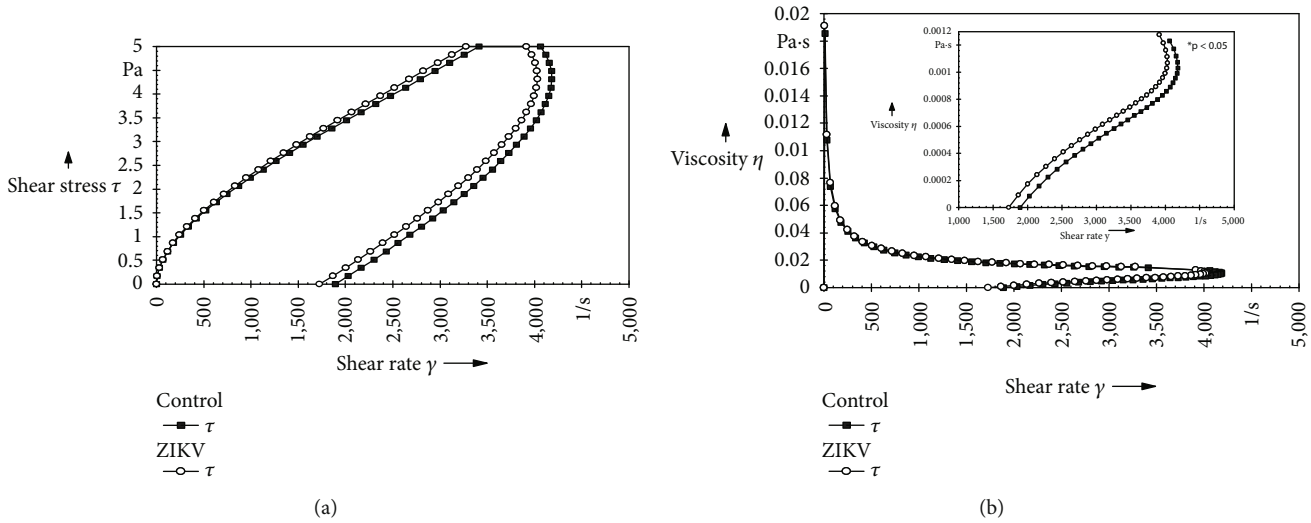

Figure 1: Rheological profile of the colostrum supernatant according with maternal ZIKV infection. (a) Flow curve of the colostrum supernatant from mothers infected or not infected with ZIKV during pregnancy. Viscosity curve (b) of the colostrum supernatant from ZIKV-infected mothers during pregnancy or control group. *Amplification of the region with a statistical difference ($p < 0.05$); it was assessed by ANOVA (two-way) and Tukey's test.

period and during breastfeeding [29]. Accordingly, our results revealed change in cytokines and viscosity in human colostrum of mothers who had ZIKV infection during their gestational period.

In Brazil, the diagnosis of ZIKV infection depends on the identification of the virus by RT-PCR performed during the acute period of infection [10]. The virus is detectable in the blood during the acute viraemia period, and it

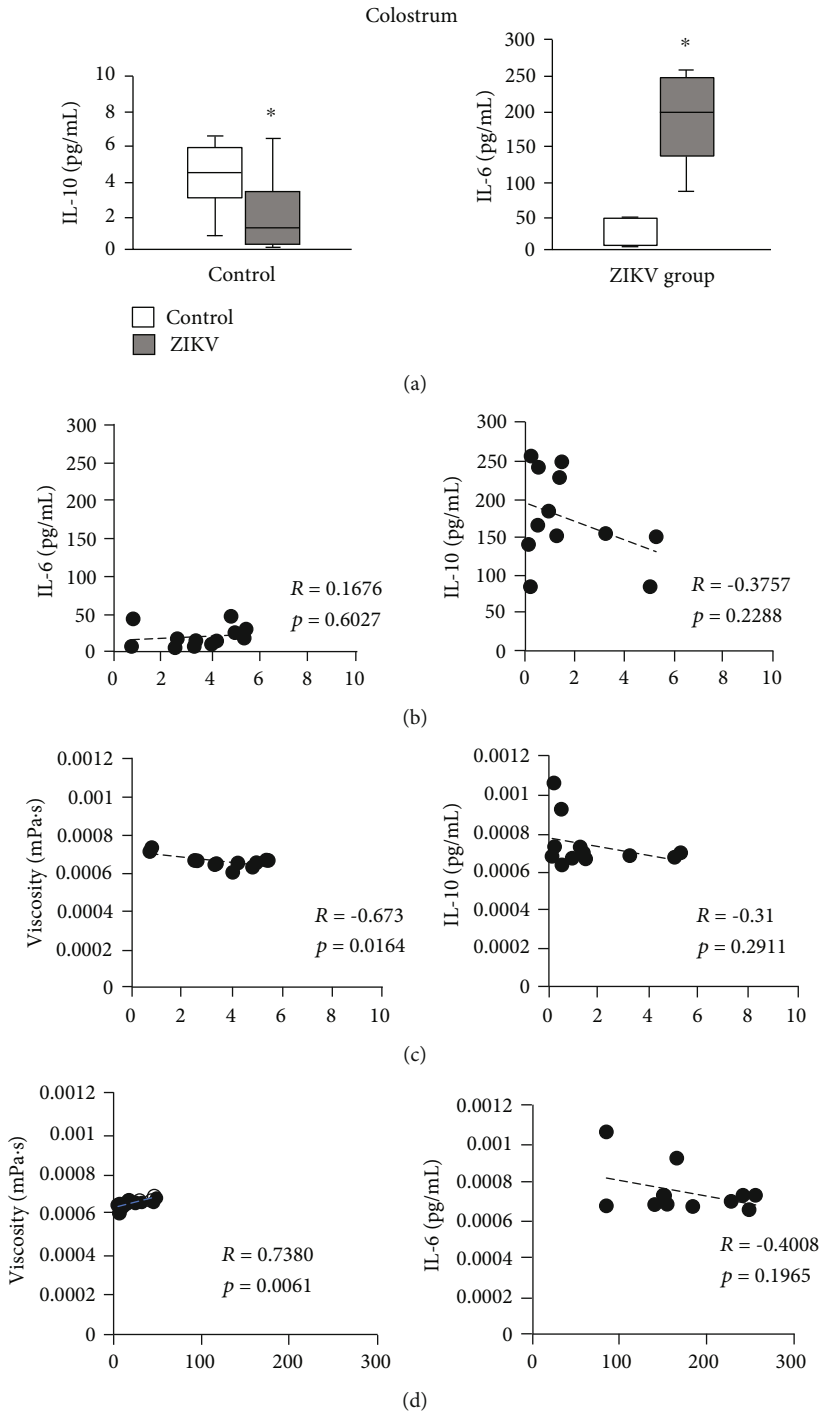

Figure 2: Cytokine levels and correlations with the viscosity of colostrum supernatant according to maternal ZIKV infection. (a) IL-10 and IL-6 levels of the colostrum supernatant from mothers infected or not infected with ZIKV during pregnancy. (b) Pearson's correlation between IL-10 and IL-6 levels for control and ZIKV groups. (c) Pearson's correlation between viscosity and IL-10 levels for both groups. (d) Pearson's correlation between viscosity and IL-6 levels for both groups. *Statistical difference ($p < 0.05$). *Statistical difference between the groups ($p < 0.05$); it was assessed by ANOVA and Tukey's test ($n = 12$).

is eliminated through the urine, usually for more than 10 days [30]. While in biological fluids such as semen, ZIKV is present up to 117 days after the onset of symptoms [12]. It also has been found in colostrum and human milk [11, 31, 32].

In this study, we did not observe the presence of ZIKV RNA in colostrum of mothers who had the viral infection during the gestational period. Possibly, the nondetection of ZIKV in these colostrum samples was due to the fact that women donors were out of the viraemia period of the

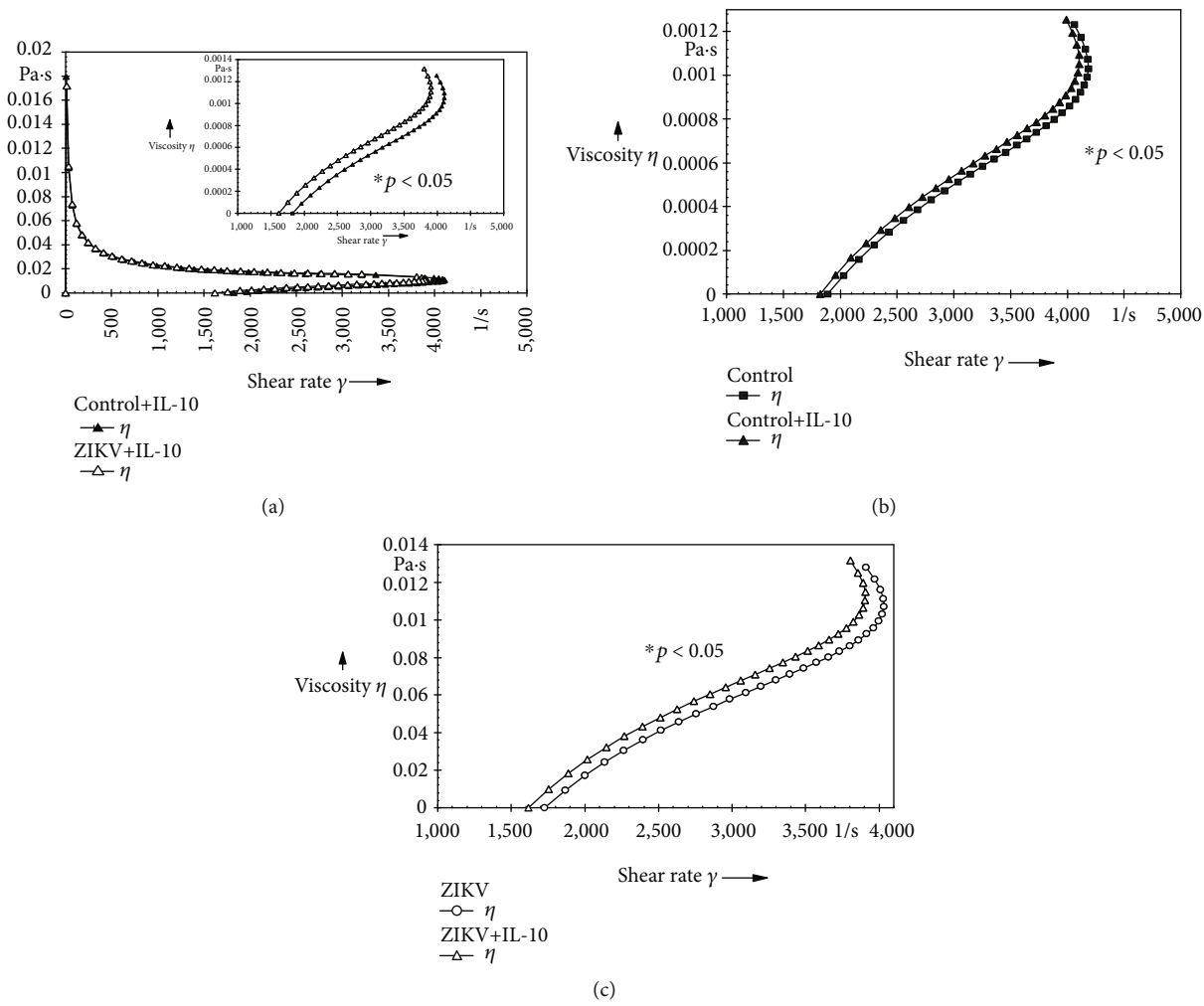

Figure 3: Cytokine modulation in the colostrum supernatant viscosity from individuals with or without ZIKV infection. (a) Viscosity curve of the colostrum supernatant after treatment with IL-10. (b) Viscosity curve of the colostrum supernatant between the control and control plus IL-10 groups. (c) Viscosity curve of the colostrum supernatant between the ZIKV and ZIKV plus IL-10 groups. *Amplification of the region with a statistical difference ($p < 0.05$); it was assessed by ANOVA (two-way) and Tukey's test.

disease. In the studied population, ZIKV infection occurred mostly within the first three months of gestation.

The gestational week of maternal infection may influence the presence or absence of ZIKV in colostrum and breast milk. In this sense, a study describes the case of pregnant women with Zika infection at the 36th week of gestation, that even 30 days after the onset of signs and symptoms, ZIVK was present in colostrum (2.44×10^6 copies/mL) and in the breast milk (9 days postpartum and 216,000 copies/mL), with no signs of infection in the infant [32].

It is worth remembering that the neonate is very susceptible to infections by bacteria and viruses [33]. Therefore, it is essential that the child be breastfed. Breastfeeding promotes the passage of maternal antibodies to the infant and is an additional protection in cases of infection until the baby's immune system is developed [34–38]. In addition human milk to directly modulating the baby's immunological development, due to the cytokine profile in its constituents [14, 39].

Possibly, cytokines play an important role in the replication and dissemination of ZIKV. Therefore, their concentrations in biological fluids from viral infections may be altered [12].

Changes in the cytokine profile, due to inflammatory processes in the presence of microorganisms, may alter the viscosity of biological fluids. Therefore, viscosity analysis is a tool to assist the clinical diagnosis of diseases [20] and, in addition, to represent a fundamental physical property for the quality indicator of human milk [40].

It is of great relevance that the fact that among biological fluids, breastfeeding represents a less efficient transmission pathway than other body fluids [11]. The outcomes of studies that detected infectious ZIKV particles in colostrum and human milk, without conclusive cases of infant infection are instigating [11, 32]. Therefore, we assume that maternal infection with ZIKV, during the gestational period, causes changes in human colostrum, by mechanisms involved in altering the viscosity and in the profile of inflammatory

cytokines. Thus, benefiting the health of the infant against possible negative impacts caused by ZIKV.

To explore this hypothesis, the viscosity was analyzed by rheology. The rheological parameters of the colostrum supernatant curve, independent of maternal infection by ZIKV, did not show ideal liquid characteristics. The lack of overlapping of the upward and downward curves leads to the formation of the hysteresis area that defines the magnitude of the thixotropic property in the sample [25].

In this research, the thixotropy of human colostrum was affected by maternal infection from ZIKV in the gestational period (independent of gestational age), resulting in a significant difference in viscosity between the analyzed groups. This fact suggests that the increase in viscosity, described in the colostrum of ZIKV group, represents a protection, which can serve as a mechanical barrier, developed by the mammary gland, that it makes difficult the dissemination of ZIKV.

Given its originality, it is difficult to compare rheological parameters of human colostrum or biological fluids from individuals who had ZIKV with others study. It is known that the use of bioactives may alter the viscosity of the biological fluid of the affected group and provide strategic pathways to manage the disease [20, 25]. These bioactives usually modulate the inflammatory process caused by the infection [20]. The development and resolution of the inflammatory process are regulated by a complex network of cytokines that have pro- and anti-inflammatory effects. The effective action of a proinflammatory cytokine depends on the synergy with other inflammatory cytokines and antagonists (anti-inflammatory) that are usually elevated at the infection area [41]. In this process, the cytokines IL-10 and IL-6 are fundamental and they are present in colostrum and breast milk [14, 39].

The cytokine IL-10 is mainly known for its regulatory activity and for inhibiting the proinflammatory responses of innate and adaptive immunity, thus preventing tissue damage due to exacerbated immune response [42], while IL-6 is responsible for activating responses of cellular components of the innate immune system and coordinates lymphocyte proliferation [43]. It is generally elevated in most inflammatory stages but eventually exhibits anti-inflammatory activity. It is also involved in the regulation of metabolic, regenerative, and neural processes [44].

In this study, a significant reduction in IL-10 levels and a significant increase in IL-6 concentrations were observed as a function of maternal infection by ZIKV in the gestational period. It emphasizes that both groups were clinically healthy at the time of colostrum collection; thus, this change in colostrum inflammatory cytokines does not refer to other diseases. In the scientific literature, there are gaps in the profile of colostrum and human milk cytokines in patients with ZIKV infection.

Study with blood samples described an increase in IL-6 levels, without changes in IL-10 levels, for the group of individuals infected by ZIKV, when compared to noninfected individuals [13]. While in the semen, patients infected with ZIKV had higher concentrations of IL-6 and IL-10 than the control, in order to evidence the persistent inflammation since the beginning of the infection [12]. Levels of IL-10 or IL-6 may be variable and may increase or decrease in relation to the control, according to the type of biological fluid, virus strain, and days after the onset of symptoms [12, 43].

In this study, no significant correlation was found between IL-10 levels and IL-6 levels in colostrum. However, these cytokines showed a correlation with viscosity for the control group.

It was observed that, in healthy subjects, IL-10 and IL-6 cytokine concentrations were, respectively, inversely or directly correlated with viscosity. It is indicative that in healthy individuals, a balance occurs between inflammation mediators (IL-10 and IL-6) to maintain colostrum viscosity. The same did not happen for the ZIKV group, suggesting that the elevation of colostrum viscosity for this group was not directly due to the elevation of IL-6. Possibly, the change in the cytokine profile triggered the release of other biological components that reflected the increase in viscosity.

It is likely that the changes observed in colostrum IL-10 and IL-6 cytokines reflect protective mechanisms of breastfeeding since IL-10, in the viral response, can impair the initiation of T cells in the early stages of adaptive immunity, which can be used as a mechanism of scape that promotes viral persistence [42].

Another interesting fact is that IL-6 induces significant increases in secretory Immunoglobulin A (SIgA) [45, 46], which is present in human colostrum [36] and is the most abundant immunoglobulin found in the lumen of the human intestine. It represents, therefore, the first line of defense of intestinal protection against pathogens [36, 47].

It is also essential to state that the action of IL-10 under the viscosity of colostrum was dependent on its concentration, whereas, in endogenous concentrations in healthy individuals, it has an inverse correlation with viscosity and while used at a higher level (exogenous stimulation), it increased viscosity in both groups. Thus, we can infer that the use of components with anti-inflammatory action in puerperae should be used with caution, because they interfere in the alteration of cytokine levels that provide colostrum with a feasible biological protection against ZIKV infection to the infant.

Another important point to debate is that between the mother and infant dyad, there is an interaction mechanism that can alter immunological components of breast milk due to infections in the infant. The human milk promotes the process inflammatory regulation with the aim of conferring additional immunological support to the infant [48]. In addition, the human milk and the infant's saliva appear to represent a biochemical synergism which boosts early baby's innate immunity [49]. So, the detection alterations in the IL-10 and IL-6 cytokines levels on colostrum of ZIKV group may be related with a baby's health status. Newborns at the time of delivery did not have health complications. It is possible that inflammatory process resulting from gestational ZIKV infection trigger consequences for the fetus that not were detected by standard routine initial examinations but that may appear at a later period. This interaction could not be evaluated due to the limitation of this study that does not cover cord blood analysis.

New research approaches should be conducted to investigate rheological properties and action of the mammary gland as an organ of the immune system in mothers with ZIKV infection aiming to understand the mechanisms of milk flow and of nutritional and immunological components.

The results of the present study reinforce the importance of a rigid control of ZIKV infection during pregnancy in order to maintain the normal flow of milk and that the immunity components are properly provided. Despite the abnormalities in rheological and immunological parameters, women that were infected with ZIKV should be strongly encouraged to breastfeed their children, since the presence of the virus in the secretion was not evidenced. In addition to being an excellent source of food for newborns, breast milk decreases the high rates of maternal and infant complications.

5. Conclusions

Maternal infection by ZIKV during gestation triggers increased viscosity and changes in IL-10 and IL-6 cytokine levels when compared to colostrum in noninfected women. The lower levels of anti-inflammatory mediators and higher inflammatory cytokines may possibly alter the viscosity and may represent a possible mechanism of adaptation of breastfeeding against a response to ZIKV.

Data Availability

The data used to support the findings of this study are available from the corresponding author upon request.

Conflicts of Interest

The authors declare no conflict of interest.

Acknowledgments

Funding for this research was provided by Fundação de Amparo à Pesquisa do Estado de São Paulo (FAPESP no: 2015/19922-0; no: 2015/01051-3; no: 2019/24232-4) and Conselho Nacional de Desenvolvimento Científico e Tecnológico (CNPq no: 303983/2016-7; no: 403383/2016-1; and no: 305725/2018-1).

References

[1] C. Zanluca, V. C. A. Melo, A. L. P. Mosimann, G. I. V. Santos, C. N. D. Santos, and K. Luz, "First report of autochthonous transmission of Zika virus in Brazil," *Memórias do Instituto Oswaldo Cruz*, vol. 110, no. 4, pp. 569–572, 2015.

[2] A. Fajardo, J. Cristina, and P. Moreno, "Emergence and spreading potential of Zika virus," *Frontiers in Microbiology*, vol. 7, article 1667, 2016.

[3] G. A. Calvet, E. O. Kara, S. P. Giozza et al., "Study on the persistence of Zika virus (ZIKV) in body fluids of patients with ZIKV infection in Brazil," *BMC Infectious Diseases*, vol. 18, no. 49, pp. 1–17, 2018.

[4] R. Lowe, C. Barcellos, P. Brasil et al., "The Zika virus epidemic in Brazil: from discovery to future implications," *International Journal of Environmental Research and Public Health*, vol. 15, no. 96, pp. 1–18, 2018.

[5] World Health Organization, *Zika virus*February 2019, https://www.who.int/news-room/fact-sheets/detail/zika-virus.

[6] H. E. Cumming and N. M. Bourke, "Type I IFNs in the female reproductive tract: The first line of defense in an ever-changing battleground," *Journal of Leukocyte Biology*, vol. 105, no. 2, pp. 353–361, 2019.

[7] A. Gordon, L. Gresh, S. Ojeda et al., "Prior dengue virus infection and risk of Zika: a pediatric cohort in Nicaragua," *PLoS Medicine*, vol. 16, no. 1, article e1002726, 2019.

[8] G. V. França, L. Schuler-Faccini, W. K. Oliveira et al., "Congenital Zika virus syndrome in Brazil: a case series of the first 1501 livebirths with complete investigation," *Lancet*, vol. 388, no. 10047, pp. 891–897, 2016.

[9] O. J. Brady, A. Osgood-Zimmerman, N. J. Kassebaum et al., "The association between Zika virus infection and microcephaly in Brazil 2015–2017: an observational analysis of over 4 million births," *PLoS Medicine*, vol. 16, no. 3, pp. 1–21, 2019.

[10] P. Brasil, J. P. Pereira Jr., M. E. Moreira et al., "Zika virus infection in pregnant women in Rio de Janeiro," *The New England Journal of Medicine*, vol. 375, no. 24, pp. 2321–2334, 2016.

[11] M. G. Cavalcanti, M. J. Cabral-Castro, J. L. S. Gonçalves, L. S. Santana, E. S. Pimenta, and J. M. Peralta, "Zika virus shedding in human milk during lactation: an unlikely source of infection?," *International Journal of Infectious Diseases*, vol. 57, pp. 70–72, 2017.

[12] D. B. L. Oliveira, G. S. Durigon, E. A. Mendes et al., "Persistence and intra-host genetic evolution of Zika virus infection in symptomatic adults: a special view in the male reproductive system," *Viruses*, vol. 10, no. 11, p. 615, 2018.

[13] F. G. Naveca, G. S. Pontes, A. Y. Chang et al., "Analysis of the immunological biomarker profile during acute Zika virus infection reveals the overexpression of CXCL10, a chemokine linked to neuronal damage," *Memórias do Instituto Oswaldo Cruz*, vol. 113, no. 6, article e170542, 2018.

[14] R. Garofalo, "Cytokines in human milk," *The Journal of Pediatrics*, vol. 156, no. 2, 2 Suppl, pp. S36–S40, 2010.

[15] A. Marcuzzi, L. Vecchi Brumatti, L. Caruso et al., "Presence of IL-9 in paired samples of human colostrum and transitional milk," *Journal of Human Lactation*, vol. 29, no. 1, pp. 26–31, 2013.

[16] O. Radillo, A. Norcio, R. Addobbati, and G. Zauli, "Presence of CTAK/CCL27, MCP-3/CCL7 and LIF in human colostrum and breast milk," *Cytokine*, vol. 61, no. 1, pp. 26–28, 2013.

[17] D. L. G. Fagundes, E. L. França, G. Morceli, M. V. C. Rudge, I. M. P. Calderon, and A. C. Honorio-França, "The role of cytokines in the functional activity of phagocytes in blood and colostrum of diabetic mothers," *Clinical and Developmental Immunology*, vol. 2013, Article ID 590190, 8 pages, 2013.

[18] D. L. G. Fagundes, E. L. França, R. T. da Silva Fernandes et al., "Changes in T-cell phenotype and cytokines profile in maternal blood, cord blood and colostrum of diabetic mothers," *The Journal of Maternal-Fetal& Neonatal Medicine*, vol. 29, no. 6, pp. 998–1004, 2016.

[19] Q. L. C. Pereira, C. C. P. Hara, R. T. S. Fernandes et al., "Human colostrum action against Giardia lamblia infection influenced by hormones and advanced maternal age," *Parasitology Research*, vol. 117, no. 6, pp. 1783–1791, 2018.

[20] E. F. Scherer, D. G. Cantarini, R. Siqueira et al., "Cytokine modulation of human blood viscosity from vivax malaria patients," *Acta Tropica*, vol. 158, no. 1, pp. 139–147, 2016.

[21] M. B. Almeida, J. A. Almeida, M. E. Moreira, and F. R. Novak, "Adequacy of human milk viscosity to respond to infants with dysphagia: experimental study," *Journal of Applied Oral Science*, vol. 19, no. 6, pp. 554–559, 2011.

[22] R. S. Lanciotti, O. L. Kosoy, J. J. Laven et al., "Genetic and serologic properties of Zika virus associated with an epidemic, Yap State, Micronesia, 2007," *Emerging Infectious Diseases*, vol. 14, no. 8, pp. 1232–1239, 2008.

[23] D. Cecilia, M. Kakade, K. Alagarasu et al., "Development of a multiplex real-time RT-PCR assay for simultaneous detection of dengue and chikungunya viruses," *Archives of Virology*, vol. 160, no. 1, pp. 323–327, 2015.

[24] P. Patel, O. Landt, M. Kaiser et al., "Development of one-step quantitative reverse transcription PCR for the rapid detection of flaviviruses," *Virology Journal*, vol. 10, no. 1, pp. 1–11, 2013.

[25] E. L. França, E. B. Ribeiro, E. F. Scherer et al., "Effects of _Momordica charantia_ L. on the Blood Rheological Properties in Diabetic Patients," *BioMed Research International*, vol. 2014, Article ID 840379, 8 pages, 2014.

[26] E. L. França, R. V. Bitencourt, M. Fujimori, T. Cristina de Morais, I. de Mattos Paranhos Calderon, and A. C. Honorio-França, "Human colostral phagocytes eliminate enterotoxigenic Escherichia coli opsonized by colostrum supernatant," *Journal of Microbiology, Immunology and Infection*, vol. 44, no. 1, pp. 1–7, 2011.

[27] A. C. Honorio-França, C. C. P. Hara, J. V. S. Ormonde, G. T. Nunes, and E. L. França, "Human colostrum melatonin exhibits a day-night variation and modulates the activity of colostral phagocytes," *Journal of Applied Biomedicine*, vol. 11, no. 3, pp. 153–162, 2013.

[28] A. C. Honorio-França, G. T. Nunes, D. L. Fagundes et al., "Intracellular calcium is a target of modulation of apoptosis in MCF-7 cells in the presence of IgA adsorbed to polyethylene glycol," *OncoTargets and Therapy*, vol. 9, no. 1, pp. 617–626, 2016.

[29] G. C. Valentine, M. D. Seferovic, S. W. Fowler et al., "Timing of gestational exposure to Zika virus is associated with postnatal growth restriction in a murine model," *American Journal of Obstetrics and Gynecology*, vol. 219, no. 4, pp. 403.e1–403.e9, 2018.

[30] A. C. Gourinat, O. O'Connor, E. Calvez, C. Goarant, and M. Dupont-Rouzeyrol, "Detection of Zika virus in urine," *Emerging Infectious Diseases*, vol. 21, no. 1, pp. 84–86, 2015.

[31] S. Pfaender, N. J. Vielle, N. Ebert, E. Steinmann, M. P. Alves, and V. Thiel, "Inactivation of Zika virus in human breast milk by prolonged storage or pasteurization," *Virus Research*, vol. 228, no. 1, pp. 58–60, 2017.

[32] J. R. Sotelo, A. B. Sotelo, F. J. B. Sotelo et al., "Persistence of Zika virus in breast milk after infection in late stage of pregnancy," *Emerging Infectious Diseases*, vol. 23, no. 5, pp. 856-857, 2017.

[33] P. A. Sirois, G. Pridjian, S. McRae et al., "Developmental outcomes in young children born to mothers with West Nile illness during pregnancy," *Birth Defects Research Part A Clinical and Molecular Teratology*, vol. 100, no. 10, pp. 792–796, 2014.

[34] A. S. Goldman, C. Garza, B. L. Nichols, and R. M. Goldblum, "Immunologic factors in human milk during the first year of lactation," *The Journal of Pediatrics*, vol. 100, no. 4, pp. 563–567, 1982.

[35] E. L. França, T. R. Nicomedes, I. M. P. Calderon, and A. C. Honório-França, "Time-dependent alterations of soluble and cellular components in human milk," *Biological Rhythm Research*, vol. 41, no. 5, pp. 333–347, 2010.

[36] E. L. França, G. Morceli, D. L. Fagundes, M. V. C. Rudge, I. D. M. P. Calderon, and A. C. Honorio-França, "Secretory IgA–Fcα receptor interaction modulating phagocytosis and microbicidal activity by phagocytes in human colostrum of diabetics," *APMIS*, vol. 119, no. 10, pp. 710–719, 2011.

[37] O. Ballard and A. L. Morrow, "Human milk composition: nutrients and bioactive factors," *Pediatric Clinics of North America*, vol. 60, no. 1, pp. 49–74, 2013.

[38] G. Morceli, A. C. Honorio-França, D. L. Fagundes, I. M. Calderon, and E. L. França, "Antioxidant effect of melatonin on the functional activity of colostral phagocytes in diabetic women," *PLoS One*, vol. 8, no. 2, pp. e56915–e56918, 2013.

[39] T. C. Morais, A. C. Honorio-França, R. R. Silva, M. Fujimori, D. L. G. Fagundes, and E. L. França, "Temporal fluctuations of cytokine concentrations in human milk," *Biological Rhythm Research*, vol. 46, no. 6, pp. 811–821, 2015.

[40] S. Sunarić, M. Denić, J. Lalić et al., "Physicochemical and biochemical parameters in milk of Serbian breastfeeding women," *Turkish Journal of Medical Sciences*, vol. 47, no. 1, pp. 246–251, 2017.

[41] S. T. Ahmed and L. B. Ivashkiv, "Inhibition of IL-6 and IL-10 signaling and Stat activation by inflammatory and stress pathways," *The Journal of Immunology*, vol. 165, no. 9, pp. 5227–5237, 2000.

[42] J. M. Rojas, M. Avia, V. Martín, and N. Sevilla, "IL-10: a multifunctional cytokine in viral infections," *The Journal of Immunology Research*, vol. 2017, article 6104054, 14 pages, 2017.

[43] F. Colavita, V. Bordoni, C. Caglioti et al., "ZIKV infection induces an inflammatory response but fails to activate types I, II, and III IFN response in human PBMC," *Mediators of Inflammation*, vol. 2018, Article ID 2450540, 6 pages, 2018.

[44] J. Scheller, A. Chalaris, D. Schmidt-Arras, and S. Rose-John, "The pro- and anti-inflammatory properties of the cytokine interleukin-6," *Biochimica et Biophysica Acta (BBA) - Molecular Cell Research*, vol. 1813, no. 5, pp. 878–888, 2011.

[45] J. R. McGhee, K. Fujihashi, C. Lue, K. W. Beagley, J. Mestecky, and H. Kiyono, "Role of IL-6 in human antigen-specific and polyclonal IgA responses," *Advances in Experimental Medicine and Biology*, vol. 310, pp. 113–121, 1991.

[46] K. Fujihashi, Y. Kono, and Y. H. Kiyono, "Effects of IL6 on B cells in mucosal immune response and inflammation," *Research in Immunology*, vol. 143, no. 7, pp. 744–749, 1992.

[47] N. J. Mantis, N. Rol, and B. Corthésy, "Secretory IgA′s complex roles in immunity and mucosal homeostasis in the gut," *Mucosal immunology*, vol. 4, no. 6, pp. 603–611, 2011.

[48] S. S. Al-Shehri, C. L. Knox, H. G. Liley et al., "Breastmilk-Saliva interactions boost innate immunity by regulating the oral microbiome in early infancy," *PLoS ONE*, vol. 10, no. 9, article e0135047, 2015.

[49] F. Hassiotou, A. R. Hepworth, P. Metzger et al., "Maternal and infant infections stimulate a rapid leukocyte response in breastmilk," *Clinical & Translational Immunology*, vol. 2, no. 4, p. e3, 2013.